8-2022

Load Modeling and Evaluation of LEDs for Hardware Test Bed Application

Jillian M. Ruff
University of Tennessee, Knoxville, jruff4@vols.utk.edu

To the Graduate Council:

I am submitting herewith a thesis written by Jillian M. Ruff entitled "Load Modeling and Evaluation of LEDs for Hardware Test Bed Application." I have examined the final electronic copy of this thesis for form and content and recommend that it be accepted in partial fulfillment of the requirements for the degree of Master of Science, with a major in Electrical Engineering.

Leon M. Tolbert, Major Professor

We have read this thesis and recommend its acceptance:

Leon M. Tolbert, Hua Kevin Bai, Han Helen Cui

Accepted for the Council:
Dixie L. Thompson

Vice Provost and Dean of the Graduate School

(Original signatures are on file with official student records.)

Load Modeling and Evaluation of LEDs for Hardware Test Bed Application

A Thesis Presented for the
Master of Science
Degree
The University of Tennessee, Knoxville

Jillian Ruff
August 2022

DEDICATION

To my parents, Kenneth and Elisa Ruff; my sister, Katelin Creek; my Brother-in-law, Craig Creek; and finally, my niece and soon to be nephew, Cecelia Grae Creek and Peanut. Without their love and support, I would not be where I am today. For that, I am eternally grateful. May the world be a brighter place with this knowledge.

ACKNOWLEDGEMENTS

My profound gratitude goes to my professor and mentor, Dr. Leon Tolbert. Without Dr. Tolbert, I would not have had the confidence to pursue higher education in achieving my Masters. As an undergraduate, Dr. Tolbert saw a future for me in Power Electronics and fought for my opportunity to achieve a comprehensive position within his field of research. Throughout my time in this program, I have had the opportunity to develop and hone my skills as an Electrical Engineer. Gaining more than just an education, I have acquired a plethora of skills through research and laboratory analysis, preparing me tremendously for anything my future may hold. Despite adjustments in lieu of the COVID-19 pandemic, Dr. Tolbert remained available to guide his team to success, fostering an environment for those he mentored to flourish.

I would also like to thank Peter Chenyang Jiang for serving as my mentor at Oak Ridge National Laboratory (ORNL). Peter worked to provide me with a foundational skillset which assisted in my achieving a position as a graduate research assistant. Throughout my time working with Peter, I was able to cultivate a research-oriented mindset and develop advanced laboratory experience. Peter created a safe environment where the education of his team was at the forefront. He saw the potential of those he worked with and pushed them to be their best, while providing them the ability to make an impact on his many projects. I am honored to have had the opportunity to work with and learn from him.

Additional appreciation is extended to my peers at The University of Tennessee, Knoxville. Throughout the duration of my degree, my fellow researchers and professors fostered a supportive environment for growth, in the pursuit of knowledge. Completion of this thesis would not have been possible without the support of graduate students Niu Jia, Dennis Chertkovsky, Xingyue Tian, Jingjing Sun, and Vince Wilson. All of these students made exponential effort to assist me

throughout the duration of the program, especially during laboratory testing and affiliated coursework. They not only encouraged and supported my work at UTK, but also became dear friends to me throughout the process.

Gratitude is further extended to my graduate committee members, and professors, Dr. Kevin Bai and Dr. Helen Cui, at The University of Tennessee. I am incredibly grateful for the influence they have had on not only this thesis, but also my education. Their dedication toward my studies and accomplished work has prevailed through the pursuit of not only my Master's Degree, but also my Bachelor's Degree, in Electrical Engineering. I am honored to have had their continual guidance and active presence within my life throughout the evolution of my education.

Lastly, I would like to thank the National Science Foundation (NSF) and the Center for Ultra-Wide-Area Resilient Electric Energy Transition Networks (CURENT) for providing me with excellent resources and funding opportunities for my graduate studies. Also, I am grateful for the financial support provided by the DOE Wide Bandgap Traineeship funded by DOE EERE's Advanced Manufacturing Office.

ABSTRACT

The lighting industry was revolutionized with the emergence of LED lighting. Over the last 15 years, LED lighting device sales and utilization have grown immensely. The growth and popularity of LEDs is due to improved operation of the device when compared to previous lighting technologies. Efficient performance of the device is critical due to the growth of global energy consumption.

As nonrenewable generation fuel is finite, utilities have begun the transition to renewable energy generation. Generation and distribution systems become inherently complex to comprehend and maintain with incorporation of emerging supply and load technologies. With the unprecedented growth of LED bulbs, there are concerns regarding the impact of their integration on power systems.

In determination of the effects, which LED bulb adoption posed within the power grid, investigation of this device as a grid-load was pursued. This thesis reviews existing studies pertaining to LEDs and power grid load modeling methodologies. Load modeling aids in establishing a balance between energy generation and consumption, comprehensively characterizing relationships between electrical generation, transmission, distribution, and loads.

Due to the complexities of large networked systems, device load models are constructed and aggregated in emulation of the interactive relationships throughout the power grid. This thesis includes a study of preestablished LED bulb ZIP load models and formulation of a component-based load model for improved characterization of a conventional LED lighting device. Load modeling was conducted with reference to the UTK HTB, for future integration and improved grid emulation.

Factors, such as shape, size, illumination, and the power rating of popular LED bulbs is examined. Through investigation of typical LED bulb topologies, a model is formulated, in representation of device behavior as a load. The established load model's characteristics are tested with comparison to physical device operation in a laboratory environment.

The LED bulb component-based model is simulated under dynamic conditions in portrayal of device behavior under fault scenarios. An interactive interface is formulated for simulation of load behavior throughout grid level events. Detailed analysis of data and methods of implementation is provided, in characterization of the LED bulb's load profile.

TABLE OF CONTENTS

LIST OF TABLES

LIST OF FIGURES

CHAPTER 1
INTRODUCTION

1.1Background

1.1.1 The Role of Lighting

As a modern society, both citizens and industries of the United States of America (U.S.) operate with the integration of a complex system commonly referred to as the U.S. Power Grid. An understated luxury of living in this region is the ability to access energy supplied by this grid. Currently, electricity can act not only as an amenity to provide ease throughout living, but also provides vital support to those in need.

We as a nation are seeing entire industries migrate toward relying entirely on electricity. Whether it may be utilized in hospitals, schools, automotive, or an individual home, the population demands for a reliable supply of electricity throughout the country. As citizens of the U.S. become more reliant upon the integration of technology, the necessity for energy distribution steadily rises [59-61].

A vast majority of the population has grown accustomed to a lifestyle that calls for the continuous supply of electricity. Electricity, generated at power plants throughout the nation, is distributed to commercial and residential areas through a transmission system, known as the power grid. A simplified visualization of this energy generation and distribution system is shown in Figure 1.

Transmission of electricity take place through the transmission line system within the power grid. This complex networked system allows the public to utilize electricity through various platforms, devices, and technologies. One of the most common platforms integrated within the power grid is that of lighting.

The consumption of electricity for the purpose of lighting is of utmost importance to the public. Historically, access to lighting devices has allowed for increased productivity levels within society. Humans, by nature, are non-nocturnal creatures. As a result, they were previously limited in productivity by the ability to access lighting sources.

Humans, as a species lacks the anatomical connections within their optical cones to enable vision in the dark. This concept is seen in Figure 2, illustrating a comparison of a nocturnal and diurnal eye. Humans have evolved with the anatomical optical structure referred to as the diurnal eye.

In opposition to the diurnal eye, species that have improved vision in low light environments, have evolved to possess optical structures referred to as nocturnal eyes. Nocturnal eyes are characterized with unobstructed vision in low light environments. The structure of optical cones within nocturnal eyes are better suited under conditions where external lighting is not present.

In opposition, diurnal eyes are those which humans possess. Mankind lacks the genetic trait which enables vision in the dark. However, the population has not let evolution stand in the way. Resourcefulness and innovation have paved the way for people to utilize more than just the daylight hours for productivity [62-64].

1.1.2 Historic Emergence of Lighting Devices

In ancient civilizations, fire was harnessed as a source of light in the form of, what is now recognized as, a candle. The candle acted as a source of lighting for centuries throughout the world. Earliest depictions of the candle date to Ancient Egyptian civilizations as seen in Figure 3, depicting photographic evidence of a candle artifact found in the tomb of King Tutankhamun.

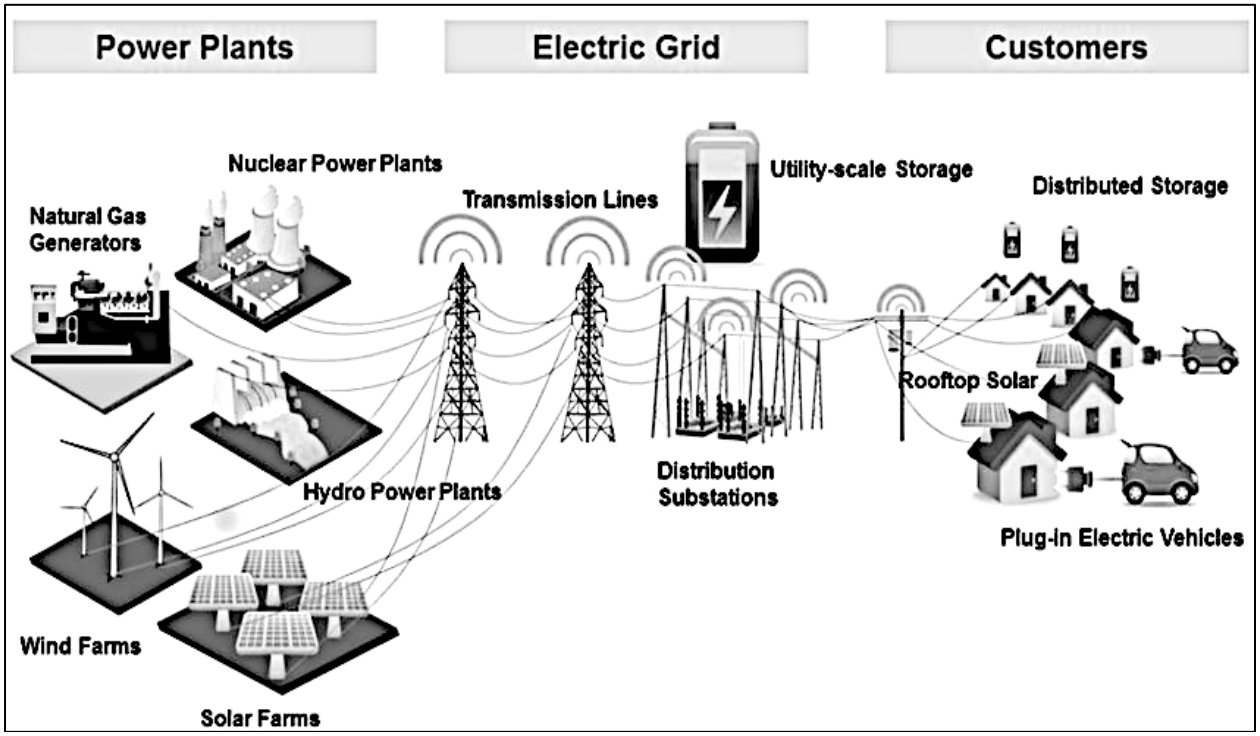

Figure 1. The Power Grid

Simplified representation of the power grid network for generation and distribution of power to consumers in use of integrated devices [65].

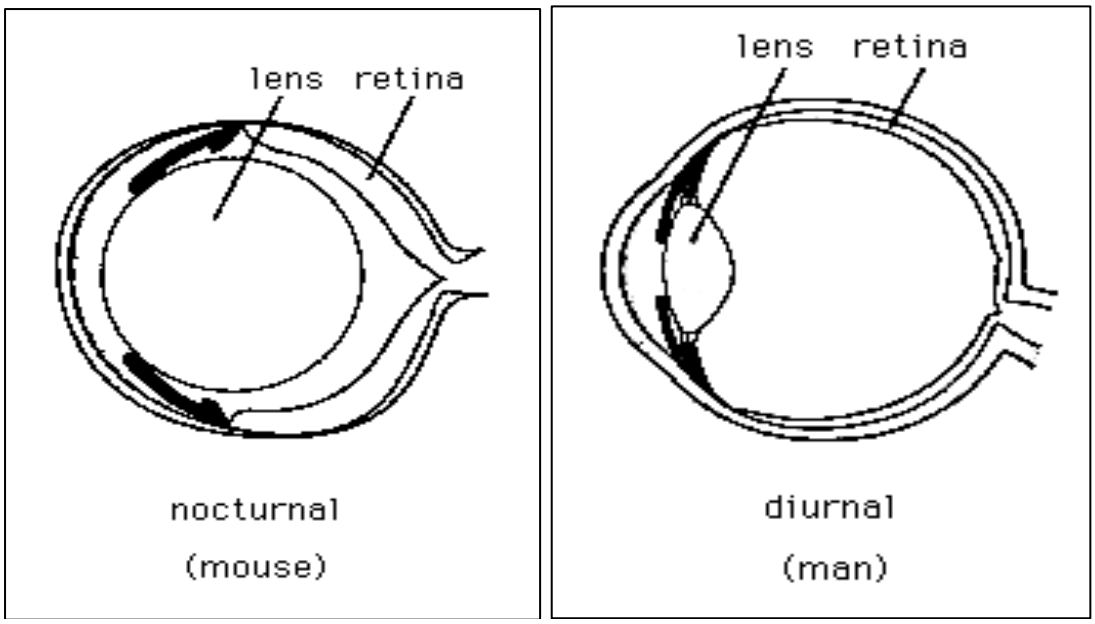

Figure 2. Anatomy of the Eye

Simplified visualization of a nocturnal eye (left) which enables night vision is provided for comparison with the human diurnal eye (right), which lacks the ability to adequately see in the dark [64].

Despite its controlled burn, the candle still posed fire risk to those who used it as a primary source of light.

In addition to the flammability hazards associated with the candle, the apparatus's lifespan in the production of light was limited in duration. In operation, the intensity of illumination was dim. Often, multiple candles were required for adequate area lighting. In recognition of the many downfalls associated this ancient lighting system, a Scottish inventor, by the name of William Murdoch, created the next technological advancement in lighting [67].

In the early 1800's, William Murdoch was credited for the next lighting innovation, using coal gas to formulate a lamp apparatus. This invention, known as the gas lamp, pictured in Figure 4, received high praise when compared to its predecessors. The lifespan of the lighting apparatus was much longer than that of the candle.

Gas emitted from burning coal was transported through a system of pipes to provide for longevity of the flame. More successful at illuminating larger areas at a time, the gas lamp grew in popularity. Despite an overwhelming integration into society as a primary form of illumination device, the gas lamp still posed safety risks with usage, due to its flammable nature [68].

Noting the hazards associated with harnessing flame as a lighting apparatus, one of America's greatest inventors harnessed electricity for the purpose of lighting. The incandescent light bulb was developed by Thomas Edison in the late 1800's and is pictured in Figure 5. It was designed to supply more consistent, longer lasting, and higher quality light. An innovation for its time, the incandescent bulb was acknowledged as the first historical iteration of the light bulb. Harnessing electricity, this revolutionary device supplied light to the public.

Electrical current passed through carbon metal filament wire within the incandescent light bulb. Impacted by the presence of electrical current, the temperature of the wire would begin to

increase drastically. At such a high temperature, the wire glowed, emitting light. To protect the heated wire from air, it was placed inside of a glass blown bulb filled with inert gas. The incandescent lamp was then marketed to the public and found widespread use in the 1900s.

The incandescent bulb stood as the first commercially practical form of electric lighting to be used across the globe. This variety of lamp still operates as a form of lighting in modern society. With this technological innovation in lighting apparatus available, scientists have since been able to refine the utilization of electricity for the purpose of lighting. In efforts to achieve superior longevity and overall efficiency of the light bulb, scientists have worked to improve upon the incandescent lamp [70].

To achieve more power and less heat in comparison to the incandescent lamp, the next major historical trend of lighting invented was that of the fluorescent light bulb. Depiction of an early implementation of the fluorescent lamp is provided in Figure 6. An American electrical engineer, by the name of Peter Cooper Hewitt, pioneered the invention of the lamp in the early 1900s.

In the beginning stages of this invention, electrical current was passed through mercury gas sealed in a glass tube to produce light. Acting as a less expensive and more efficient alternative to the incandescent lamp, fluorescent lamps took over the market. Despite their accolades, the fluorescent lamp possessed a displeasurable blue-green tinted glow, criticized by the public [71].

Throughout a span of 30 years, scientists worked to enhance the fluorescent bulb. Fluorescent bulbs were marketed to the public through the invention of an inexpensive, compact spiral package. The fluorescent lamp had evolved to become Compact Fluorescent Lights (CFL) with package implementation pictured in Figure 7. Incorporation of a coating of fluorescence within the bulb provided for a more appealing illuminance. Offering a superior quality of light

emission, longer lifespan of the bulb, and a cheaper alternative to that of the fluorescent lamp, CFL was integrated into commercial spaces.

Growing in popularity, the public began to gravitate toward CFL over fluorescent lamps due to these assets. While these bulbs proved more efficient and effective, there was still room for improvement in the evolving, electrically dependent world. A comparison of the predominant historical bulb implementations outlines the quantitative comparison of attributes in Table 1. With associated attributes and emphasis upon the pitfalls of each implementation, scientists progressed toward the development of the Light Emitting Diode (LED) light bulb [73-74].

1.1.3 Evolution of LED Lighting

LEDs are semiconductor devices that emit light when current is applied across them. When positive and negative charges, which reside within the device, are put in the presence of current, they begin to move throughout the device. Physical science surrounding the movement of charged particles in the operation of LEDs is exemplified through Figure 8. Movement of these charged particles releases energy in the form of photons, more commonly recognized as visible light. As an electrical component, LEDs are praised for their minimal consumption of energy, small dimensions, prolonged lifetime, and fast switching abilities. However, in the earliest stages of development, LEDs were microscopic, making them an ill-fit for practical, everyday usage for lighting [76], [78].

Initial discovery of the light emitting properties of LEDs began in the early 1900s. Henry Joseph Round, an experimenter from Britain's Marconi Laboratory, applied voltage across a Silicon-Carbide crystal. Upon doing so, he observed that as current was run through the crystal, yellow light was emitted. Investigation into the theory behind this reaction soon followed and was published by Russian scientist Oleg Vladimirovich Losev, approximately 20 years later.

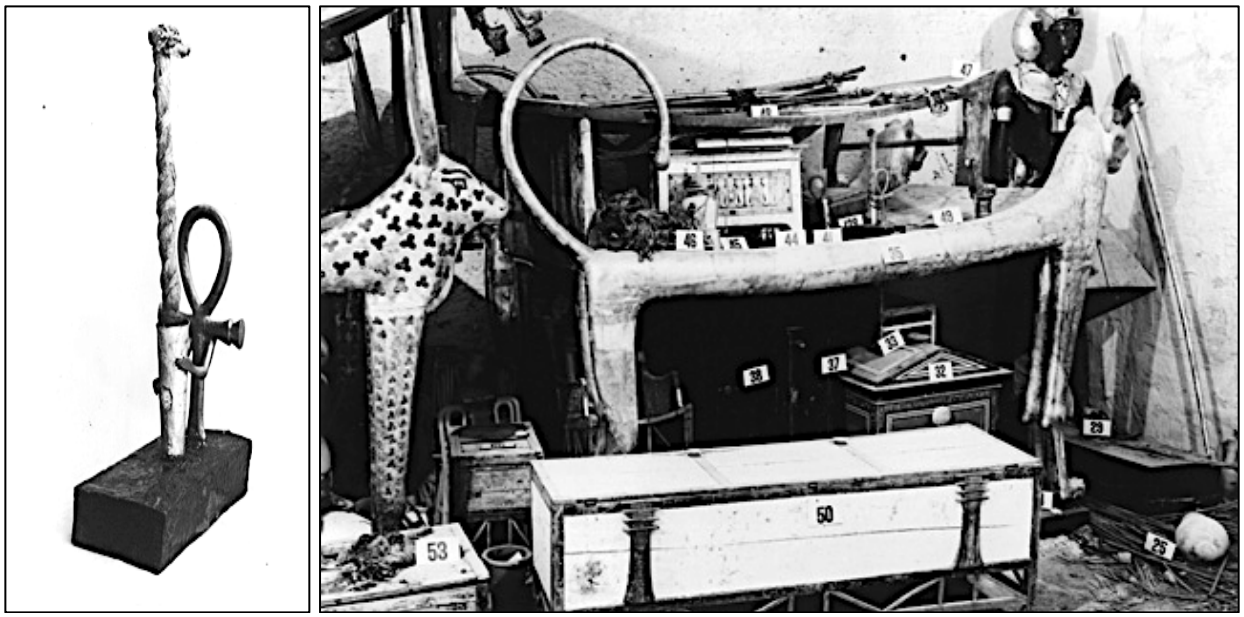

Figure 3. Ancient Egyptian Candle

Photos from the excavation site of King Tutankhamun's tomb which indicate the presence of candlesticks in Ancient Egyptian civilizations [66].

Figure 4. William Murdoch's Gas Lamp

Photo of one implementation of the gas lamp, invented by William Murdoch, for the use of public street lighting. [69].

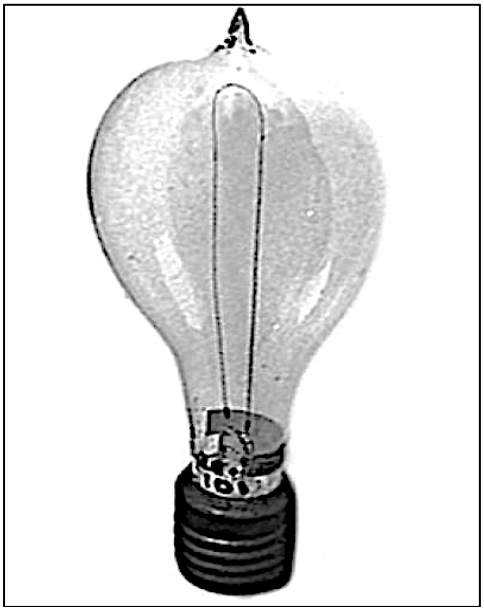

Figure 5. Thomas Edison's Incandescent Bulb
Photo of the incandescent bulb, brought to market by Thomas Edison, for the use of residential area lighting. [70].

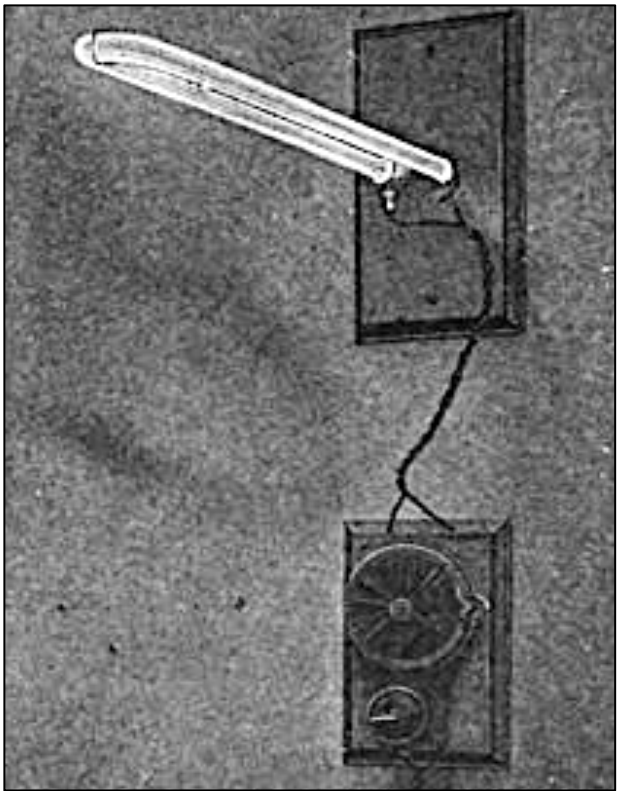

Figure 6. Peter Cooper Hewitt's Fluorescent Lamp
Fluorescent lamp, which was invented and patented by Peter Cooper Hewitt as the next form of area lighting [71].

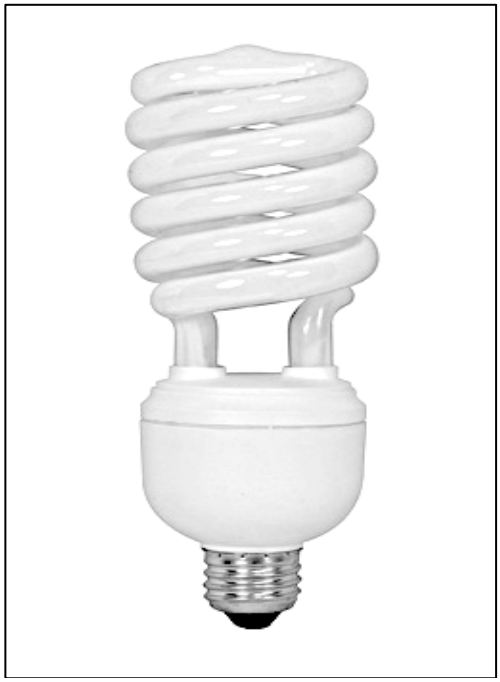

Figure 7. Standard CFL Bulb

Modern implementation of a typical CFL bulb available on the consumer market for purchase, to be used in residential area lighting [72].

Table 1. Power, Cost, and Lifespan Comparison of Bulbs

Type	Incandescent	CFL	LED
Watts used	60 W	14 W	7 W
Average cost per bulb	$1	$2	$4 or less
Average lifespan	1200 hours	8000 hours	25000 hours
Bulbs needed for 25000 hours	21	3	1
Total purchase price of bulbs over 20 years	$21	$6	$4
Cost of electricity (25000 hours at $0.15 per kWh)	$169	$52	$30
Total estimated cost over 20 years	$211	$54	$34

Quantitative comparison of the lifespan, power consumption, and cost of primary historical light bulbs to provide insight into the effective efficiency of each lighting iteration. [74].

Over the span of several decades, research on LEDs continued at a conservative pace. Occasional emission of infrared light was proved possible by simple diodes when connected to current. Soon after, Gallium-Arsenide was found to consistently emit infrared light in the presence of current and was patented as an infrared LED. It was not until Nick Holonyak Jr.'s research in the 1960s, that LEDs' light production entered the visible part of the frequency spectrum.

Holonyak, coined as the Father of LEDs, had made a breakthrough that led to the discovery of various LEDs that ranged in different colored light emission as shown in Table 2. Many researchers, throughout the globe, worked to establish LEDs that operated at different frequencies within the visual light spectrum. In the late 1900s, the brightness of the LED was refined and increased by researchers. Invention of high brightness LEDs allowed for the device's application in fiber optics for telecommunications.

Continued research on LEDs improved upon their performance as a source of lighting. Advantages of these devices became apparent with further research into the material configuration of the devices. Ability to control the color and brightness of the device was a key innovation, which highlighted LEDs as a cutting-edge light source. Being the first form of lighting with a wide range of controllability aspects, the U.S. Department of Energy (DOE) began to encourage further research into LEDs. The DOE pushed for research toward the development of LEDs for commercial and residential applications.

Innovative packaging methods, implemented by Fairchild Semiconductors, effectively reduced the market cost of LEDs. By formulating the device using a planar process of chip production, seen in Figure 9, LEDs became a commercial product with the possibility for a variety of applications. LED lights stand as, arguably, one of the most advantageous sources of light [74-78], [2].

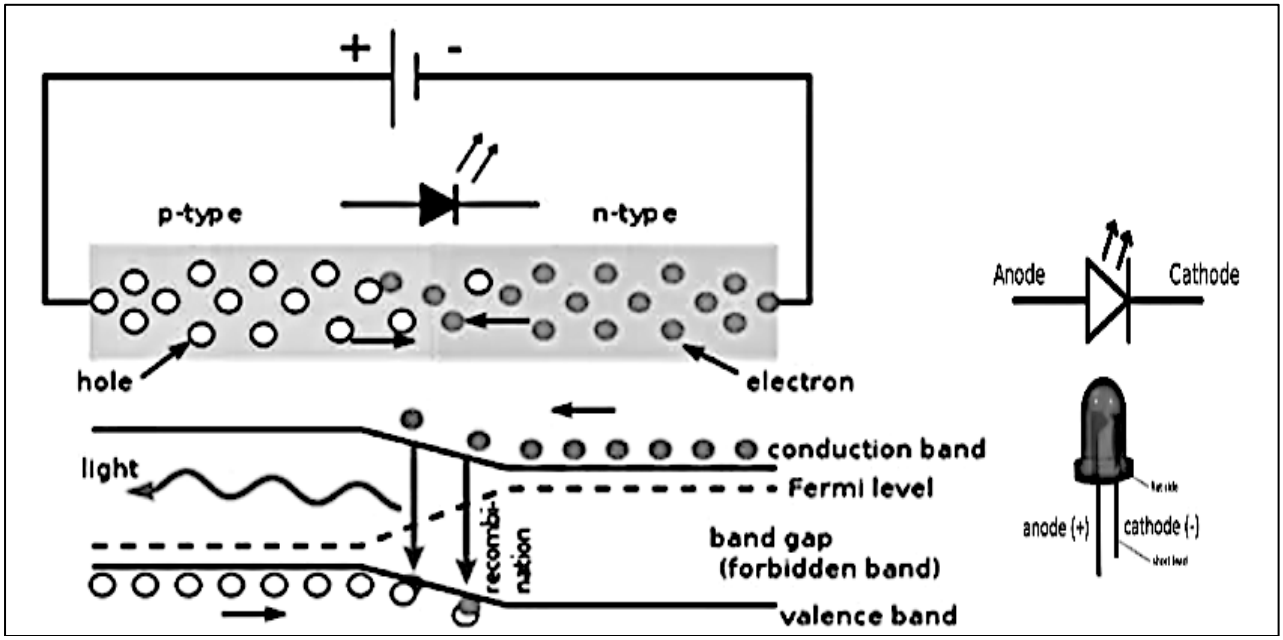

Figure 8. Inner Workings of Light Emitting Diodes

Representation of how a light emitting diode functions with attention to the microscopic physical structure and movement of particles in emission of light [78].

Table 2. Comparison of Bulb Light Emission Spectrums

Light Source	Spectrum
LED	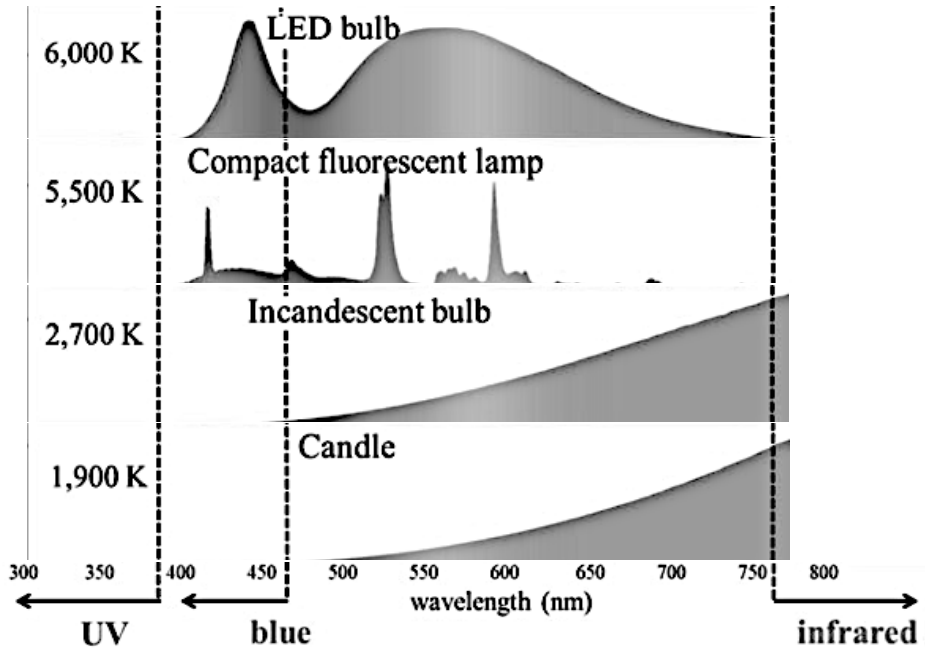
CFL	
Incandescent	
Candle	

Comparison of the spectrum of light emissions for LED, CFL and Incandescent bulbs, along with Candles based upon wavelength with indication of infrared, UV and blue light ranges which are categorized as detrimental to health and unfavorable in visual perception of users [79].

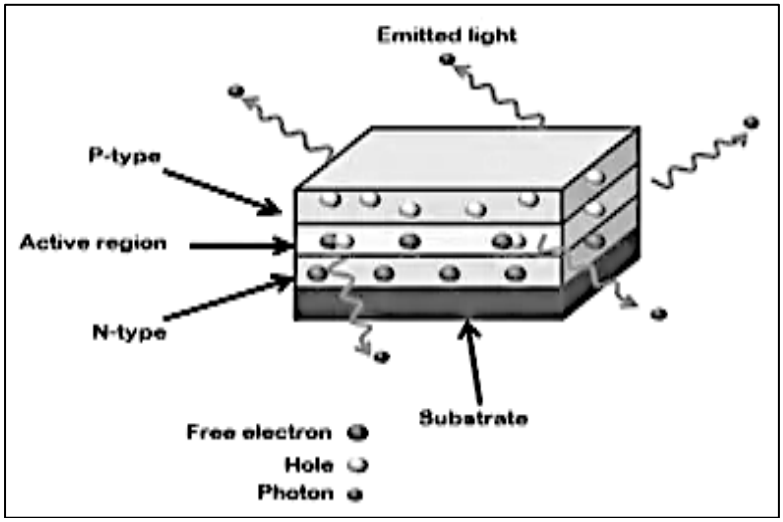

Figure 9. Planar Model of Light Emitting Diode

Planar design of a LED as a chip with microscopic physical attributes which show the process which takes place in the emission of light [78].

1.1.4 Why LED Lighting?

Credited as the most energy efficient bulb available, LEDs offer a plethora of virtues. When compared to the incandescent, fluorescent, and CFL lamp, LEDs produce more light per consumed unit of power. Superior optical power may be attributed to the LED lamp's ability to convert electricity almost entirely to light. Whereas most competing lighting technology releases energy in the form of heat. The duration of time for an LED to turn on and off has been determined to be the quickest of all electric light sources. Quantitative comparison of the characteristics associated with competing lighting devices is provided in Table 3 [2], [80].

In addition to this, the dimensions of an LED are considerably smaller than competing lamps. Durability of materials lends to the device's resistance to damage. Other bulbs are composed of materials more fragile in nature, such as glass. Being substantially less likely to break increases the longevity of a LED lamp. Also contributing to the superior lifespan of these devices is how they produce light.

Other bulbs rely on the heating of metal filament for their operation, which does not occur in LEDs. Over time, the continued production of heat within fluorescent, incandescent, and CFL bulbs deteriorates components, which shortens their respective lifespans, all of which is quantified in Table 3. In addition to this, the illuminance of the LED bulb surpasses its predecessors at lower rated power. Thus, the superior efficiency of the LED lighting apparatus is emphasized through comparison in Table 4 [2], [80], [81].

The implementation of LEDs in electrical appliances is vast. From mobile phones to traffic lights, LEDs have become an economically friendly source of lighting. Their small size and spectrum of colored light emission gives new opportunities for freedom in design when compared

to traditional light sources. Adding to this, LEDs provide better quality of light due to their uniform distribution of luminance, glare, and color properties.

Since there are many physical and physiological factors that influence one's perception of lighting quality, it cannot be defined in terms of a photometric measure. Rather, it is important to note the quality and quantity of light affecting its visual appreciation. Appreciation principles rely on qualitative response to what is seen and how it is seen. Lighting provides an environment in which physical and visual functions may effectively be completed.

Most consider lighting a form of comfort enabling people to perform tasks in the evening or at night, but the appreciation of this commodity is reliant upon several factors. Users credit the LED light for its high illuminance and adjustable colored emission. LEDs' uniformity and colored light properties have been noted to enhance the human experience. They are praised for providing a quality environment at an overall lesser cost.

Considering the high cost of electricity, LEDs are more economically efficient than their predecessors. While fluorescent lamps require multiple bulb or tube replacements due to burnout, durability of LED lamps provide for longevity in usage. With this, LED lights require less maintenance than competing devices. Furthermore, LED lamps are credited in making the overall cost less expensive for lighting.

Adding to this, LED lamps have reduced carbon dioxide emissions in comparison to fluorescent lamps. LED lamps do not contain harmful substances. Unlike fluorescent lamps, LEDs do not emit toxic gasses when discarded. In addition, they do not contain mercury, which is a health hazard associated with CFL usage. Both of which have been found to be harmful to not only humans, but also to the environment.

Overall, LEDs are beneficial due to their lower maintenance cost associated with their prolonged-life, human performance factors of visual comfort, color range, task performance, and visibility. Although the initial cost associated with LEDs may be higher than other artificial lighting sources, their endurance is longer, power consumption lower, and maintenance cost negligible [3].

LED lamps are praised for their high efficiency and prolonged lifespan in comparison to other bulbs. Due to these characteristics, they have been and continue to be integrated throughout a plethora of technologies. These technologies may be observed across both the commercial and residential market. Notable LED implementations include those within general, communication, and critical lighting systems.

This wide span of applications for LED lights may be attributed to their operational abilities at low energy consumption and pollution rates. When compared to other light bulbs, LEDs possess lower intrinsic impedance and ultraviolet radiation emission rates. Having small ratings such as these lends to the LED bulb being an ideal choice of device for lighting necessities [4].

Despite their many accolades, it may be noted that LED light bulbs are not the cheapest source of light, but rather the second cheapest. Presently, CFL bulbs are acknowledged as being the most inexpensive option for lighting. However, due to the prolonged lifespan of LED bulbs, users will ultimately spend more when choosing CFL as seen in Table 3.

According to device ratings, approximately three CFL bulbs will be purchased throughout the operation of one LED lamp. With this and unit pricing observed, LED bulbs are determined to be the most cost-effective source of light as seen in Table 3 [2], [74].

Table 3. Comparison of Tested Bulb Operating Characteristics

Type	LED	CFL	Incandescent
Average Life	50000 hrs	10000 hrs	1200 hrs
Power	6-8 W	13-15 W	60 W
Light Output	100 Lumens/W	50 Lumens/W	10 Lumens/W
Heat Emission	3.4 Btu/hr	30 Btu/hr	85 Btu/hr
Electricity Use[1]	350 kWh	700 kWh	3000 kWh
Bulbs Needed for Use[1]	1	5	42
Mercury Content	None	1-5 mg	None
Sensitivity to Temperatures	None	Above 120 °F and Below -10 °F	Some
Sensitive to Humidity	None	Yes	Some
On/Off Cycling	No Effect	Lifespan Reduction	Some
Turns on Instantly	Yes	Some Delay	Yes
Durability	Very Durable	Fragile	Fragile

[1] Use for 50,000 hours

Characteristic response of lighting devices for comparison of efficiency and attributes in operation [80].

Table 4. Comparison of Bulb Rated Power at Desired Illuminance

Bulb	Lumens				
	200+	400+	700+	900+	1300+
Incandescent	25 W	40 W	60 W	75 W	100 W
CFL	6 W	9 W	12 W	15 W	20 W
LED	4 W	6 W	10 W	13 W	18 W

Comparison of the power consumption requirements of each bulb to reach a specified illuminance, which illustrates the superior efficiency of LED bulbs in opposition to Incandescent and CFL bulbs [81].

1.1.5 LED Lighting and the Power Grid

Estimated to make up 84% of lighting product sales within the next ten years, LEDs are considered a predominant form of light bulb throughout the world, shown in Figure 11. In the present day, LED lamps have taken over as the most utilized form of light bulb in residential areas, followed by CFL as seen in Figure 10. Due to the growing demand for LED light bulbs as a primary commercial and residential lighting product, it should be noted their impending effect on the power grid [82], [83].

According to the U.S. Energy Information Administration (EIA), over 7% of the total end use energy consumption in residential, industrial, and commercial sectors in 2020 was from lighting, shown in Figure 12. With respect to year 2021, LED lighting consumed approximately 287 billion kilowatt-hours of energy, showing expectation of a large impact of integration within the grid. of Further the influence of lighting devices within these sectors is addressed in Table 5, which exhibits the data collected by the EIA's Annual Energy Review. Compilation of these datasets is implemented in determination of the percent distribution of lighting on these sectors and organized visualization [84].

Acknowledgement of this statistic allows for scientific minds to proactively work toward providing the power consumed by lights within the grid. Through load modeling and emulation techniques, potential grid failures due to LED usage may be mitigated. In doing so, increased stability and reliability of the power grid may be achieved, so that citizens continuously have access to lighting for comfort, vitality, safety, progress, and prosper [83-84].

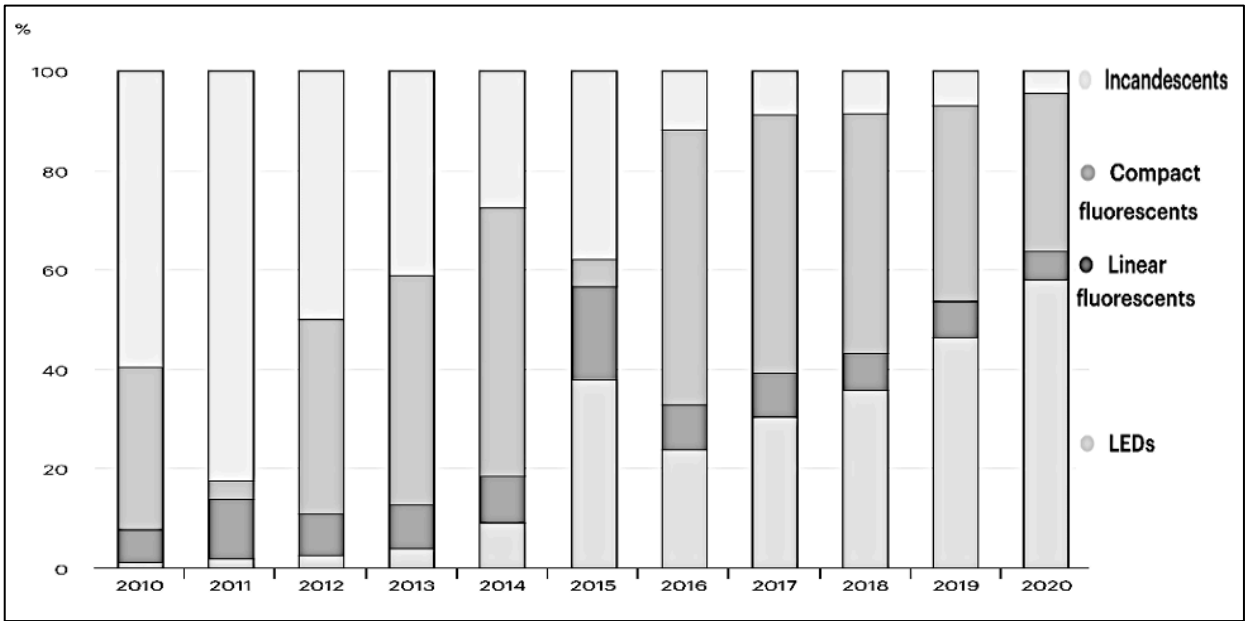

Figure 10. Past Decade of Lighting Market Trends

Percent breakdown of all lighting sales within the market, each year, by separating100% of the sales into the various categories of bulb type. It is noted that in LED sales have steadily risen over the course of the decade and surpassed all other bulbs in recent years and has shown a steady positive trend in market sales [82].

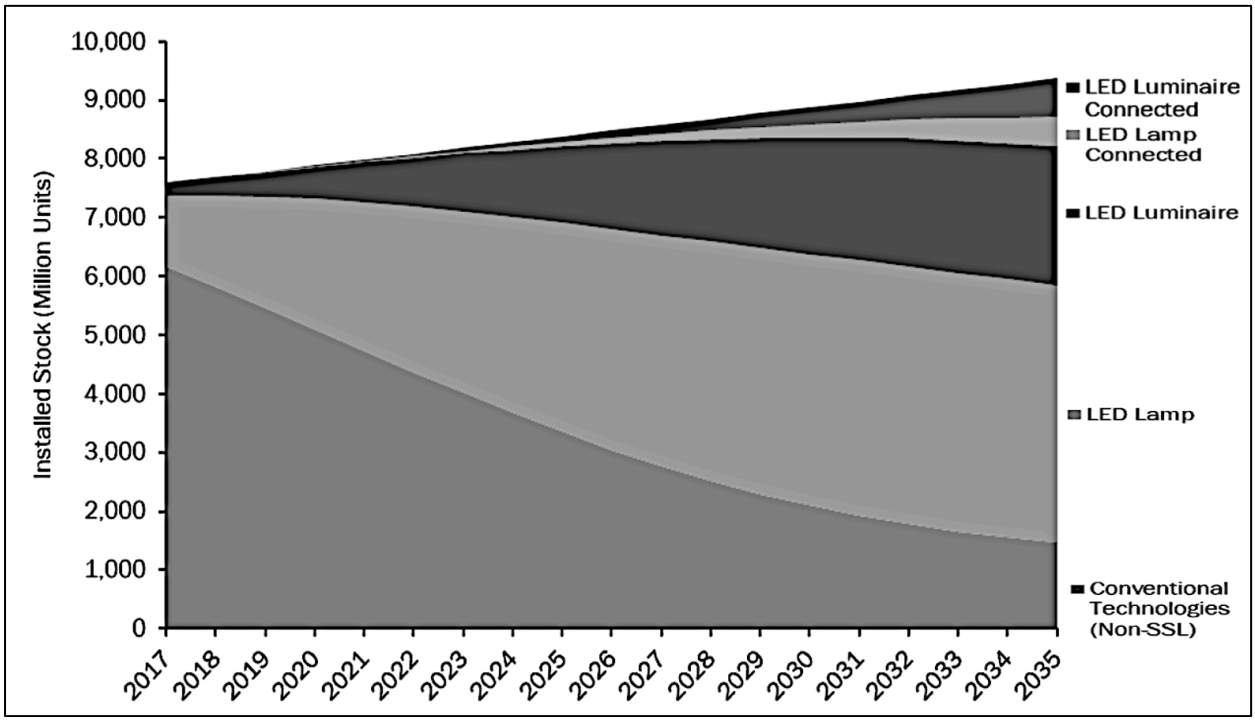

Figure 11. Market Projections for LED vs Non-LED Devices

Market projections for LED-based lighting devices in comparison to opposing lighting devices. LEDs are predicted to take leadership in the market, while non-LED-based lighting apparatus sales are predicted to fall drastically [83].

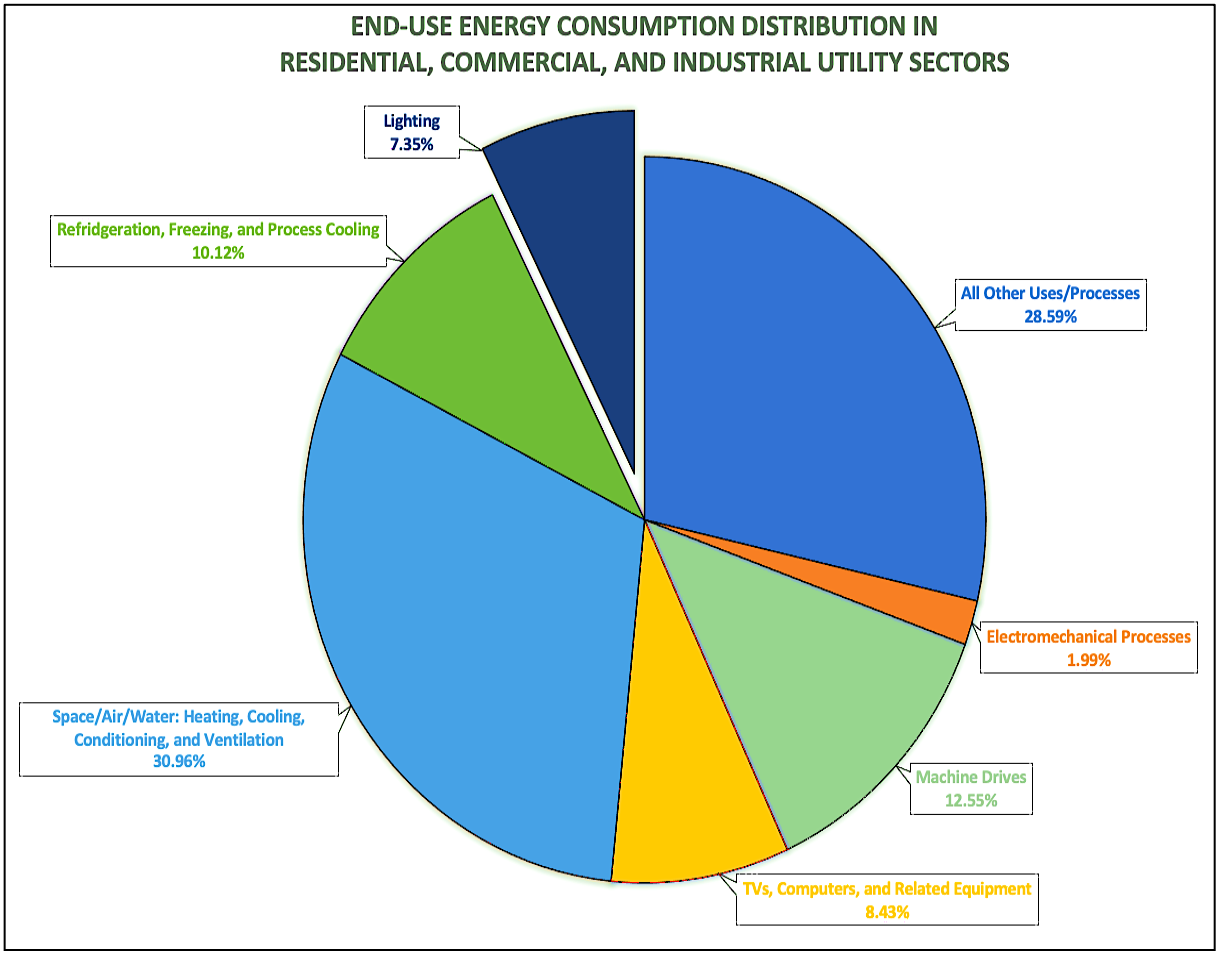

Figure 12. End-Use Energy Consumption Percent Distribution

Annual Energy Review Data on Commercial, Industrial, and Residential Sector's End Use Energy Consumption's Percent Distribution. Depicting the influence of Lighting on these sectors to be approximately 7.35% [84].

Table 5. End Use Energy Consumption Distribution

Sector	End Use	~ %	Electricity Sales and Direct Use (trillion kWh)
Commercial	Computers and Office Equipment	17.3	0.2249
	Refrigeration	14.8	0.1924
	Space Cooling	12.0	0.1560
	Ventilation	11.4	0.1482
	Lighting	**12.1**	**0.1573**
	Space and Water Heating	3.10	0.0403
	All Other Uses	29.3	0.3809
	Total	100	1.3
Industrial	Machine Drive	51.6	0.4644
	Process and Boiler Heater	11.1	0.0999
	Facility Heating, Ventilation, A/C, and Cooling	8.40	0.0756
	Electromechanical Processes	8.20	0.0738
	Process Cooling and Refrigeration	8.40	0.7560
	Other Processes and Facility Uses	6.40	0.0576
	Lighting	**5.90**	**0.0531**
	Total	100	0.9
Residential	Space Heating	14.2	0.2130
	Space Cooling	15.7	0.2355
	Water Heating	11.8	0.1770
	Refrigeration and Freezers	7.10	0.1065
	Lighting	**4.10**	**0.0615**
	Televisions and Related Equipment	4.10	0.0615
	Computers and Related Equipment	1.70	0.0255
	All Other Uses	41.3	0.6195
	Total	100	1.5
Combined Sectors (Commercial, Residential, and Industrial)	Refrigeration, Freezers, and Process Cooling	10.12	0.3745
	Space/Facility Heating and Cooling, Boiler/Water Heating and Process, A/C, and Ventilation	30.96	1.1455
	Computers, Televisions, and Related/Office Equipment	8.43	0.3119
	Machine Drive	12.55	0.4644
	Electromechanical Processes	1.99	0.0738
	All Other Uses/Processes	28.59	1.0580
	Lighting	**7.35**	**0.2719**
	Combined Sectors Total	100	3.7

Annual Energy Review Data on Commercial, Industrial, and Residential Sector's End Use Energy Consumption's Distribution. Depicting the influence of each end use on these sectors and showing the influence of Lighting [84].

1.1.6 Aim of Thesis and Subsequent Chapters

With this rapid adoption of LEDs in the U.S. and their presence being a large percentage of the load on the grid, a better understanding of how LEDs impact the grid, and vice versa, is needed to ensure continued reliable operation of the electric grid. This thesis establishes an aggregate, component-based load model, for the purposes of characterization of the operation and affiliated effects which typical marketed LED lighting devices have when integrated within the U.S. power grid.

1.2 Thesis Outline

1.2.1 Chapter Two Overview

Chapter two provides a review of established literature pertaining to LEDs and load modeling. It begins with the portrayal of the previous research on the benefits and pitfalls of LEDs in operation and description of the underlying processes which take place in LED bulbs for the establishment of functionality. Historical evolution, adoption, and integration of LEDs is discussed, and the benefits of these devices are highlighted with direct comparison to competing illumination systems.

The various applications of LED-based lighting devices are further addressed along with the necessity of load modeling for these devices. Concepts associated with load modeling are described and previous research related to ZIP load modeling of LEDs observed with conclusions made for the necessity of component-based modeling of LED lighting devices.

Established systems at The University of Tennessee, are described in detail in an effort to describe the work being done to characterize complex systems, such as the power grid network. Grid emulation inspiration and associated implementation are depicted through the hardware

testbed interface. Associated drive for the inclusion of emerging technologies is given emphasis. Desire for load modeling of integrated devices within the power system is addressed and importance of LED bulb inclusion highlighted

1.2.2 Chapter Three Overview

Chapter three includes a description of the process employed in development of the component-based load model that best represents standard LED Bulbs. Study of the various iterations of available device implementation is addressed. Operational principles, associated with both the device and country-wide standards, are applied in comprehension of the LED bulb's inner-workings. Factors such as size, shape, illuminance, and power rating are included in description of the most prevalent LED bulb.

Study of lighting market trends further corroborates consumer preferences of manufactured LED lights. Comparison is made between popularly marketed devices and device-specific designs. Industry-standard design guides are correlated to device-specific modules in formulation of a load model that best represents a standard LED bulb. The component-based load model is chosen with power electronic topology design and component parameters explicitly defined.

1.2.3 Chapter Four Overview

Chapter four illustrates the testing procedure utilized in the laboratory for analysis of an LED bulb's behavioral response to ambient conditions. Equipment utilized and processes employed in establishing the laboratory test configuration are discussed. Data extraction techniques and compilation of measured data is expressed. Laboratory findings are provided with analysis of the characteristic exhibited.

Formulation of a simulated topology for testing of the component-based load model is highlighted with effort to emulate measured laboratory conditions. Behavior is recorded in

simulation software at synonymous test conditions to those visualized in laboratory testing. Results are provided for comparison to the laboratory DUT, in verification of the established model.

1.2.4 Chapter Five Overview

Chapter 5 provides an overview of dynamic characterization and the motivation behind investigation of load model dynamic response. Correlation is made to preexisting systems established in UTK's HTB grid emulator. In analysis of the LED bulb's component-based load model under dynamic conditions, a procedure was established in portrayal of the model's behavior under disturbances ranging in magnitude and duration.

Implementation techniques utilized in observation of this behavior are addressed with formulated simulation and results analyzed. The relationship between fault magnitude and duration to device operating behavior is explored. Potential effects of the device's dynamic response on grid operation are addressed through worst case load model profile. Dynamic characterization through load modeling is posed to provide an opportunity in preemptively addressing and mitigating failures of both system and device.

Adjustments of the dynamic test simulation of the load model are addressed, in the formulation of an interactive interface. Adaption of the simulated model is addressed in creation of a dashboard for interaction with the load model. Further, methodology in implementation of user controlled and induced disturbances for real-time visualization of dynamic load model response and device functionality is expressed.

Established systems at The University of Tennessee, are described in detail in an effort to describe the work being done to characterize complex systems, such as the power grid network. Grid emulation inspiration and associated implementation are depicted through the hardware testbed interface. Associated drive for the inclusion of emerging technologies is given emphasis.

Desire for load modeling of integrated devices within the power system is addressed and importance of LED bulb inclusion highlighted.

1.2.5 Chapter Six Overview

Chapter 6 provides a summary of this thesis and the main contributions provided by this research. In addition, some suggestions for future work, are addressed. Topics of study are suggested for future work with utilization of the work done within this thesis. Improved precision in grid emulation is posed through utilization and tuning of the established load model to the variety of marketed LED devices. Characterization of a wider dynamic disturbance range provides for the design of compensation technologies in attaining improved grid reliability. Further, work toward maintaining supply conditions for consistent operation of the device and affiliated grid technologies and the integration of the model within grid emulator systems is suggested.

CHAPTER 2
LITERATURE REVIEW

2.1 Light Emitting Diodes in Lighting Devices

2.1.1 Introduction of LEDs to the Lighting Industry

Optimization of energy usage in the production of light has been a mission for many since Thomas Edison's first incandescent lamp. In the present day, innovation arose with the use of semiconductors within LED lamps. Able to convert electrons to photons, LED lamps operate with proficiency across the visual spectrum. The LED illuminance range can produce any color including white light. The performance and efficiency of the LED lamp is outstanding in comparison to its lighting predecessors as seen in Table 6 in comparison to fluorescents [1], [3].

The use of LEDs for lighting has been a positive technological advancement. It is interesting to note that the emergence of the solid-state lighting (SSL) industry began with the invention of LEDs. Initially, fabrication costs related to the production of internal electrical components caused a delay in the adoption of SSL LEDs in the market. However, LED-based technologies spurred a developmental revolution with substantial profits. These diodes became critical within the global economy [1], [2].

2.1.2 Commercialization of Light Emitting Diodes

LEDs were first commercialized in the 1960s. Adopted as a high-tech alternative to incandescent, fluorescent, and CFL bulbs, LEDs saved both energy and costs. Presently, SSL LED bulbs are common in the consumer market and have reached attractive prices to users as illustrated in Table 7. LED manufacturers are producing state of the art diodes that innovate the lighting industry, through research and design to produce a vast array of commercial devices.

Table 6. Power Consumption in Area Study

Power	Fluorescent	LED
Total	2000 W (20 W * 100)	1200 W (12 W * 100)
Per Unit Area	6.0 W/m^2 (2000 W / 335.2 m^2)	3.6 W/m^2 (1200 W / 335.2 m^2)

Study of the Power Consumption and per unit area power consumption of fluorescent and LED lamps used in area lighting, illustrating the high efficiency of LED Lamps as opposed to competing lamps [3].

Table 7. 60-Month Period Lamp Cost Analysis

Type	Incandescent	Fluorescent	LED
No. of Lamps	1	1	1
Lamp Wattage (W)	60	18	12
Average Life (hrs)	1000	8000	35000
Burning Time (hrs/yr)	2688	2688	2688
Re-Lamping Cost (Rs)	80	1100	4500
Replacement Cost (Rs)	200	200	200
Electricity Cost (Rs/kWh)	9.5	9.5	9.5
CO_2 Emission Factor (CO_2/kWh)	0.5	0.5	0.5
Connected Load with Ballast (kW)	0.06	0.02	0.012
Operation over 60 Months (hrs)	13440	13440	13440
No. of Lamps Required over 60 Months	14	1.68	1
Lamp Replacement and Re-Lamping Cost (Rs)	3920	2600	0
Power Consumption over 60 Months (kWh)	806.4	268.8	161.28
Electricity Cost after 60 Months (LKR)	7660.8	2253.6	1532.16
Total Cost over 60 Months (LKR)	11580.8	4853.6	1532.16
CO_2 Emissions over 60 Months (kgCO_2)	403.2	134.4	80.64

Cost analysis of Incandescent, Fluorescent, and LED lamps over a period of 60 months which illustrates the cost effectiveness of LED lamps in comparison to other lamps, where costs, Rs, are measured in Indian Rupee and LKR signifies the cost in Sri Lankan Rupee [3].

Collaboration, in this regard, between scientific research and manufacture of a marketable device has led to several advancements in SSL LEDs [2], [3].

2.1.3 Applications and Benefits

LEDs have obtained favor due to their lower energy consumption over other innovations. It is important to note that energy consumption of LEDs is only one aspect of their usefulness. The quality of illumination is an important factor, but the benefits associated with energy savings, cost effectiveness, user's psychological health, and waste disposal are also integral in comprehensively determining their accolades, quantified through experimentation complete among 80 participants. Quantification of the study, illustrating preference of LED devices to fluorescent bulbs, is provided in Table 8 [3].

Due to technological advancements and continuous industrial growth, it is estimated that global energy consumption will increase by substantial margins. Consequently, it is essential to recognize the need for energy efficiency within devices. Such a device must be established for long term use and supply on a global level. Considering these factors, LEDs are an efficient and economical lighting source both on a commercial and residential plane.

With sizable applications which continue to flourish, LEDs have made and will continue to make an impact on the power industry. As such, the need for research surrounding their impending effect on the power grid is imminent. Load modeling of grid integrated technologies, such as LED lights, aids in the design, analysis, and control of complex power systems. Due to the LED light's widening range of applications, formulation of a load model, which accurately depicts device behavior within complex networks, is crucial [4].

Table 8. Survey of Human Response to Lamps

Score	Visibility		Mood Effect		Visual Comfort		Color Appearance		Work Performance		Preference to Stay	
	FL	LED	FL	LED	FL	LED	FL	LED	FL	LED	FL	LED
Very Poor	2	0	2	0	6	0	3	0	3	0	0	0
Not Bad	25	0	20	0	23	0	25	0	25	0	16	0
Good	47	5	53	8	50	7	51	3	47	3	58	8
Very Good	5	15	4	21	1	20	1	24	2	25	6	28
Great	1	60	1	51	0	53	0	53	3	52	0	44
Total	80	80	80	80	80	80	80	80	80	80	80	80

Survey of 80 participants illustrating the benefits and preference of LED lamps in comparison to fluorescent [3].

2.2 Power System Emulation

2.2.1 Load Modeling and Power Systems

Load modeling is a technique utilized by engineers to formulate a more comprehensive understanding of device behavior and operation within electric networks. The modeling of loads aids in the analysis of power systems providing controllability, stability, and management of increasingly complex designs. As power systems require a balance between energy generation and consumption, load modeling aids in the establishment of system equilibrium [5], [4].

The primary use of load modeling throughout various applications is the assessment of voltage and frequency stability. Additionally, power quality analysis throughout load classes may be established through the modeling of loads. A standard diagram depicting an aggregate model is visualized in Figure 13. Whether residential, industrial, or commercial, load analysis is integral in the modeling of power systems [4].

Briefly, a power system is a network of electrical components that include generation, transmission, distribution, and loads. A key element in power system design is emulation. The modeling of loads in connection with the system is key in system emulation. However, the calculations associated with load modeling are complex and complicated in derivation. Complications arise as load model derivation should account for all devices in the power system that are consuming electrical energy [7], [8].

2.2.2 Importance and Evolution of Testbed Emulation

For decades, older technologies have managed the electric grid. With the emphasis on energy conservation and emergence of newer digital electronics, upgrades are being made with the intention of making the electric grid a smarter system. Today, grid research has progressed, with

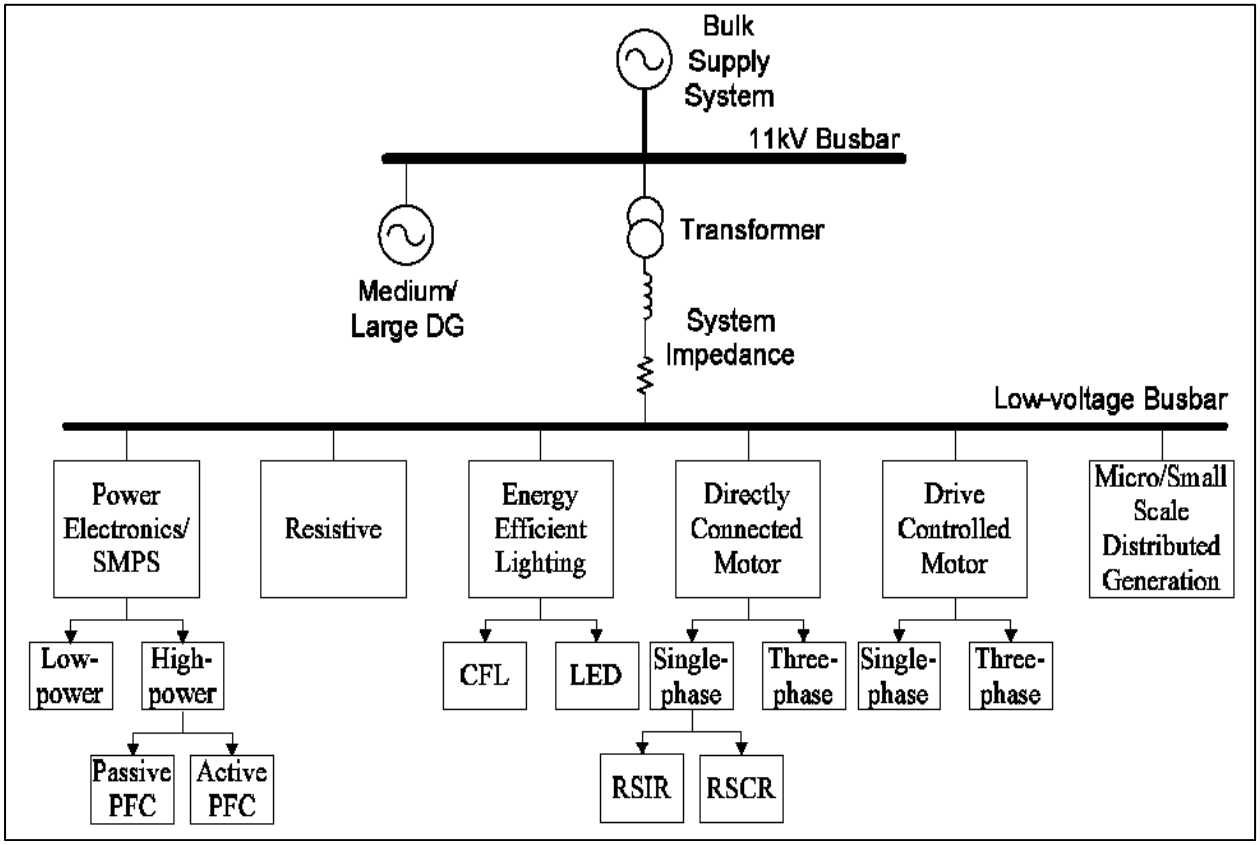

Figure 13. System Aggregate Model Diagram

Exemplary diagram of an aggregate system model which incorporates LED lighting [6].

with the ability to capture data and exchange actionable information in the evolution of grid architecture.

Rapidly emerging integrations within the grid are driving a need for improved characterization of affiliated devices. The integration of new technologies in the grid can result in unexpected outcomes when aggregated across the overarching power system. Testbeds provide a laboratory environment to model these changes within the power grid, without the risks associated in a live production setting. Testbeds have the ability to sample and measure different components and systems, through the incorporation of software, physical hardware, and network components [14].

2.2.3 The University of Tennessee Hardware Testbed

The University of Tennessee's College of Engineering has committed 16,000 ft^2 of space to a center that houses the Center for Ultra-Wide-Area Resilient Electric Energy Transmission Networks (CURENT). This center is home to an array of research areas, including the HTB, Large-scale System Testbed, FNET monitoring/ visualization lab, and affiliated power systems and power electronics lab facilities. The UTK testbed system provides for the monitoring and control of power electronic devices in the pursuit of knowledge surrounding these devices. The organization is dedicated to comprehensively characterizing the impact of power electronic devices on the power grid and the development of enabling technologies [15].

UTK's HTB is a platform which has been formulated through converter-based emulation for testing of the power grid. The platform models a real microgrid system with a topology that is simplified for testing of grid level scenarios. Conventional techniques of microgrid testing have relied upon the deployment of a physical system or the utilization of a hardware in the loop (HIL)

platform. Contrary to conventional testbed implementation, the HTB platform is a more cost effective, flexible, and efficient method of verification through control algorithms [14 - 15].

Praised for its superior operation, this platform has been formulated through methods proven to be more closely related to a real system when compared to HIL techniques. Alternate techniques neglect to incorporate factors, such as actual measurement error and communication time delay, which are included in the HTB platform. In this regard, implementation of the HTB is carried out through the programming of converters in emulation of power system component behavior [14], [16].

The UTK HTB includes both a hardware and large-scale testbed configuration. In the large-scale testbed, a real-time grid platform simulates the power grid. By doing so, it provides for the ability to effectively model disturbances throughout the grid. In addition to investigation of physical device behavior, the testbed also incorporates a communications layer. Within the communication layer, network-based communication devices and control methods are implemented.

Researchers within the organization have modeled the system in representation of the North American grid. Resizing of the model has been carried out, through the reduction of the system's dynamic model, for software simulation. In better representation of the future power grid, approximately 20% of power generation, within the HTB, was modeled as renewable resource-based generation.

Improvements to the system include the incorporation of an open-source simulator of the power system, additional renewable energy capacity, energy storage, and communications network emulation. Modules, within the established system, are connected through a communication network. A closed loop emulator, operating with an open-source power system simulator

(ANDES), permits the streaming of data in operation. By doing so, grid measurements within the testbed are obtained, with respect to raw simulation data. Further, UTK's in-house visualization platform, exhibited in Figure 14, provides an avenue for researchers to interact with parameters and switching algorithms, for control and analysis of the system, throughout various scenarios/conditions [14], [22 - 23].

Additionally, power electronic converters are utilized in the emulation of the electric grid. Researchers have formulated a system that fosters the ability to emulate bulk power grids, overseen by the Northeast Regional Power Coordinating Council (NERC) and Western Electricity Coordinating Council (WECC), depicted in Figure 15. In doing so, the high penetration of renewables and use of multi-terminal, high-voltage, direct current (HVDC) to move power over long distances has been investigated. The established system allows that converters can be programmed to emulate various, grid-based technologies, such as generators or loads, with a wide range of characteristics [14], [23].

Currently, UTK developed a variety of emulators, including wind generation, solar generation, three-phase loads, energy storage elements, transmission line emulators, faults emulation, synchronous generation, and a real-time interface that enables digital power system simulation. Established efforts for microgrid emulation, have been enacted in partnership with EPB Chattanooga, a regional electric utility. UTK has successfully utilized the established testbed in analysis of controllers prior to their implementation within the EPB system [14 - 15].

With the rapid emergence of new technologies, changes are happening that not only dramatically affect the power grid, but also the in-depth comprehension of grid in operation. Through tremendous upgrades in the ability of software to measure and report power grid changes, researchers are better equipped to understand how new technology, when aggregated, will affect

the power system. New hardware testbed platforms are being developed that link both the computational-based and physical world, with the ability to run technical and practical tests through algorithms, as illustrated within the HTB [6], [15].

2.2.4 Power Electronic and Load Modeling in Testbed Emulation

As America's electric demand continues to evolve, testbed systems, like UTK's HTB, will require continued adjustment in the accurate reflection the power grid's demand side input. As market trends indicate the surge in adoption of LED lightbulbs, these devices have redefined the global lighting industry demands. The operational efficiency associate with LED bulbs and their rapid integration throughout utility sectors has permanently changed the trajectory of power consumption through lighting. Thus, LED lamps have resulted in an aggregated change in load demand with significant impact to the power grid [6].

Due to the present and impending effects of LED lamps within the power grid, testbed systems require modification that includes monitoring and analysis of LED lighting throughout the system. Current testbed systems include the framework and architecture to support power system functions, but also offer the ability for additional layers for forecasting, visualization, analysis, and communications. Through the inclusion of an LED load model, data aggregation will more effectively portray power system operation [6], [14].

In this regard, the incorporation of the lighting device will further establish comprehension of not only power grid changes, but also the effects on the affiliated device's operation. Inclusion of the LED lamp load within the testbed platform will provide for device characterization that enables the simulation of grid scenarios with improved accuracy. Formulation of an LED Load model, in this regard, allows the plethora of LED lamps, presently utilized within the grid, to be incorporated within the system. By doing so, energy generation and demand may obtain improved

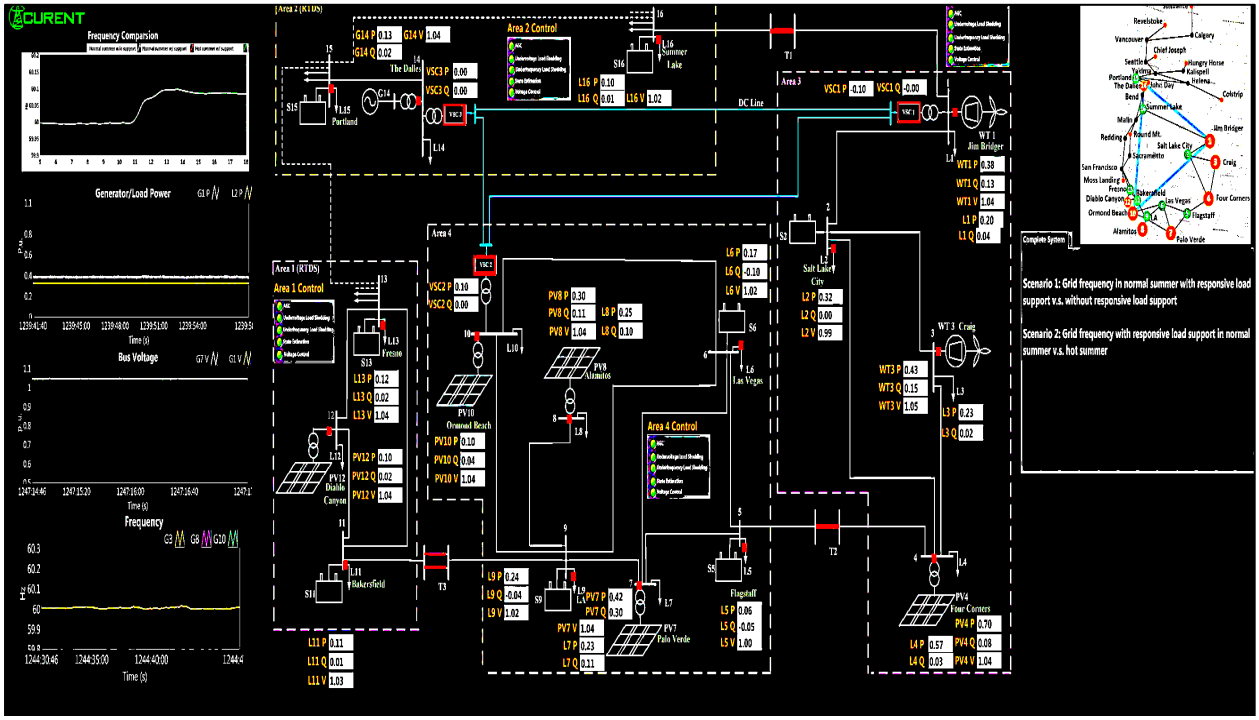

Figure 14. UTK HTB Visualization

Depiction of the HTB visualization located at UTK, allowing interactive control and analysis of the WECC Power Grid, including frequency test scenario, for analysis of responsive load support effects on the power system [22].

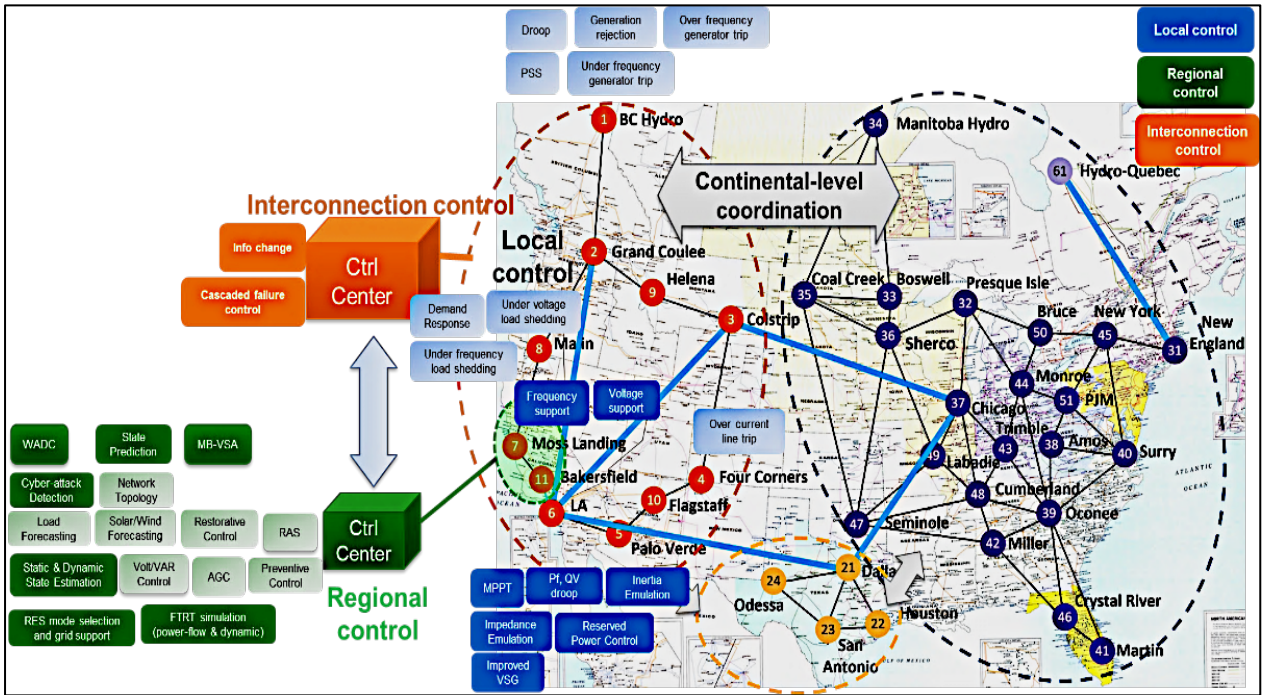

Figure 15. UTK HTB Regional Focus with Affiliated Methodology Overview

Visualization of the HTB system's established application regions, including the WECC and NERC, with synopsis of implementation avenues in representation [23].

balance, in real-time, without jeopardizing the reliability of the grid or the quality of device operation [1], [4], [6], [17].

2.3 Load Modeling

2.3.1 Comprehension Through Load Modeling

Across a large power system, it is difficult to accurately represent every individual power consuming device. Because of this, aggregate load models are used for the analysis of power systems. Load modeling helps in analyzing the performance of a power system. This process provides a mathematical representation of the relationship between power and voltage [8].

For the betterment of system performance, load models must be maintained to incorporate the emergence of new technologies. As electronic innovations arise, engineers employ modeling techniques to characterize their behavior as a load. By doing so, a simplistic mathematical representation is obtained for ease in application and analysis of the overall power systems [5].

By means of mathematical relation, an algebraic function is formulated through load modeling. This function works to define the instantaneous operating conditions of the device under analysis in conjunction with the system of integration. As such, respect is paid toward the input voltage magnitude and/or the frequency, which is affiliated with the system and load. It describes a prediction of the load behavior and operation under various supply conditions, including those where sudden changes in voltage and frequency occur.

This analytical representation is derived to express the power-voltage relationship associated with the load. Derivation of the mathematical model includes equations which incorporate the rated voltages *(V)*, rated frequency *(f)*, active power *(P)*, and reactive power *(Q)* values as shown in **(1)** and **(2)**. Formulation of this relationship provides a simplified approach to

achieve a comprehensive understanding of networked electronic devices, as seen in power systems.

$$\boldsymbol{P} = \mathbf{f}(\boldsymbol{V}, \boldsymbol{f}) \quad (1)$$

$$\boldsymbol{Q} = \mathbf{f}(\boldsymbol{V}, \boldsymbol{f}) \quad (2)$$

Building a reliable system requires the knowledge of these load characteristics, which may be achieved through the load modeling process. However, this process is complicated due to the large number of devices that are integrated within power systems. Variation of load types adds to the difficulty of device and system analysis. The struggle to derive an accurate load composition estimation is an added complexity when modeling loads. Each affiliated device must be observed in characterization of its response to changes in voltage, frequency, capacity, and duty cycle [4].

A typical aggregated load demand model will have load classes that include residential, commercial, and industrial demand, as shown in Figure 16. Industrial demand is more challenging due to the diversity of equipment required and comprehension of load demands. For this reason, large industrial loads may need to be individually modelled. Residential and commercial load demands can be better represented by standard aggregate load models [6].

Conventional techniques of load modeling aim to describe this relationship between power and voltage within the tested device through mathematical analysis. Load modeling provides knowledge on the operation of a device under a range of conditions. As a result, device performance, when used in connection with preexisting electronic systems, is better understood.

Insight on the power-voltage relationship allows for the mitigation of potential failures within the overall power grid. Load modeling allows for increased stability within the entire system to be achieved. Fundamentally, the process of load modeling begins with determination of the variety of load. Identification of the load variety relies upon the device's operational behavior, which is categorized as either static or dynamic in nature [5].

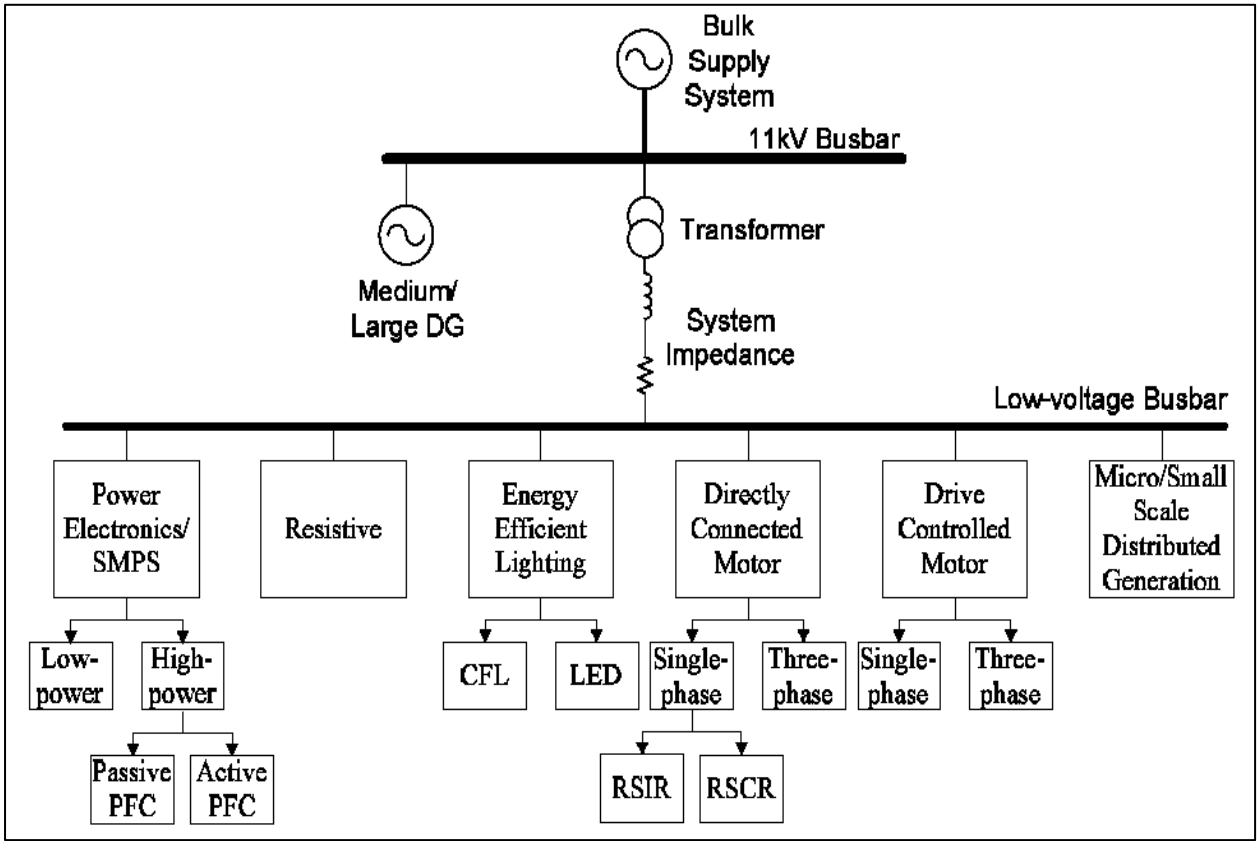

Figure 16. System Aggregate Model Diagram

Exemplary diagram of an aggregate system model which incorporates LED lighting [6].

2.3.2 Characterization of Load Type

Static loads are fixed, continuous loads that have minimal variation over short time intervals. They are time-independent models that show load behavior in a constant state and can be represented by a mathematical relationship that is based on voltage dependency. Static load modeling references the instantaneous operating conditions of the device in characterization as a load. This steady state analysis is subject to vary with input voltage. While static loads are easily characterized during and after a load disturbance, representation becomes difficult under voltage collapse.

On the other hand, dynamic loads describe those with rapidly changing behavior. Dynamic loads give detailed representation of the voltage stability characteristics of a device. They are separated into classifications according to the effect that voltage has on the load. Dynamic loads are inherently more complex due to their fast response to voltage and frequency variations.

Dynamic loads demonstrate an active-reactive power relationship as a function of voltage and time, while static loads' behavior is inherently steady state and time-independent. Loads categorized as dynamic show variations in response based upon external operating conditions. As a result, dynamic load models provide insightful voltage stability analysis [4].

Following the determination of load type, various techniques may be employed to identify the parameters of the load model. Identification of the load model parameters allows for a simple mathematical representation of the device to be established. This analytical simplification aids in a device's successful integration within more complex systems. Derivation of load model parameters may be completed through either real-time measurement or electrical component analysis [5].

2.3.3 Methodology of Load Modeling

Measurement-based load modeling is implemented through the real-time data analysis of device behavior during laboratory testing. Advantageous for its emphasis on the physical device's response during testing, this technique is easily applied to a wide variety of loads. Despite praise for the method's versatility, measurement-based modeling is an estimation of the load parameters at conditions specified during testing. As a result, measurement-based load models are not beneficial in application within systems operating outside of those tested during data acquisition.

Additional work toward the measurement-based technique incorporates the use of Artificial Neural Networks (ANNs) to more accurately model devices as loads. ANNs work toward analyzing the relationship between a device's measured input and output conditions. Input-Output dataset analysis allows ANNs to optimize measurement-based load model parameters. A simplified visualization of the ANN structure which takes measurements as input data and outputs an estimated load model is provided in Figure 17.

ANNs formulate load models with better representation of device behavior. The positive impact of ANNs on load modeling is reliant upon the collection of measured data in large quantities. In accordance with sizable statistics, the ANN's computational ability must meet the respective processing requirements to estimate an accurate load model. While praised for the optimization of load parameters, ANNs do not establish a universal load model for integration. Rather, ANN load models are specified for the singular system in which data is collected.

Measurement-based load modeling works to formulate a simplistic mathematical representation of data acquired on device operation. From the gathered measurements, an equation is derived which best represents the estimated behavior of the device during testing. Research of this method has determined several common equations which sufficiently model a variety of

devices in the market. Of these mathematical models, selection of representation is determined based upon optimal fit for depicting device behavior.

Static models are one example of a prevalent mathematical representation. Devices best fit to a static model exhibit an active-reactive power relationship over time that depends on input voltage and frequency. Models with this static behavior often portray resistive type loads. However, static models may also be used to approximate dynamic loads, such as induction motors. When applied for the approximation of dynamic loads, the static model is not considered to be precise [5].

2.3.4 Behavioral Characteristics of Load Models

Static models can be classified as one of three general behavior-based models: constant impedance *($Z_{p,q}$)*, constant current *($I_{p,q}$)*, or constant power load models *($P_{p,q}$)*. These behavioral types are separated as a standard representation describing how the device responds. Behavior in this nature is easily observable during testing. As such, behavioral categorization provides a simplified model for load expression.

Constant impedance models are observed to have a relationship between active *(P)* and reactive power *(Q)* as a function of the squared voltage magnitude with model-based constant impedance coefficient, referenced in **(3)** and **(4).** They may also be referred to as the admittance models. This behavioral type is easily observable as a parabolic trend between active and reactive power with dependency on the voltage condition, depicted in Figure 18.

$$\boldsymbol{P} = \mathbf{f}(\boldsymbol{Z_p}, \boldsymbol{V^2}) \quad \textbf{(3)}$$

$$\boldsymbol{Q} = \mathbf{f}(\boldsymbol{Z_q}, \boldsymbol{V^2}) \quad \textbf{(4)}$$

Similarly, constant current models are representative of an active-reactive power relationship. However, this relationship is observed to vary with voltage magnitude and incorporate a model-based constant current coefficient, shown in **(5)** and **(6)**. Constant current type

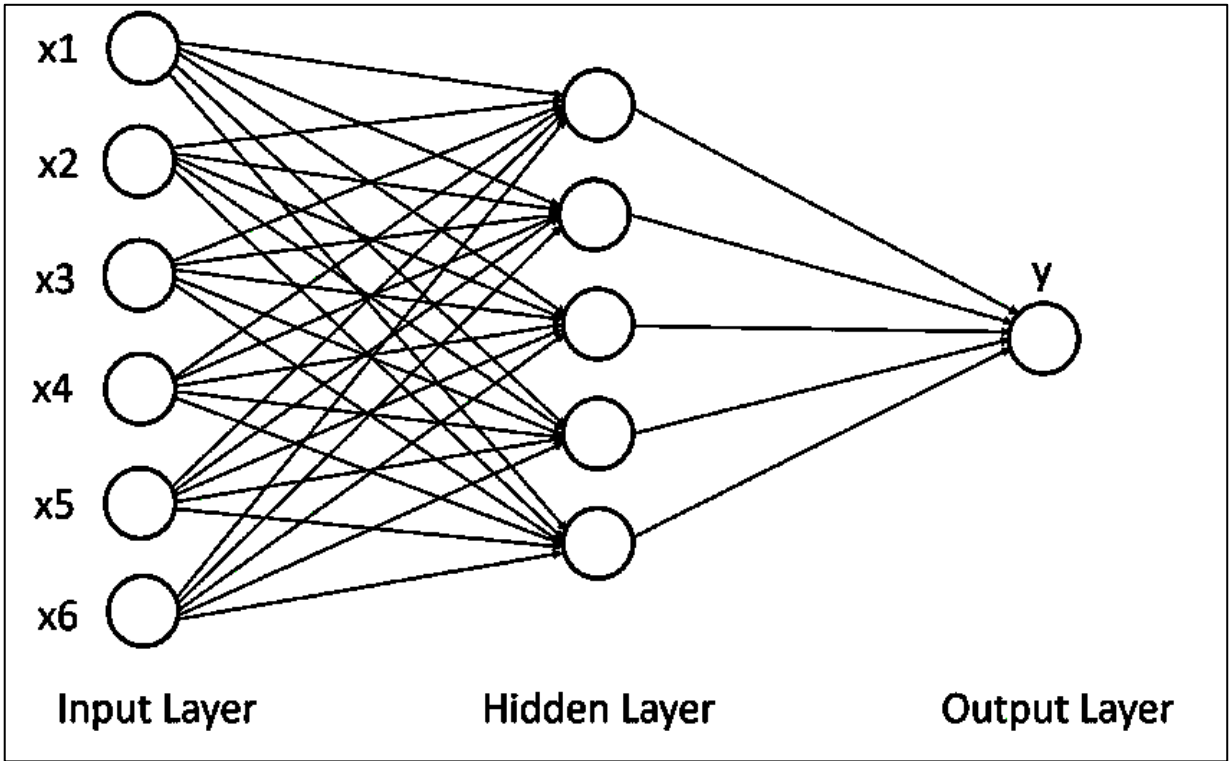

Figure 17. Measurement-Based Artificial Neural Network Structure

Simplified diagram of an Artificial Neural Network (ANN) used for improved estimation of load models. Input layer signifies the input measured data acquired during testing and the output layer signifies the ANN approximated load model [11].

loads are distinguished by a linear relationship that is dependent upon the input voltage condition as shown in Figure 18.

$$\boldsymbol{P} = \mathbf{f}(\boldsymbol{I_p}, \boldsymbol{V}) \quad (5)$$

$$\boldsymbol{Q} = \mathbf{f}(\boldsymbol{I_q}, \boldsymbol{V}) \quad (6)$$

Lastly, static models may behave as a constant power load. Often referred to as a constant PQ or MVA load model, this model describes a load that draws constant active and reactive power without correlation to voltage magnitude, exhibited in **(7)** and **(8)**. Graphical visualization of this relationship is depicted through a horizontal, constant value regardless of input voltage condition, visualized in Figure 18 [4].

$$\boldsymbol{P} = \mathbf{f}(\boldsymbol{P_p}) \quad (7)$$

$$\boldsymbol{Q} = \mathbf{f}(\boldsymbol{P_q}) \quad (8)$$

Commonly utilized for characterization of both static and dynamic loads is the ZIP model. ZIP models use a polynomial fit to exhibit the relationship between device power and voltage. The polynomial function incorporates estimated coefficients which correspond to the device's intrinsic electrical properties during tested operation. These ZIP model parameters include the approximate device impedance *($Z_{p,q}$)*, current *($I_{p,q}$)*, and power *($P_{p,q}$)* constants. The ZIP model operates as a function of voltage and is a summation of the constant models, with incorporation of the device's nominal power *(P_o, Q_o)* and nominal voltage *(V_o)* ratings, modeled in **(9)** and **(10)** [5].

$$\boldsymbol{P} = \boldsymbol{P_o}(\boldsymbol{Z_p}\left(\frac{\boldsymbol{V}}{\boldsymbol{V_o}}\right)^2 + \boldsymbol{I_p}(\frac{\boldsymbol{V}}{\boldsymbol{V_o}}) + \boldsymbol{P_p}) \quad (9)$$

$$\boldsymbol{Q} = \boldsymbol{Q_o}(\boldsymbol{Z_q}\left(\frac{\boldsymbol{V}}{\boldsymbol{V_o}}\right)^2 + \boldsymbol{I_q}(\frac{\boldsymbol{V}}{\boldsymbol{V_o}}) + \boldsymbol{P_q}) \quad (10)$$

It is common to represent large, aggregated loads as a combination of these three and is referred to as a ZIP load where the percentage of Z, I, and P add up to 100%, indicated in **(11)**. These ZIP coefficients work toward characterization of a load that behaves with constant impedance, constant current, and constant power static response. They are used to represent device

power consumption as a function of voltage. This model provides better matching to non-linear load characteristics. In conjunction with the three parameters of the ZIP model, there is the phase angle-based ZIP model [4], [6].

$$\mathbf{1} = \left|\boldsymbol{Z_{p,q}} + \boldsymbol{I_{p,q}} + \boldsymbol{P_{p,q}}\right| \quad \textbf{(11)}$$

Ohm's Law, provided in **(12)**, acts to describe the relationship between voltage and current throughout a resistive load *(R)*. Continuation of this fundamental principle allows for the calculation of power throughout the resistive load, as seen in **(13)**. Thus, purely resistive, constant loads are theorized to operate entirely through the consumption of active power *(P)*.

$$\boldsymbol{V = IR} \quad \textbf{(12)}$$

$$\boldsymbol{P = VI = V^2R = I^2R} \quad \textbf{(13)}$$

In application to real-time circuits, the instantaneous voltage *(v)* and current *(i)* conditions operate as a function of time *(t)*. These components can be portrayed through wave equation, represented in **(14)** through **(16)**. These analytical representations incorporate angular frequency *(ω)*, with respect to operational frequency *(f)*, peak voltage/current *(V_m / I_m),* and phase delay from a standard sinusoid *($\theta_{v,i}$)*, which can be applied within Ohm's Law for the derivation of instantaneous power *(p)*, shown in **(17)**.

$$\boldsymbol{v(t) = V_m \sin(\omega t + \theta_v)} \quad \textbf{(14)}$$

$$\boldsymbol{i(t) = I_m \sin(\omega t + \theta_i)} \quad \textbf{(15)}$$

$$\boldsymbol{\omega = 2\pi f} \quad \textbf{(16)}$$

$$\boldsymbol{p(t) = v(t) * i(t)} \quad \textbf{(17)}$$

In connection with Ohm's Law, purely resistive loads exhibit current and voltage waveforms that operate in-phase, with respective component's phase delays equivalent. However, this equivalence is not universal to all load types. As a result, when the difference in phase delays of each component *(ϕ),* depicted in **(18)**, is not equivalent to zero, the expression for real power

becomes **(19)**, through application of trigonometric identity simplification, with an additional reactive power component *(Q)* present within the circuit, depicted in **(20)**.

$$\boldsymbol{\phi = \theta_v - \theta_i} \quad \textbf{(18)}$$

$$\boldsymbol{P = \frac{V_m I_m}{2} \cos(\phi)} \quad \textbf{(19)}$$

$$\boldsymbol{Q = \frac{V_m I_m}{2} \sin(\phi)} \quad \textbf{(20)}$$

The term 'reactive' is used to describe power that flows bidirectionally from load to source. This category of power does not actively contribute to work done within the system. Reactive power becomes applicable when voltage and current waveforms, within a circuit, are out of phase with each other. In opposition to the purely resistive load, purely inductive loads are characterized as those which solely consume reactive power. Purely inductive loads depict a phase delay difference equivalent to **(21)**. Whereas purely capacitive loads depict a phase delay difference equivalent to **(22)** and generate reactive power [12], [18], [20].

$$\boldsymbol{\phi = \theta_v - \theta_i = 90°} \quad \textbf{(21)}$$

$$\boldsymbol{\phi = \theta_v - \theta_i = -90°} \quad \textbf{(22)}$$

Comprehension, of these principles, aids in the categorization of load characteristics when applied to the ZIP model. When the sum is of the ZIP model coefficients is negative this indicates a load which primarily depicts capacitive behavior. Likewise, a positive sum is reflective of a load which primarily functions in an inductive nature [12].

As LEDs operate similarly to an ideal diode, where current flow is permitted through the component, in source to load orientation, when instantaneous voltage is greater than the LED's intrinsic threshold voltage. In optimization of an LEDs light production, front end rectifiers are often used in conjunction with the device. The front-end rectifier acts to adjust the passage of the voltage source so a positive orientation is maintained at the LED, illustrated in Figure 19. Thus, the LED is host to active and reactive power characteristics which is neither purely resistive,

inductive, or capacitive in nature. Thus, load modeling such as that which is obtained through the ZIP model aids in characterization [19].

Another analytical variation of the ZIP model is the phase angle-based ZIP model. The phase angle-based ZIP model is representative of the active-reactive power relationship as a function of the load component phase angle at each voltage level. This relationship is exhibited in **(23)** and **(24)**, including terminal voltage *(V_a),* apparent power *(S_o),* calculated in **(25)**, and fraction of load characterized by constant ZIP parameter *($Z_{\%}$, $I_{\%}$, $P_{\%}$)*. Incorporation of the correlation between component phase angles allows for the calculation of active and reactive power through ZIP modeling. However, the derivation of an accurate ZIP model affects its applicability in analysis [4].

$$\boldsymbol{P = \frac{V_a^2}{V_o^2} S_o Z_{\%} \cos(Z_\theta) + \frac{V_a}{V_o} S_o I_{\%} \cos(I_\theta) + S_o P_{\%} \cos(P_\theta)} \quad \textbf{(23)}$$

$$\boldsymbol{P = \frac{V_a^2}{V_o^2} S_o Z_{\%} \sin(Z_\theta) + \frac{V_a}{V_o} S_o I_{\%} \sin(I_\theta) + S_o P_{\%} \sin(P_\theta)} \quad \textbf{(24)}$$

$$\boldsymbol{S = \frac{V_m I_m}{2} = \sqrt{P^2 + Q^2}} \quad \textbf{(25)}$$

Similarly, the exponential load model is another mathematical representation, which describes the relationship between device voltage and power, shown in **(26)** and **(27)**. In the format of an exponential equation, the exponential model is often utilized in characterization of mixed variety loads. This model incorporates an exponential coefficient *($n_{p,q}$)*, which is equivalent to 2, 1, or 0, in depiction of a constant impedance, current, and power loads respectively. Mixed variety load modeling refers to devices which may include static and dynamic components, such as induction motors.

$$\boldsymbol{P = P_o (\frac{V}{V_o})^{n_p}} \quad \textbf{(26)}$$

$$\boldsymbol{Q = Q_o (\frac{V}{V_o})^{n_q}} \quad \textbf{(27)}$$

The exponential model provides ease in derivation, as it incorporates fewer load parameters in comparison to the ZIP model. This model also holds potential for simple transition to the ZIP model with the inclusion of additional load parameters. Like the ZIP model, frequency changes within the system are eliminated by the exponential model to represent loads with negligible response to frequency variation [5], [4].

Derivation of a third analytical load type, known as the frequency dependent model (FD), may be achieved from both the ZIP and exponential model. The FD model takes the product of the ZIP and exponential models by a factor which corresponds to system frequency *(f_F)*, shown in **(28)**. Incorporation of the frequency factor, within the FD model, highlights an additional relationship between the intrinsic frequency dependence of the device *(k_f),* nominal frequency *(f_o),* and load frequency *(f)* in device characterization.

$$\boldsymbol{f_F = 1 + k_f(f - f_o)} \qquad \textbf{(28)}$$

These common mathematical representations of load models are advantageous due to their basis upon data acquired through real-time testing, depicting the electrical relationships of a device during operation, with ease in comprehension. Reflecting the location of device integration within a system, these measurement-based models offer a generic method that is easily applied to a range of loads. These established methodologies forgo the need for research on device composition, as knowledge surrounding the device's physical electrical configuration is not guaranteed in availability. In such cases, where device design is unknown, these measurement-based models are employed [5].

2.3.5 Basis of Modeling

Insight on the LED bulb's operational behavior is obtained through the modeling of the device as a load. In doing so, the intrinsic characteristics associated with the device are defined for

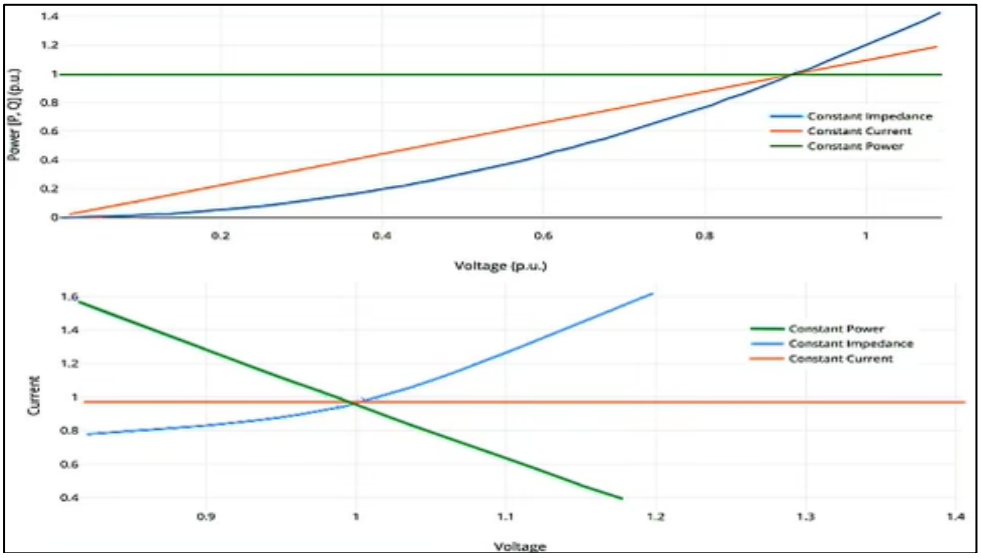

Figure 18. Constant Load Behavior Graphical Representation

Visualization of constant load behavior on P-V plot (top) and I-V plot (bottom).

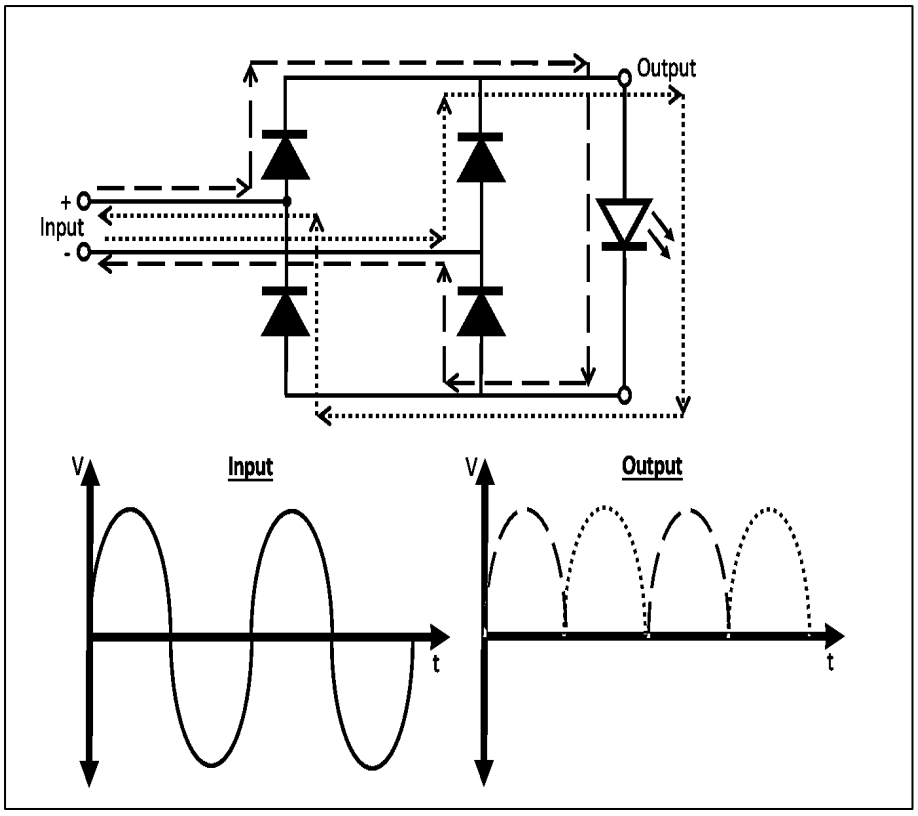

Figure 19. Rectifier Voltage Diagram

Visualization of rectifier circuit and the resultant voltage waveform established with ac voltage input signal and loop orientation highlighted.

portrayal. Modeling, in this regard, permits application within the affiliated system for analysis of not only the apparatus, but also the ambient network. Methodologies include measurement-based and component-based techniques, in the formulation of an accurate load model for device characterization.

Accuracy, in the portrayal of device behavior through load modeling, directly corresponds to the modeling approach employed. Formulation of a load model is an inherently complex task. Methodologies, in formulation and representation of the device as a load, are employed with respect to end-use application, means of establishment, and device specific characteristics. Additionally, determination of a measurement or component-based approach of load modeling relies upon the technique's inherent benefits and pitfalls, some of which are outlined in Table 9 [4 - 6].

2.3.6 Measurement Based Modeling

Measurement-based models are formulated with a data driven approach. They are derived through a modeling technique which aims to identify load parameters mathematically. Datasets are obtained through observance of the changes in device active and reactive power changes resulting from applied voltage and frequency. These changes are recorded for analysis through either intentional lab testing or natural power system monitoring. As such, the means of data is collected, for the purpose of load modeling, must be considered. Once the data is obtained, the load model is derived and validated [4].

While simplistic in procurement, measurement-based models pose potential risks in application. Failure to model device behavior may occur at operating conditions outside of those included in input data. Measurement-based methods act as a mere snapshot of device behavior through a tested duration of time in a defined location. As a result, their potential for successful

Table 9. Measurement vs Component-Based Load Modeling Approach

Technique	Advantages	Disadvantages
Measurement-Based	- Based on data from actual systems. - Provide accurate models for measured locations and time. - A generic method that can be applied to various models. - No need to have deep understanding of loads.	- Unable to account for different operation conditions. - Models are developed using data measured in certain periods at specific locations, which lacks generalizability. - Measurements with large disturbances are hard to obtain.
Component-Based	- Field measurement is not required. - Physical representation of end-use devices. - Can be applied to different operation conditions. - Demand side management is considered.	- Requires characteristics of individual load components. - Accurate and comprehensive load composition information is difficult to obtain. - Device specific. Model is not an adaptive procedure for modeling of other devices.

A comparison of the attributes and shortcomings associated with the measurement and component-based load modeling techniques in application and accurate characterization of a device [5].

application within a system is narrow because of uncertainty in how well a measurement-based model can be extended to other systems or even for different operating conditions within the same system.

In addition to the narrow range of applications for measurement-based models, accuracy in modeling is difficult to achieve. Accurate characterization of device behavior during large system disturbances proves problematic. Acquisition of data, which describes device response to the variety of potential grid disturbances, is an insurmountable process. Consequently, failure to incorporate device response to these disturbances can negatively affect overall power system performance [5].

With respect to disadvantages, the measurement-based approach is criticized for having less accuracy in modeling large disturbance operations and cannot be generalized, due to being performed for a specified operating condition. As such, these models provide little flexibility in application. They offer no clear understanding of the actual load composition, which is subject to modeling. The developed model is inherently specific to the measurement location, conditions, and time, making measurement-based models inapplicable within extraneous systems [4], [6].

The measurement-based approach is generally not the approach of choice in application due to the costs associated with data procurement along with the difficulty of characterizing load response. Characterization difficulty arises due to the vast potential of variations that might occur within the system, such as the effects of seasonal change on load response. Issues are observed with measurement devices and grid level events where changes in voltage and frequency do not act continuously. As modeling requires a prominent definition of voltage and frequency behavior, the measurement-based approach consequently becomes less advantageous. Component-based load modeling techniques mitigate some of these concerns [4], [1].

2.3.7 Component-Based Load Modeling

Component-based load models focus on the electronic configuration of the device under analysis. Implementation of the component-based model requires extensive research surrounding the load characteristics of the device. Analytical analysis on power electronics associated with the device must be carried out. Eliminating the need for field measurement, component-based models precisely illustrate the physical composition of the device. As a result, the derived load model is considered universally applicable across systems and operating conditions. They additionally account for the demands associated with and management of the device's operation [1].

The component-based approach begins with analysis of the load components which are connected to the system. Aggregate component-based load models are developed incrementally in emulation of networked power systems. Loads are categorized within either industrial, commercial, and residential classes. Data acquisition on the individual components, which the load is composed of, and the identification of load class are used to develop component-based load models.

Component-based load models are considerably more adaptable than measurement-based methodologies. They can represent both static and dynamic characteristics associated with complex loads. To do so in an accurate manner, this approach requires extensive knowledge of the load composition. Additionally, the percent power consumption of each load component must be addressed in the formulation of the load model.

The benefit of the component-based approach is that field measurement is not required for application in the approach. As a result, this method is more cost-effective with easier application. It can be used to model both steady-state and dynamic conditions of operation in representation of device characteristics that are connected to the power system. The main disadvantage of the

component-based approach is the requirement of individual characteristics of load components for modeling. It is often difficult to get a complete composition of the load, along with its inability to adjust to the integration of modern loads whose behavior is different from previous historical loads [4].

Despite the many accolades associated with component-based models, disadvantages arise due to the requirement of individual load component behaviors within the device. This methodology of load modeling is dependent upon the in-depth comprehension of the device configuration. Thus, the model becomes inherently device specific, lacking simplicity in adaptation to newly emerging technologies, such as LED lights [1].

2.4 Load Modeling of LED Lamps

2.4.1 Determination of LED Load Type

When examining LED bulbs, the extremely high efficiency of this new technology compared to other earlier forms of lighting is apparent. Due to this, the establishment of a load model to depict this innovation is vital. To start the discussion, we must understand some simple mechanics. First, we acknowledge that a load is any device powered by an electrical circuit. The term has been derived from the load put on the circuit from the current demanded for operation of the device.

Loads can be broken down into different groups based upon their output behavior. Load groups may be categorized inherently as inductive, resistive, or capacitive in nature. Likewise, electrical components can be separated within these groups based upon their typical output response.

Previous research has drawn the conclusion that because incandescent light bulbs are resistive loads then LED bulbs must also be primarily resistive. LED lights are driven by conversion of input AC to DC in illumination of the incorporated diodes. They have been considered resistive in previous load models as they rely on active power to function. However, this is not an accurate assumption.

Because LEDs do not generate heat for the purpose of light production, this assumption is inherently flawed. When compared to incandescent lights, LED's lamps are not completely resistive loads. LED lights incorporate power electronic converters which are composed of capacitive, inductive, and switching elements. As such, characterization of this device becomes more complex than estimation of a nearly resistive power factor based upon previous bulbs [10].

2.4.2 Existing LED Load Modeling

Previously, researchers have pursued a measurement-based approach when modeling LED lights. LED lights have had various forms of ZIP coefficient representation. Previous determination of the ZIP parameters for an LED lighting load provided the ability to approximate the behavioral response of the device at measured conditions. Additionally, the ZIP model has provided generalized insight into the effects of LED usage within affiliated electrical distribution systems.

Determination of established LED ZIP load models have been accomplished through data acquisition. Measurements utilized in previous LED modeling only included the operational range specified by device manufacturers. Past findings have claimed that the characterization of LED load type is dependent upon input voltage conditions, but primarily fell within the constant power model. Inconclusive determination of load type and confined operational range during testing has

led to concerns about the accuracy of these LED ZIP load models, especially as new technologies emerge.

LED lights have had technological innovation throughout their development lifespan. As such, these measurement techniques must be maintained and kept up to date. Accurate ZIP model parameters must reflect LED devices throughout the market. As time progresses, previously obtained LED ZIP models become increasingly inapplicable, as newly efficient methods of implementation emerge within the power electronic industry. Thus, researchers across the globe work to maintain LED ZIP models to reflect emerging technologies within the grid.

The most recent work found on LED ZIP load models was formulated from laboratory tested datasets. Corresponding measurements neglected the characterization of device behavior during grid level transient events. Data acquired during this testing has been completed within a conservative range which only reflected the device's rated operating conditions. From the acquired data, an estimation of ZIP load parameters had been established.

Parametric results obtained within the study portrayed device behavior as a simplified polynomial expression with inclusion of a caveat regarding accuracy. Emphasis had been drawn toward the inaccuracy of the ZIP load model for LED reactive power analysis. In addition, there has been discussion regarding the contingency of the ZIP load model's effectiveness in relation to the device's power rating.

Despite these concerns, previous findings have been beneficial in characterizing the effect of input voltage on device illumination and power consumption. However, it was explained that this operational behavior was not universal in representation across various LED devices. As such, this earlier LED ZIP Load Model still contained a substantial margin of error in application.

2.4.3 LED Lamp ZIP Load Model

Prior research, put forth in an effort toward characterization of LED lamp behavior, has employed measurement-based techniques to formulate the device's load model. The developed load model was estimated through the application of laboratory-acquired data to the measurement-based ZIP analytical model. In implementation, prior research employed a laboratory test procedure that involved the ramping of applied power supply voltage to the bulb.

Data logging occurred at each operating condition and included the input voltage, current, and power of the device under test (DUT) at each input scenario. Following the acquisition of data, as described, measurements were analyzed and applied to the ZIP analytical model, in characterization of the device as a load. The established ZIP parameters in this research are tabulated in Table 10.

The methodology utilized in derivation of LED ZIP model parameters was proven advantageous for the corresponding study's application. However, the formulated analytical model was device specific and did not provide a general model to depict behavior of LED bulbs as a whole. Additionally, procurement of data was completed at steady-state operating conditions.

In doing so, the dynamic response of the bulb was not illustrated in measurements. Accuracy of measurement-based load models is limited to the conditions which testing exhibits. As a result, the established ZIP model would not encompass the device's transient response throughout the array of potential grid scenarios [4].

2.4.4 Future LED Load Modeling

In the future, consideration can be given to merging both the component-based and measurement-based approaches of load modeling. Utilizing load signatures, attention can be paid

Table 10. Established LED Bulb ZIP Model Parameters

Brand	Power Rating (W)	Z_p	I_p	P_p	Z_q	I_q	P_q
EcoSmart	5.5	-1.43	3.90	-1.11	0.74	-1.96	0.25
GE	9	-22.51	45.82	-22.26	23.25	-47.48	22.95
EcoSmart	9	-6.81	16.27	-8.26	5.24	-12.84	6.54
EcoSmart	9	-9.11	20.71	-10.55	10.30	-23.21	11.86
Great Value	9	-5.65	14.46	-7.96	0.38	-4.43	3.10
EcoSmart	9.5	-8.36	18.43	-9.03	8.95	-18.42	8.35
Cree	10	2.33	-4.07	2.68	-9.46	16.61	-8.28
Great value	12.5	-5.85	15.47	-8.38	2.66	-8.83	5.15
GE	13	-1.47	3.27	-0.81	0.27	-2.21	0.87
EcoSmart	13	-13.92	29.35	-14.44	12.28	-26.38	13.03
Sylvania	14	0.00	0.00	1.00	0.00	-0.39	-0.56
Great Value	14	0.00	0.00	0.94	-1.25	2.05	-1.79
Feit Electric	15	-10.92	24.84	-12.93	8.74	-20.09	10.42
EcoSmart	15.5	-10.21	22.05	-10.81	10.45	-21.11	9.57
Feit Electric	17.5	0.00	0.00	1.00	1.60	-4.36	1.84
Sylvania	22	-1.11	1.95	0.11	0.52	-1.38	-0.05
Feit Electric	28	0.00	0.00	1.00	12.72	-26.94	13.20

ZIP model parameters of the associated LED bulbs that has been deduced in prior research and testing of the affiliated device behavior at steady-state operation [4].

toward incremental load characteristic analysis. As such, an understanding of load composition may be established from data recorded and a model formed [4].

2.5 Project Description

Work exhibited in this thesis outlines a proposed LED load model for analysis. It aims to formulate a component-based model to be applied in representation of common LED lighting devices on the market. This power electronic schematic is formulated with intent to be generalized. Thus, this component-based model is designed with the objective of flexible applicability.

Intention is to provide a more accurate load model for analysis of conventional commercial and residential LED bulbs. This model, in turn, provides for vast potential in application. Component-based modeling, in this nature, formulates an inclusive representation of current LED devices in use. Generalized, the model provides comprehensive understanding of LED bulbs as a load. As such, the integration of LED lighting loads within power systems may be addressed in present and future work.

2.6 Contributions and Organization

This thesis works towards developing CURENT technologies through modeling, analysis, and HTB system integration of LED light bulbs as a component-based load model. The inclusion of LED lighting as a load within the wide area grid benefits operation and distribution of renewable power within power systems. Incorporation of the affiliated power electronic interfaced load model results in increased reliability of grid performance. Throughout the past decade, concepts such as this have been implemented to demonstrate CURENT's technological innovation.

With the relevant literature in mind, this thesis establishes a comprehensive component-based load model of LED light bulbs for the purpose of analysis and integration within CURENT system HTB, which has been refined over the span of 10 years. The grid models developed and implemented in the HTB have been designed with the intent to assess the effectiveness of the technologies for future grid application.

Similarly, characterization of LED light bulbs as a grid level load model provides insight on the reliability of the device, throughout the continent, for commercial and residential use. Through testing of various scenarios, a more profound understanding surrounding the operational conditions of a standard LED light bulb may be characterized in greater detail, with this accomplished by means of a universally applicable component-based load model of a broadly used LED light bulb in the consumer market.

To demonstrate the load modeling accomplishments of CURENT technologies affiliated with the HTB, much work has been completed by researchers within the organization. Including load emulation of devices which behave with both static and dynamic characteristics. Static and dynamic load emulation has been utilized to mimic real power flow within the HTB system.

Previous work made use of the constant impedance, current, and power (ZIP) model to emulate a static load, while a three-phase induction motor is utilized to emulate dynamic loads. In addition, investigations of the load characteristics affiliated with data centers have been completed with discussion of the effects posed on the power grid through power electronic analysis. Following this work, power emulation of these findings within the HTB regional network was completed, which provides insight on voltage sag events due to their incorporation within the grid as a load.

In entirety, the HTB has been formulated to illustrate the system which is the power grid. Work put forth toward the HTB has provided for the interfacing and further analysis of the complexities which contribute to the overall function of the grid in real time. These complexities include, and are not limited to, that of load modeling [14], [16 - 17].

2.7 Future Applications

In the future, the HTB will continue to focus on the modeling of various loads with respect to the power grid such as that which is proposed within this thesis, through the integration of a LED light bulb load model. HTB will also focus on the effect of including more specific varieties of load models for devices consuming power on the grid as investigated through component-based load modeling within this work. Investigation throughout this research explains component-based analysis for future modeling of emerging technologies. In addition, this work pertains to not only the grid, but also the performance of the device itself during operation within a wide range of scenarios to be tested within the HTB.

The implementation and demonstration of load modeling within CURENT technologies on the HTB additionally enables utility members and vendors to utilize the state-of-the-art technologies developed by CURENT with a more comprehensive understanding of how the grid operates for informed administration.

2.8 Chapter Two Summary

Throughout this chapter, a review of preexisting research was conducted, for the purpose of providing a comprehensive description of the concepts surrounding this thesis. Historical adaption of LEDs within lighting products was noted, along with device operational properties and

attributes associated with their integration discussed. Operational relationships are noted in correspondence to the device's intrinsic principles. Lighting market trends are addressed and shown to favor LED lamp integration. In this regard, the lamp's impending effect on grid level integration is emphasized, with importance placed on the formulation of an LED load model.

Load modeling principles are defined with applications for the analysis of complex power systems, such as the power grid through testbed emulation systems, such as the UTK HTB. Various, load models and modeling techniques are investigated with their respective characteristics and attributes discussed.

CHAPTER 3
LOAD MODELING OF LED BULBS

3.1 Determination of Load Modeling Methodology

3.1.1 Inspiration for Load Modeling Overview

Motivation toward acquiring a comprehensive understanding of power system operation places importance on the characterization LED bulbs, integrated within the grid. The associated effects, posed by the device's integration, must be investigated, in effort to maintain accurate representation of the current power system in operation. Pursuit of this understanding requires knowledge surrounding the operational behavior of the LED device, which is possible through load modeling [4 – 6].

3.1.2 Selected Approach for LED Load Modeling

With the purpose of characterizing LED lamp behavior throughout a wide range of applications and grid scenarios, an alternate methodology to previous research is utilized, in development of a load model. Measurement-based methodology has proven to produce models that are limited in accuracy to data range observed in the test environment, device specific, and negate the device's transient response to dynamic events. Aiming to formulate a model that depicts behavioral response of a typical LED lamp within the market, the component-based approach is explored [4-5].

Component-based load modeling is credited for having a wider range of application within a system. This technique formulates a topology that functions in correspondence with the device. The derived model exhibits the operational characteristics of the apparatus throughout a wider range of scenarios and incorporates the device's potential transient response during dynamic events. The component-based approach provides adaptability to the variety of LED bulbs within

the market. Since the load model investigates the power electronic structure within the device, it can be formed to represent the majority of marketed devices with minimal adjustment of parameters within the model for improved representation [5].

Additionally, this model will provide the opportunity for characterization of the device operation under applied scenarios. In doing so, the established model will illustrate LED bulb performance throughout different grid events. Ability to further characterize the device, in this regard, provides information that can be utilized in supply of reliable and persistent area lighting.

Component-based methodology that meets the desired benefits, involves careful, intentional design of the load model's topology. The established load model must not only operate with accurate depiction of device behavior, but also provide representation for majority of manufactured LED bulbs utilized throughout the grid.

3.2 LED Lamp Component-based Load Model

3.2.1 Investigation of LED Lamp Power Electronics

Design of a topology which best represents a standard LED bulb utilized throughout the grid requires comprehension of the fundamental power electronic components that operate within the device. First, analysis on the steady-state operating conditions associated with LED lights provides information on the potential power electronic module utilized within the device. The standard for power systems in U.S. commercial and residential sectors provides for 120 Volt, 60 Hertz AC power supplies. As there exists a country-wide standard for power systems within establishments, the operational rating of the device must coincide with this input condition [24].

Since the DUT produces light through the utilization of LEDs, additional information can be gathered surrounding the power electronic converter. LEDs are electrical components which

illuminate when positive threshold conditions are supplied. Under the presence of AC conditions, illumination of the diode would only take place throughout less than half of the supply condition cycle.

In this regard, flickering and/or blinking of the light would be visible during operation if output conditions were AC throughout the LED load. LED bulbs are not perceived to have this type of illumination. Thus, the affiliated power electronic module within the device is deduced to incorporate a power electronic converter topology enabling rectified operational conditions (DC) for the LED load for more consistent illumination [25].

In determination of the specific converter utilized in conventional LED lamps, the variety of marketed device implementations were explored. Since there exists a wide range of LED bulbs available to consumers, characteristics of common device utilization are addressed. Typical lighting supply mounts, found in the commercial and residential sectors, require an A19 bulb, pictured in comparison to other bulbs within Figure 20.

This bulb size is fit to be integrated within E26 mounting systems. The E26 mount is the standard size of bulb socket sold in the US, applicable to home/commercial building wiring systems in addition to supplementary lighting systems, such as decorative lamps. This sizing/shape constraint has been found to not only occupy majority of area lighting applications, but also is indicated as the most commonly purchased bulb within the market [26], [28], [49].

Further, bulbs which are described as ’60 W equivalent’ have been proven to be the preferred choice of lighting device within the market. This description has been industry-standard terminology in indication of the device’s brightness during operation. With origin tied to the brightness associated with standard area lighting obtained through incandescent bulbs, this rating is most sought after by consumers in choosing lighting devices. Acquired information, surrounding

typical light bulb shape, size, and description, in narrowing the device market in formulation of a more accurate representation of the LED light through load modeling [27].

3.2.2 Application of Device Power Electronic Analysis

Descriptive findings surrounding the standard bulb is applied to market sales trends in determination of the top LED light manufacturers. In doing so, the wide variety of LED bulbs can be further narrowed to those most prevalent in utilization. In addition, the commonly utilized LED power electronic modules of popular manufacturers are explored, along with general LED bulb AC-DC topologies. In doing so, it is determined that the most prevalent method of device construction includes a full bridge diode rectifier input in conjunction with a wide-bandgap (WBG) Silicon-Carbide (SiC) MOSFET in implementation of the device.

Next, formulation of a simplified power electronic topology that encompassed key components illustrated in typical LED bulb models is needed. Various device models were noted to vary slightly in design. The main differences included the incorporation of transformer elements, inclusion of additional active switches, and device power rating. However, fundamental circuit operation principles and generalized implementation remained consistent.

Historically, market trends show that consumer preferences in lighting device are linked to conservation of energy and minimal cost of initial purchase. LED lights have been designed with and praised for their limited power consumption in comparison to other bulbs. When choosing a topology of LED that best represented a conventional model, initial cost of purchase and power rating was considered. A standard device was chosen that possessed low power rating and cost of purchase.

As such, the Feit A19, 60W equivalent, 8.8W LED bulb topology is chosen as a baseline for the component-based load model. Depiction of the specified LED bulb is provided in Figure

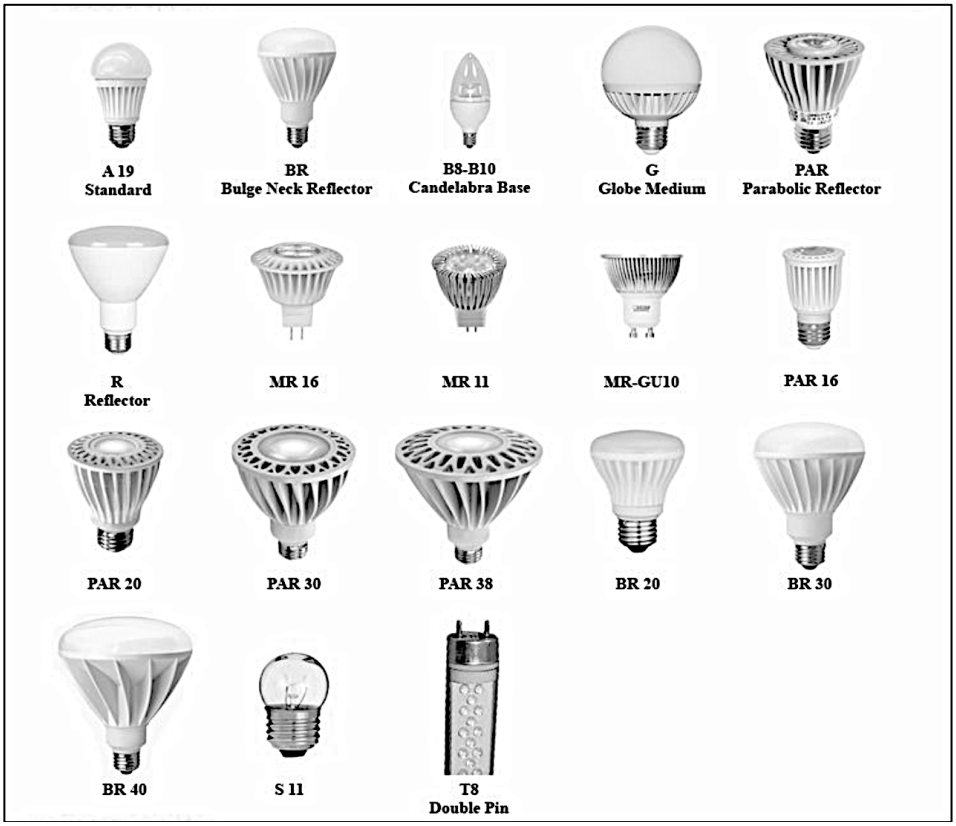

Figure 20. Comparison of Bulb Shape/Sizes

Depiction of the bulbs available within the market with focus on the shape and size variation, highlighting the A19 bulb as standard [28].

21 and the device's circuit topology is illustrated in Figure 22. Nominal ratings associated with the distributed device are outline in Table 11. Adjustments were made to the chosen topology for increased representation of a standard LED bulb. These refinements are made with respect to extraneous manufactured device schematics and LED driver design guides. Associated component parameters are further perturbed in formulation of a model which best depicts LED light operational behavior of the DUT. This simulated topology was chosen in modeling as opposed to an averaged switching model for improved representation of the device throughout operation and aim for adjustability in future modeling of LED devices within the market.

In an effort to represent a standard LED device, dimming and colored light illumination was not modeled in the chosen implementation. However, these characteristics are host for application in future research through continued modeling of the LED driver. In application, a standardized pulse generator was utilized in control and representation of the bulb. Further implementation of dimming and colored light illumination is possible through inclusion and manipulation of the LED driving system within the established model.

Further, for application to manufacturer specific LED devices, the established model parameters may be minimally perturbed with ease in replication and representation of the specified device's operational behavior ratings. This model stands as a generalized topology of a standard LED bulb. In doing so, the inductive and capacitive components within the model provide majority of influence on device operation. Thus, the parameters of this passive components may be adjusted for the purpose of application to extraneous LED manufacturers [29 – 33].

3.2.3 Formulated Component-Based Load Model

The established load model, in representation of LED lightbulb operational behavior is designed with respect to Feit Electric 8.8 W, A19 LED bulb. Since explicit information on the

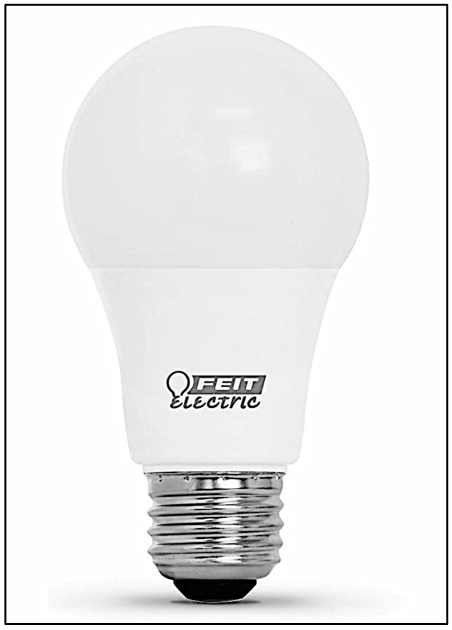

Figure 21. Feit Electric A19, 8.8 W, 60 W Equivalent LED Bulb
Physical LED bulb chosen as a baseline in the establishment of a component-based Load Model [50].

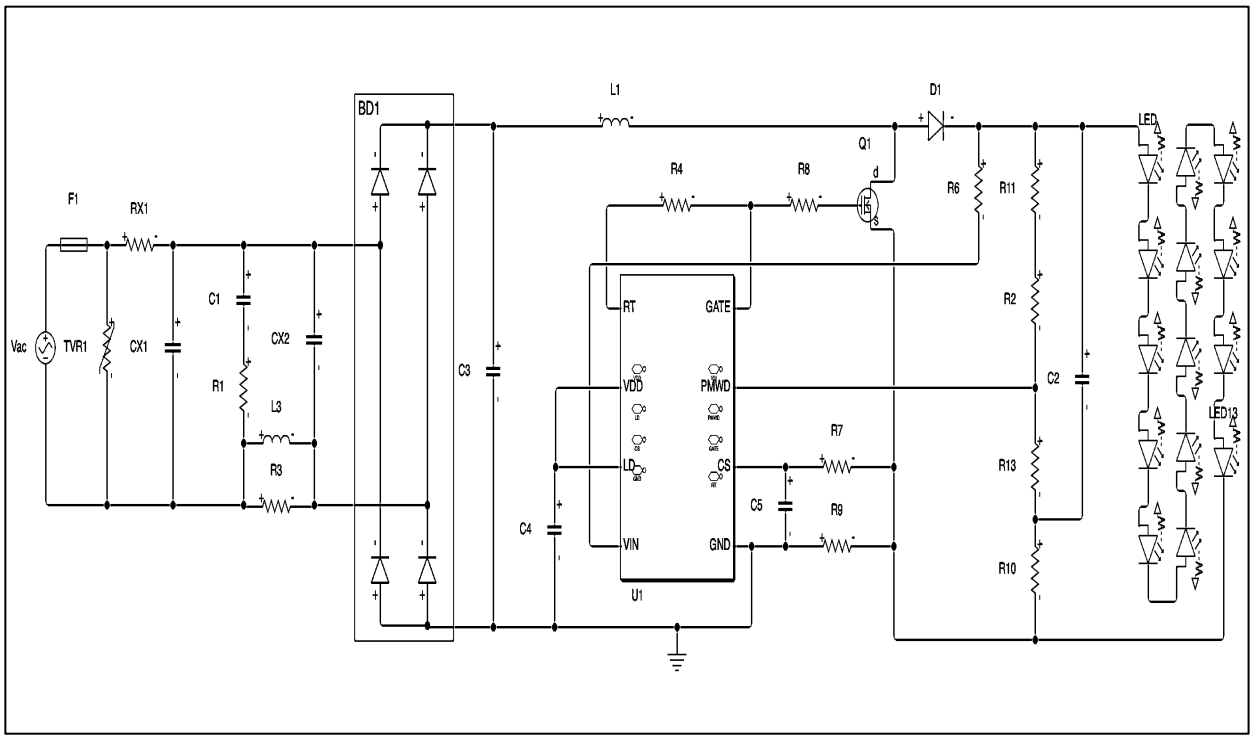

Figure 22. Feit Electric LED Bulb Circuit Topology
Formulated diagram of the Feit A19, 8.8 W, 60 W equivalent LED Bulb's internal circuit topology [32].

Table 11. Feit A19 LED Bulb Parameters

Ref.	Component Type	Description
V_{ac}	AC Power Supply	120 V, 60 Hz
F1	Fuse	2 A, 250 V
TVR1	Varistor	270 V, Part # = 7N271
RX1	Resistor	30 Ω, 0.5 W
R1		1 kΩ, 0.25 W
R3		4.7 kΩ
R4		220 kΩ
R6		1 kΩ
R7		470 Ω
R8		27 Ω
R9		2.2 Ω
R10		8.2 Ω
R11		270 kΩ
R12		240 kΩ
R13		5.1 kΩ
CX1, CX2	Capacitor	0.047 μF
C1		0.22 μF
C2		22 μF, 250 V
C3, C4, C5		Unknown
D1	Diode	Part # = RB751V
L1	Inductor	Unknown
L3		820 μH
Q1	N-Channel MOSFET	Part # = 4N60
UI	LED Controller	Part # = AP1910
BD1	Full-Wave Rectifier	Part # = ABS10

Tabulated list of components within the Feit A19 8.8 W, 60 W equivalent LED bulb including affiliated ratings and indication if rating is unknown [32].

affiliated power electronic module is not provided by the manufacturer, the model is compared to typical elements integrated throughout LED devices. Additionally, design guides for LED driver affiliated circuits are referenced in adjustment of the Feit Topology, to best represent the DUT.

Alterations made to the Feit Topology include the incorporation of an inductive element, in series with the LED load. Majority of LED driver design guides and device topologies reference the integration of this component within the load. To best portray the LED device in load modeling, this component is included in the design. Typical topologies also utilized ICs for control of the active switch. For simplified comprehension of the standard LED as a load model, the IC is modeled with inherent purpose, as a signal utilized to drive the WBG SiC device.

Parameters of each electrical component are defined to reflect the element's specified datasheet ratings. If a component was not specified within the topology, comparison was drawn to standard LED Driver and LED bulb implementations. Components that closely represented typical application were chosen for portrayal. Then, corresponding characteristics, of the chosen device, were obtained from their respective datasheet ratings and applied to the load model.

Following the preliminary establishment of the load model, a comparison is drawn to laboratory tested device operational behavior. Minor adjustments are made to the LED bulb's load model component parameters. In doing so, the load model is formed and verified to accurately represent device behavior at various operating conditions. The finalized LED bulb component-based load model is modeled in Matlab Simulink Software and portrayed in Figure 23. Electrical component ratings utilized within the modeled converter are outlined in Table 12 [29 – 34].

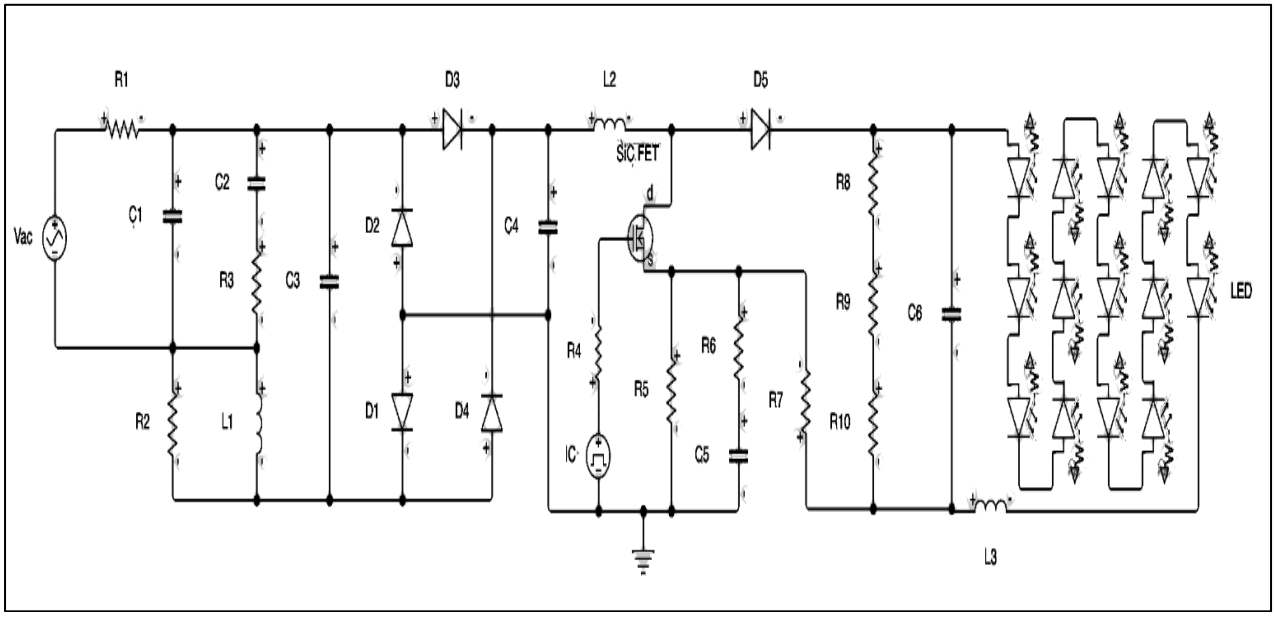

Figure 23. Established LED Bulb Component-Based Load Model

Depiction of formulated component-based load model, in representation of a standard LED bulb.

Table 12. LED Bulb Load Model Component Parameters

Ref.	Component	Description	Part #	Datasheet
Vac	AC Power Supply	*(@ Steady-State, DUT Op. Rating)* 120 V, 60 Hz	CaI-1001P	[35]
R1	Resistor	30 Ω ± 5%	CF12JT30R0TR-ND	[36]
R2		4.7 kΩ ± 5%	RC0100JR-074K7L	[38]
R3		1 kΩ ± 1%	RC0100FR-071KL	[38]
R4		27 Ω ±5%	ERJ-P6WJ270V	[44]
R5		2.2 Ω ± 5%	RC0100JR-072R2L	[38]
R6		470 Ω ± 5%	RC0100JR-07470RL	[38]
R7		8.2 Ω ± 5%	RC0100JR-078R2L	[38]
R8		270 kΩ ± 5%	ERJ-XGNJ274Y	[46]
R9		240 kΩ ± 5%	RC0100JR-07240KL	[38]
R10		5.1 kΩ ± 5%	RC0100JR-075K1L	[38]
C1, C3	Capacitor	.047 μF ± 10%	473MKP275K.X2	[37]
C2		.22 μF ± 10%	FK20X7R2E224K	[39]
C4, C5		0.1 pF ±10%	0603J300P100BQT	[42]
C6		83.5 μF ± 10%	CL05A104KA5NNNC	[47]
L1, L2	Inductor	820 μH ± 10%	RLB0608-221KL	[40]
L3	Inductor	82 mH ±5%	2534R-70J	[49]
D1, D2, D3, D4	Full-Wave Bridge Rectifier	*(Independent Diode Ratings)* [1] V_F = 0.95 V [2] R_{ON} = 2.375 Ω [3] G_{OFF} = 2.143e-7 Ω^{-1}	ABS10	[41]
D5	Schottky Barrier Diode	[1] V_F = 0.37 V [2] R_{ON} = 370 Ω [3] G_{OFF} = 1.667e-8 Ω^{-1}	RB751V40	[45]
SiC FET	N-Channel MOSFET	[4] $R_{DS(ON)}$ = 2.5 Ω [5] $I_{DS(ON)}$ = 2.2 A [6] $V_{GS(ON)}$ = 20 V [7] $V_{GS,TH}$ = 4 V [8] L_M = 0.674321 V^{-1} [9] T = 25 °C [10] R_S = 1e-4 Ω [11] R_D = 0.01 Ω [12] C_{iss} = 670 pF [13] C_{rss} = 50 pF [14] C_{oss} = 100 pF	4N60G-K08-5060R	[43]
IC	LED Driver Control IC	[15] V_{pulse} = 2.45 V [16] t_{rise} = 1 ns [17] t_{fall} = 1 ns f_{sw} = 488.28 Hz	AP1910	[30]
LED	Light Emitting Diode	[18] R_S = 0.006452 Ω [19] [I_1, I_2] = [3.64, 49.75] mA [19] [V_1, V_2] = [3.08, 3.91] V [20] $C_{junction}$ = 20 pF	OF-SMD3528WW	[48]

[1] Forward Voltage; [2] On-State Resistance; [3] Off-State Conductance; [4] Drain-Source On-State Resistance; [5] On-State Drain Current [6] On-State Gate-Source Voltage; [7] Gate-Source Threshold Voltage; [8] Channel Modulation; [9] Temperature; [10] Source Resistance [11] Drain Resistance; [12] Input Capacitance; [13] Reverse Transfer Capacitance; [14] Output Capacitance; [15] Gate Drive Signal Magnitude [16] Gate Drive Signal Rise Time; [17] Gate Drive Signal Fall Time; [18] Series Diode Connection Resistance; [19] I-V Curve Data; [20] Junction Capacitance

Outline of the component parameters that are utilized in emulation of the LED bulb in correspondence with the physical component ratings. The properties outline in description are implemented within the component-based load model for simulation of device behavioral response, for comparison to physical device operation.

3.3 Chapter Summary

In this chapter, the framework and process of designing a component-based load model in representation of an LED lamp was described. With aim to develop a load model that represented the majority of LED devices in utilization, an investigation of commonly utilized device implementations was conducted.

Further, the associated operational principles of the device were addressed, in better comprehension of the device's power electronic topology. Comparison was drawn between the most prevalent manufactured bulbs within the market. Insight was gathered with respect to the electrical configurations associated with these devices. Commonalities in topologies were highlighted with further comparison to industry standard LED driver design guides. Acquired knowledge was applied in the formulation of a LED Bulb component-based load model, and specifications in implementation were explicitly defined.

CHAPTER 4
ANALYSIS OF THE LED BULB/LOAD MODEL AT STEADY-STATE CONDITIONS

4.1 Laboratory Analysis of the LED Bulb

4.1.1 LED Bulb Under Test

Design of the established component-based load model was completed with the intention of portraying a standard LED bulb, similar to what would be utilized throughout the grid. In this regard, the formulated topology acts as a template, to be adjusted for representation of typical LED lighting devices. Through slight modification of component ratings, the model is applicable in representation of bulbs possessing power ratings that differ from that which is described. This is exhibited through comparison of popular device topology features, within the market, and inclusion of reference to LED driver design guides.

Component parameters of the established load model, referenced in Table 12, were chosen with respect to the Feit LED bulb, pictured in Figure 21. Laboratory testing was implemented on the same device, being the Feit A19 8.8 W (referred to as the 60 W equivalent) LED bulb. Choice of analyzing this bulb, through laboratory testing, provides for comparison to the established load model. Thus, accuracy of the component-based load model, in representation of device behavior, may be assessed for verification.

4.1.2 Laboratory Testing Procedure

Acquisition of real-time laboratory data provides for the characterization of a conventional LED based lighting apparatus under various operating conditions. Testing was implemented for the purpose of comparison and verification of the established component-based load model, through observation of the voltage and current conditions. Effort was made to accurately

characterize the model, in representation of LED lighting devices as a load, for various applications.

The procedure incorporated testing of both input and output conditional response of the DUT under varied operating conditions. In doing so, depiction of the behavioral relationship of the device to ambient conditions was obtained. The equipment utilized in analysis of this relationship is tabulated in Table 13 with inclusion of the affiliated purpose of each item.

As Table 13 indicates, equipment needed for the testing procedure included an AC power supply capable of producing 120 V, 60 Hz sinusoidal voltage to power the Feit A19 LED light bulb, screwed into a bulb mount. Two wires of different colors, red and black, were cut from the wire spindle in appropriate length for connections.

The Feit LED bulb, being the selected device for experimentation and analysis, was screwed into the bulb mount. The oscilloscope was acquired with voltage and current probes for measurement and observation of device operation. The voltage probe was attached with + and – clips connected to the respective bulb mount path. Additionally, the current probe was clipped to the + mount path.

The oscilloscope, with affiliated probes, provided visualization of I-V waveforms, depicting device behavior at various operating conditions. Again, use of the Digital Multimeter verified connections of the established configuration and ensured accuracy in probe measurements. Once connections were verified, the set-up, represented in Figure 24 for testing of the DUT's input condition, was complete. With the established configuration in place, associated testing and data collection began.

Tests began by applying a 0 V, 60 Hz AC voltage to the input of test configuration, with the associated power supply. Then, power supply voltage was increased by increments of 10 V, in

adjustment of the operating conditions seen by the DUT, for the purpose of input behavior characterization. With the oscilloscope, data points of the input voltage and current waveforms, of the DUT, were extracted via USB flash drive. This method of measurement was repeated in increments of 10 V, until a maximum of 120 V was recorded in observation. At all operating conditions, results were compared to the simulated component-based load model, which was run synonymously with ambient ratings of laboratory testing.

Following the testing of the DUT's input characteristics, the device's output characteristics are addressed. The test set-up utilized for model output characterization, is illustrated in Figure 25. This generalized visualization includes the incorporated equipment configured such that the DUT's output data could be recorded for analysis. Measurements, in this regard, were pursued in portrayal of the relationship between device and environment of integration.

For the measurement of the DUT's output behavior, deconstruction of the Feit A19 LED Light Bulb was conducted. Deconstruction began with removal of the DUT from the bulb mount. Once separated, a rotary tool was used to saw through the bulb's semi-transparent plastic dome, so that it could be removed. Upon removal, the internal electronics of the bulb became accessible.

Wires were cut, stripped, and soldered to their respective terminal, on the bulb's internal printed circuit board (PCB). Thus, creating a path for measurement probes to be attached. The bulb was returned and screwed back into the bulb mount assembly. Oscilloscope probes were attached to the location depicted in Figure 24, and the digital multimeter was used to test the configuration's connections in verification of implementation maintaining the necessary conduction paths.

Testing and data collection began by using the power supply and oscilloscope in accordance with the previously implemented input testing. Initial testing began by applying 0 V, 60 Hz condition, using the power supply. Voltage was then increased from the power supply in

Table 13. List of Equipment for Laboratory Testing

Device	Purpose	Part #	Description	Ref.
Power Supply	To supply sinusoidal, AC voltage to the DUT's input terminals in the range of 0 V to 120 V at a frequency of 60 Hz.	CaI-1001P	1ϕ AC 1 Channel 1000 W 1ϕ, 100 V / 240 V 270 V 3.7 A 16 Hz / 500 Hz	[52]
LED Bulb	DUT	OM60DM/950CA/8	A19 8.8 W 60 W Equivalent	[50]
Bulb Mount	Frame used to apply the supplied power to the with ease and position bulb in stationary orientation.	R50-49875-000	600 W 250 V	[51]
Oscilloscope	Device used in observation of the DUT's operational characteristics at input and output terminals, including current and voltage waveforms.	MDO41404C-SA0	1000 MHz 2.5 GS/s / 5 GS/s	[52]
Voltage Probe	Utilized in measurement of input and output voltage condition of the DUT for oscilloscope portrayal.	THDP0200	1500 V / 150 V 200 MHz / 5 MHz	[52]
Current Probe	Utilized in measurement of input and output current condition of the DUT for oscilloscope portrayal.	TCP0030A	5 A / 30 A	[52]
Digital Multimeter	Used to verify proper connections prior to testing.	2701	N/A	[52]
Soldering Iron	Implements the necessary connections of separate entities.	3020-XTS	75 W 90 ℃ / 480 ℃	[53]
Solder Spindle	Bonds separate entities in the formulation of connections.	3020-XTS	60-40 Tin Lead Rosin Core	[53]
Red Wire Spindle	Establishes connection path between separate devices. Color denotes positive (+) terminal.	EC-0744	Single Strand 22 AWG Red	[54]
Black Wire Spindle	Establishes connection path between separate devices. Color denotes negative (-) terminal.	EC-2734	Single Strand 22 AWG Black	[55]
Wire Stripper	Removal of wire casing for soldering.	STR-22-10	22 – 10 AWG	[56]
Rotary Tool	Removal of LED bulb case for output condition testing.	63389	5000 – 2500 RPM 9.6 V	[57]
Screwdriver	Fastening of bulb mount terminals.	85076	603 Phillips	[58]
USB Flash Drive	Extraction of observed data from oscilloscope.	N/A	N/A	N/A
Electrical Tape	Covers connections for safety and security.	N/A	N/A	N/A

Outline of the equipment utilized in realization of the laboratory testing procedure.

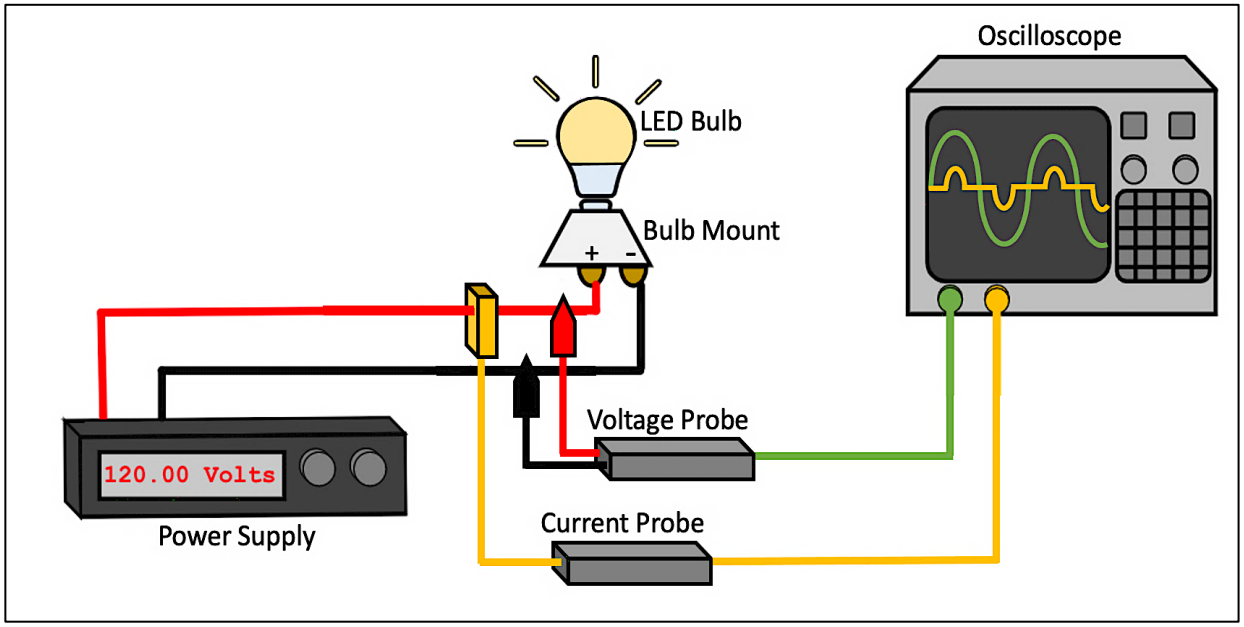

Figure 24. Input Condition Laboratory Testing Configuration

Graphic depicting the test configuration utilized in monitoring and analysis of the input behavioral response of the LED bulb at various operating conditions.

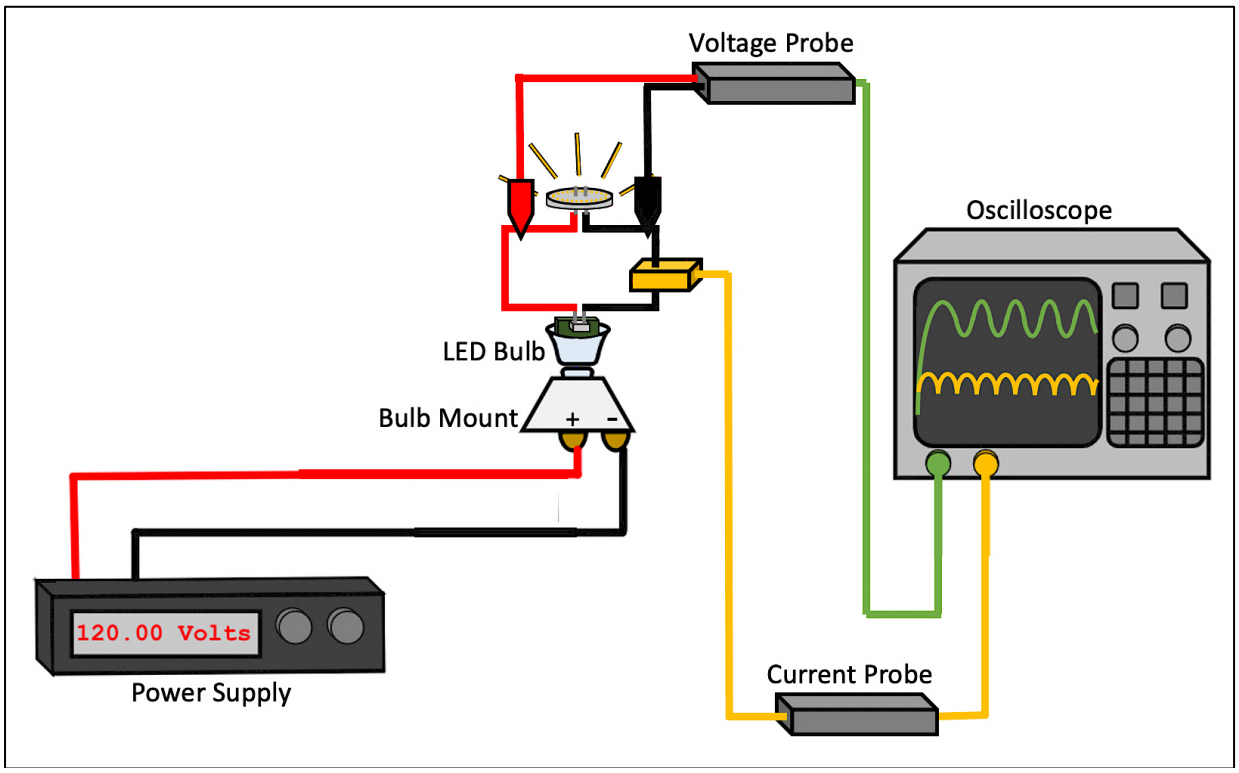

Figure 25. Output Condition Laboratory Testing Configuration

Graphic depicting the test configuration utilized in monitoring and analysis of the output behavioral response of the LED bulb at various operating conditions.

increments of 10 V, in adjustment of the ambient conditions seen by the DUT, for the purpose of characterization. Again, measurements were taken and recorded at each operational rating. Data points were extracted from the oscilloscope using a USB flash drive. Upon reaching the maximum condition of 120 V RMS, data collection was complete. Comparison was drawn between measured results and those visualized in the load model simulation. In doing so, verification of the established component-based model, at each operating condition, was achieved.

After extracting the laboratory acquired data, results were compiled for additional interpretation using MATLAB. Comparison was drawn between compiled laboratory waveforms and simulated results. Detailed analysis determined that the component-based simulation circuit required minor tuning to passive component ratings for a better representation of the DUT. After doing so, the developed load-model fully and successfully represented the laboratory tested device's behavior.

4.1.3 Laboratory Testing Data Extraction

Through completion of the aforementioned laboratory procedure, data characterizing the input and output behavior of the bulb was recorded in a USB drive. Laboratory analysis observed the device's current and voltage operation. Extraction of data at input and output terminals, of the DUT, was completed at ambient conditions ranging from 0 V to 120 V.

In addition to the extraction of measured waveforms, record is made that the DUT exhibited perceivable illumination under the presence of approximately 34 V. At 34 V supply conditions, the illuminance of the DUT was observed to be faint. Through the testing process, qualitative observation of the device's light emission was made. After first signs of light were observed, at 34 V, the bulb's quality of illuminance visibly brightened at each tested condition, up to 100 V.

At testing conditions greater than 100 V, the brightness of the DUT appeared to remain constant. Under supply conditions greater that 100 V, there was no change in light emission visible to the naked eye. In the range of 34 V to 120 V, the lighting of the bulb did not exhibit flickering or blinking qualities. Qualitative observation of the bulb's illumination throughout testing not only coincided with expectations discussed in load model development, but also provided justification in the analysis of the device's measured behavioral data.

In establishing a comprehensive understanding of the device's measured data, visualization of the obtained measurements was carried out. The data extracted from the oscilloscope, during testing, was in .CSV file format. Through utilization of MATLAB Software, data points for each test were plotted for analysis. Code, written in MATLAB script, read the data from each .CSV file and plotted waveforms with respect to time. The composed MATLAB script, for visualization of compiled waveforms, is pictured in Figure 26.

All measurements, taken during input testing, were compiled within the same command script. Input voltage waveforms were plotted in the same figure, for comparison of input voltage behavior at each tested operating condition. Likewise, the input current behaviors at tested operating conditions were plotted in the same figure. In doing so, the visualization showed the effect of operating condition on input behavior of the device.

Additionally, the graphical representations obtained were intentionally designed so that current and voltage plots were portrayed in the same window. Thus, the DUT's I-V relationship was easily compared for analysis. Depiction of the established input testing results is provided in Figure 26. Following the portrayal of tested device input behavior, measurements obtained for characterization of the DUT's output condition were plotted in the same manner, as shown in Figure 27 and 28.

```
%% Import Lab Data From .CSV
% 10V operating condition
Ch2_010 = readtable('jsq010_Ch2.csv');
Ch3_010 = readtable('jsq010_Ch3.csv');
% 20V operating condition
Ch2_020 = readtable('jsq020_Ch2.csv');
Ch3_020 = readtable('jsq020_Ch3.csv');
% 30V operating condition
Ch2_030 = readtable('jsq030_Ch2.csv');
Ch3_030 = readtable('jsq030_Ch3.csv');
% 40V operating condition
Ch2_040 = readtable('jsq040_Ch2.csv');
Ch3_040 = readtable('jsq040_Ch3.csv');
% 50V operating condition
Ch2_050 = readtable('jsq050_Ch2.csv');
Ch3_050 = readtable('jsq050_Ch3.csv');
% 60V operating condition
Ch2_060 = readtable('jsq060_Ch2.csv');
Ch3_060 = readtable('jsq060_Ch3.csv');
% 70V operating condition
Ch2_070 = readtable('jsq070_Ch2.csv');
Ch3_070 = readtable('jsq070_Ch3.csv');
% 80V operating condition
Ch2_080 = readtable('jsq080_Ch2.csv');
Ch3_080 = readtable('jsq080_Ch3.csv');
% 90V operating condition
Ch2_090 = readtable('jsq090_Ch2.csv');
Ch3_090 = readtable('jsq090_Ch3.csv');
% 100V operating condition
Ch2_100 = readtable('jsq100_Ch2.csv');
Ch3_100 = readtable('jsq100_Ch3.csv');
% 100V operating condition
Ch2_100 = readtable('jsq100_Ch2.csv');
Ch3_100 = readtable('jsq100_Ch3.csv');
% 110V operating condition
Ch2_110 = readtable('jsq110_Ch2.csv');
Ch3_110 = readtable('jsq110_Ch3.csv');
% 120V operating condition
Ch2_120 = readtable('jsq120_Ch2.csv');
Ch3_120 = readtable('jsq120_Ch3.csv');
```

```
%% Extract Numeric Data from imported .CSV
% 10V operating condition
 V_010 = Ch2_010.(5);
Tv_010 = Ch2_010.(4);
 I_010 = Ch3_010.(5);
Ti_010 = Ch2_010.(4);
% 20V operating condition
 V_020 = Ch2_020.(5);
Tv_020 = Ch2_020.(4);
 I_020 = Ch3_020.(5);
Ti_020 = Ch2_020.(4);
% 30V operating condition
 V_030 = Ch2_030.(5);
Tv_030 = Ch2_030.(4);
 I_030 = Ch3_030.(5);
Ti_030 = Ch2_030.(4);
% 40V operating condition
 V_040 = Ch2_040.(5);
Tv_040 = Ch2_040.(4);
 I_040 = Ch3_040.(5);
Ti_040 = Ch2_040.(4);
% 50V operating condition
 V_050 = Ch2_050.(5);
Tv_050 = Ch2_050.(4);
 I_050 = Ch3_050.(5);
Ti_050 = Ch2_050.(4);
% 60V operating condition
 V_060 = Ch2_060.(5);
Tv_060 = Ch2_060.(4);
 I_060 = Ch3_060.(5);
Ti_060 = Ch2_060.(4);
% 70V operating condition
 V_070 = Ch2_070.(5);
Tv_070 = Ch2_070.(4);
 I_070 = Ch3_070.(5);
Ti_070 = Ch2_070.(4);
% 80V operating condition
 V_080 = Ch2_080.(5);
Tv_080 = Ch2_080.(4);
 I_080 = Ch3_080.(5);
Ti_080 = Ch2_080.(4);
% 90V operating condition
 V_090 = Ch2_090.(5);
Tv_090 = Ch2_090.(4);
 I_090 = Ch3_090.(5);
Ti_090 = Ch2_090.(4);
% 100V operating condition
 V_100 = Ch2_100.(5);
Tv_100 = Ch2_100.(4);
 I_100 = Ch3_100.(5);
Ti_100 = Ch2_100.(4);
% 110V operating condition
 V_110 = Ch2_110.(5);
Tv_110 = Ch2_110.(4);
 I_110 = Ch3_110.(5);
Ti_110 = Ch2_110.(4);
% 120V operating condition
 V_120 = Ch2_120.(5);
Tv_120 = Ch2_120.(4);
 I_120 = Ch3_120.(5);
Ti_120 = Ch2_120.(4);
```

```
%% Plot signals
% All Voltage data on same plot
subplot(2,1,1);
plot(Tv_010,V_010,'DisplayName','10V')
hold on
plot(Tv_020,V_020,'DisplayName','20V');
plot(Tv_030,V_030,'DisplayName','30V');
plot(Tv_040,V_040,'DisplayName','40V');
plot(Tv_050,V_050,'DisplayName','50V');
plot(Tv_060,V_060,'DisplayName','60V');
plot(Tv_070,V_070,'DisplayName','70V');
plot(Tv_080,V_080,'DisplayName','80V');
plot(Tv_090,V_090,'DisplayName','90V');
plot(Tv_100,V_100,'DisplayName','100V');
plot(Tv_110,V_110,'DisplayName','110V');
plot(Tv_120,V_120,'DisplayName','120V');
lgd = legend;
lgd.FontSize = 10;
lgd.Title.String = 'Applied Input Voltage';
    hold off
title('Voltage vs time: [0-120V]')
% All Current Data on same Plot
subplot(2,1,2);
plot(Ti_010,I_010,'DisplayName','10V')
hold on
plot(Ti_020,I_020,'DisplayName','20V');
plot(Ti_030,I_030,'DisplayName','30V');
plot(Ti_040,I_040,'DisplayName','40V');
plot(Ti_050,I_050,'DisplayName','50V');
plot(Ti_060,I_060,'DisplayName','60V');
plot(Ti_070,I_070,'DisplayName','70V');
plot(Ti_080,I_080,'DisplayName','80V');
plot(Ti_090,I_090,'DisplayName','90V');
plot(Ti_100,I_100,'DisplayName','100V');
plot(Ti_110,I_110,'DisplayName','110V');
plot(Ti_120,I_120,'DisplayName','120V');
lgd1 = legend;
lgd1.FontSize = 10;
lgd1.Title.String = 'Applied Input Voltage';
hold off
title('Current vs time: [0-120V]')
```

Figure 26. MATLAB Code Plotting Laboratory Data

Outline of the MATLAB software script that was written to compile the recorded laboratory data.

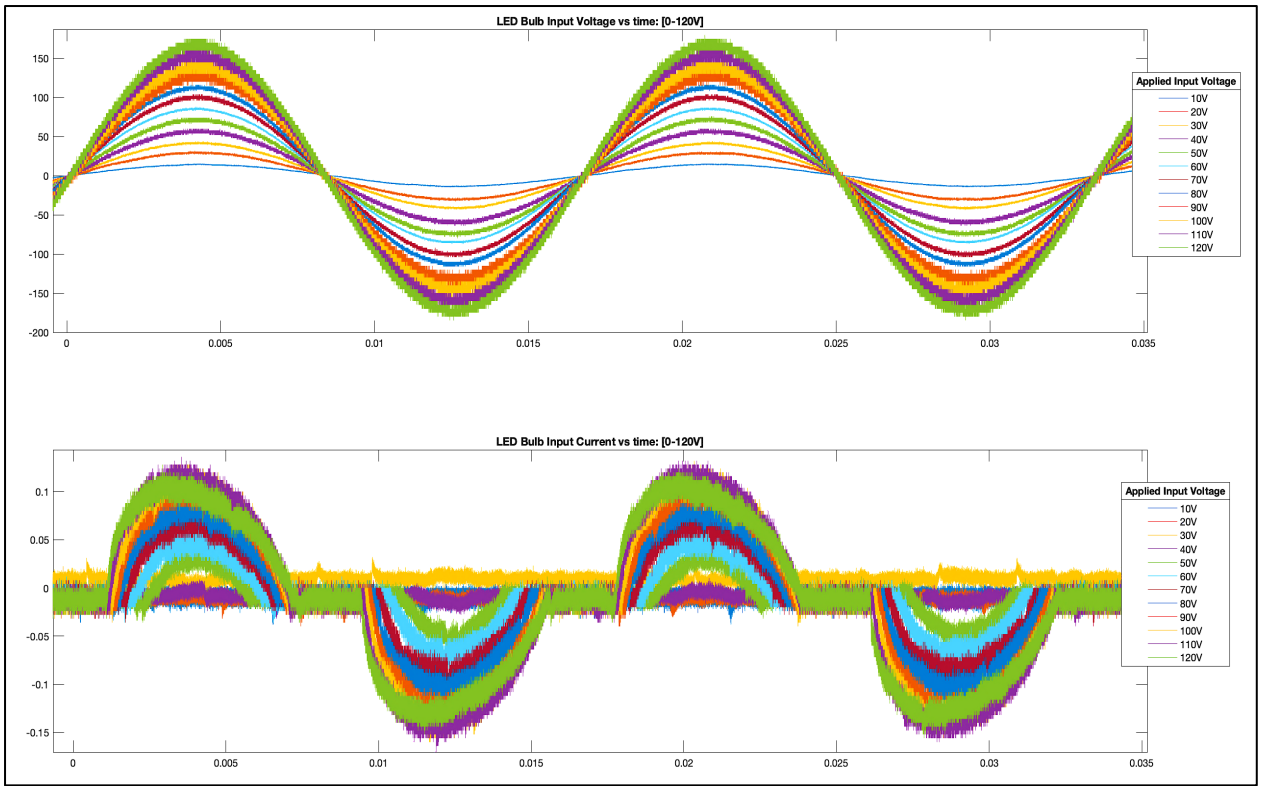

Figure 27. Input Condition Laboratory Testing Results

Graphic depicting the formulated plot depicting input response of the LED bulb at supply range 0 V to 120 V.

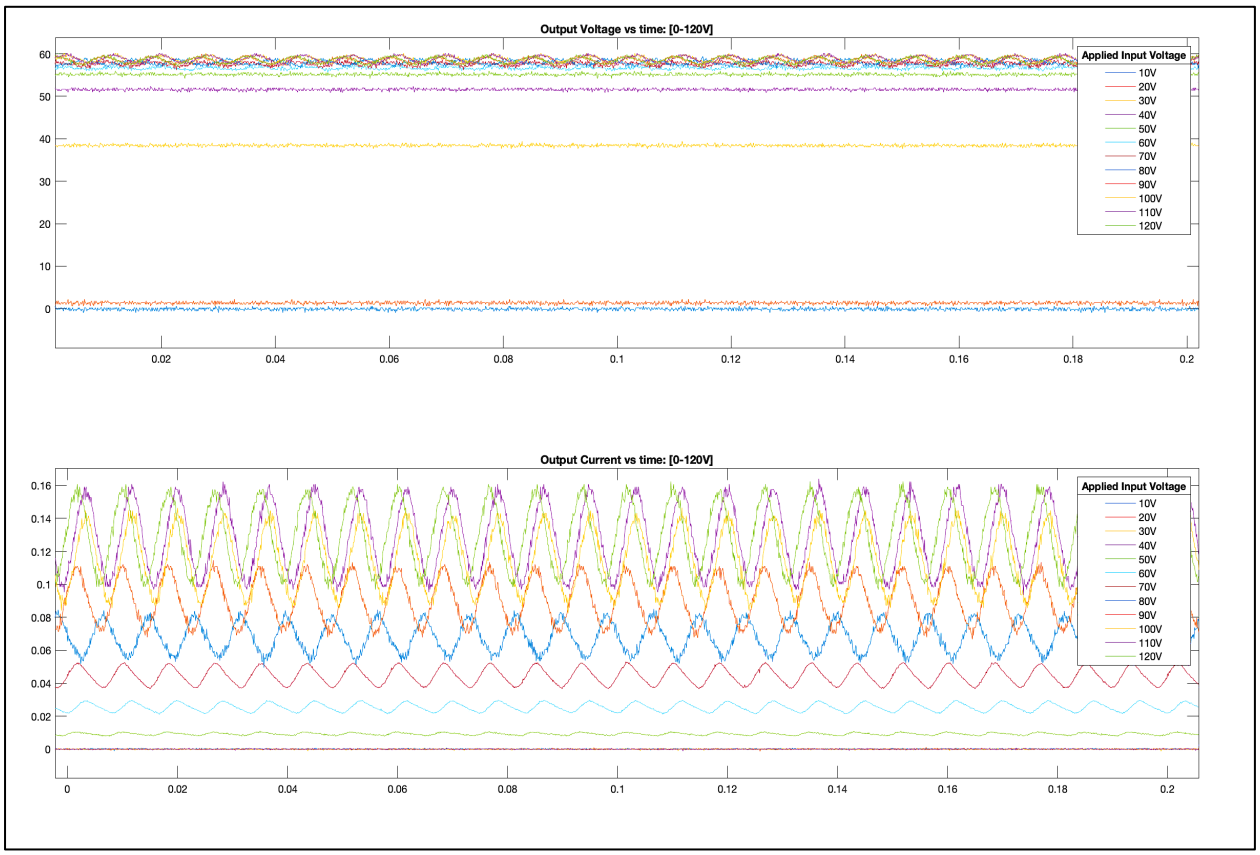

Figure 28. Output Condition Laboratory Testing Results

Graphic depicting the formulated plot depicting output response of the LED bulb at supply range 0 V to 120 V.

4.1.4 Laboratory Testing Data Analysis

Once the measured data was formatted in this regard, the LED bulb's behavioral response under tested operating conditions was observed and analyzed. The supply range that was applied, for both input and output testing, appeared to respond with two distinct behaviors. As depicted in Figures 27 and 28, measured data indicated that as supply conditions increased in magnitude, in the range of zero to approximately 100 V, the DUT's current and voltage behavior also increased, in proportion. Observation of this indicated that the LED's behavior when supply conditions were under ~100 V, exhibited a relationship that most closely related to the constant impedance load type.

When the DUT was under supply conditions larger than 100 V, the observed current and voltage behavior appeared to remain relatively constant. Minimal fluctuations within this supply range were attributed to the oscilloscope and probe's channel noise during measurement. This inference was later validated, through continued testing of the device, within and above this supply range as shown in Figure 29, illustrating the three zones of load behavior exhibited by the LED bulb.

Further testing revealed that the device's behavior within this margin remained constant in depiction, with noise fluctuations visible at varied supply states throughout testing cycles. Additionally, the marginal increase of supply conditions, greater than device operational ratings, furthered the conclusion of a constant behavioral response. Test results taken at the supply range of 110 V to 180 V are provided, with input conditions visualized in Figure 30, and output conditions visualized in Figure 31. Thus, at supply conditions larger than 100 V, the bulb's response most closely resembled a constant power type load characteristic.

The determination of load type characteristics, of the DUT, was further supported by the qualitative illuminance observations made during testing. There also existed a distinct change in output waveform oscillation and magnitude between 30 V and 40 V test conditions, coinciding with LED illumination via output load conduction. Comprehension of the behavioral response of the DUT allows for improved characterization of the DUT as a load. With improved understanding of the bulb's performance throughout ambient conditions, load modeling principles become more accurate in representation of the device. Application and comparison of laboratory findings to the component-based load model provided for not only improved representation of the device, through load modeling, but also verification of the established component-based load model.

4.2 Simulated Analysis of the Component-Based Load Model

4.2.1 Simulated LED Bulb Load Model Test Procedure

As the LED Bulb's component-based load model had been formulated to best represent the DUT, simulation testing procedure was carried out under synonymous conditions with laboratory measurements. In order to obtain data on the load model's operation, MATLAB's Simulink software was utilized. The load model, exhibited in Figure 23, was built in Simulink during the process of establishing a component-based load model. The model's affiliated component ratings were also established and are reference in Table 12.

Since the initial load model configuration had already been formulated prior to laboratory testing, implementation of acquiring data on the simulated model's behavior required minimal adjustment. Measurement probes were connected within the software to convey the model's input and output behavior. Scope components were included for the visualization of these behaviors. Integration of probe and scope components is shown in Figure 31. Inclusion of these components

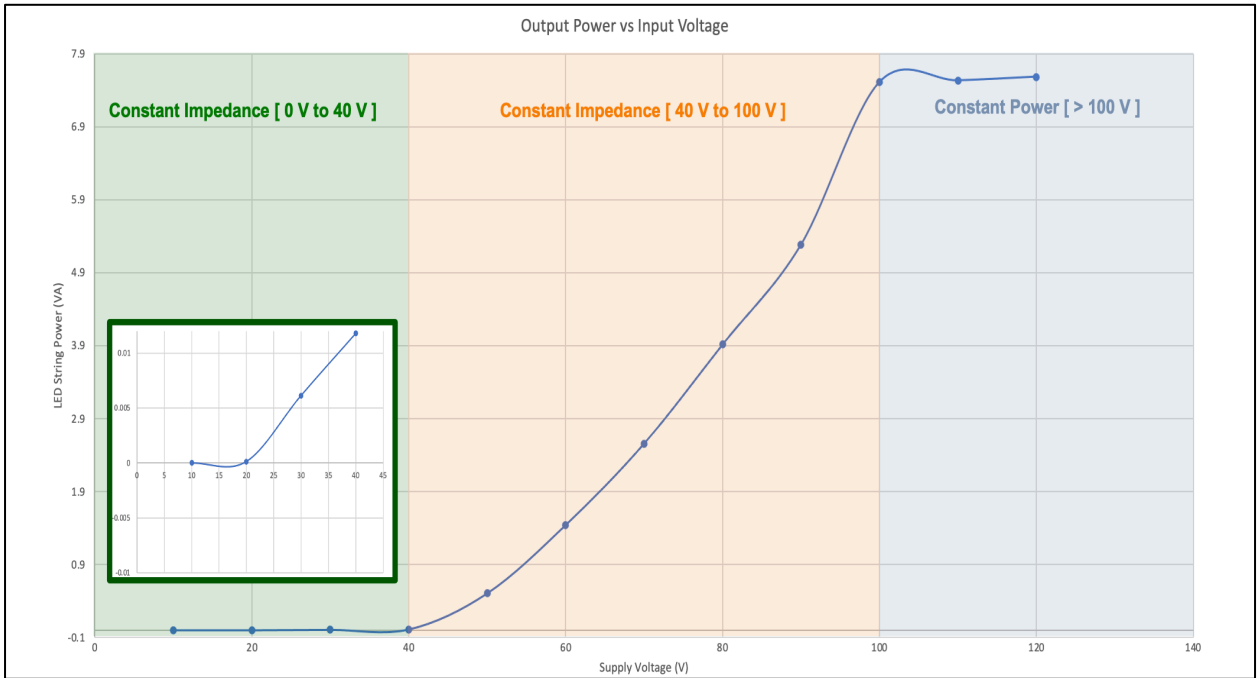

Figure 29. LED Load Behavior Regions

Zones of Load Behavior of the tested LED device with respect to supply voltage.

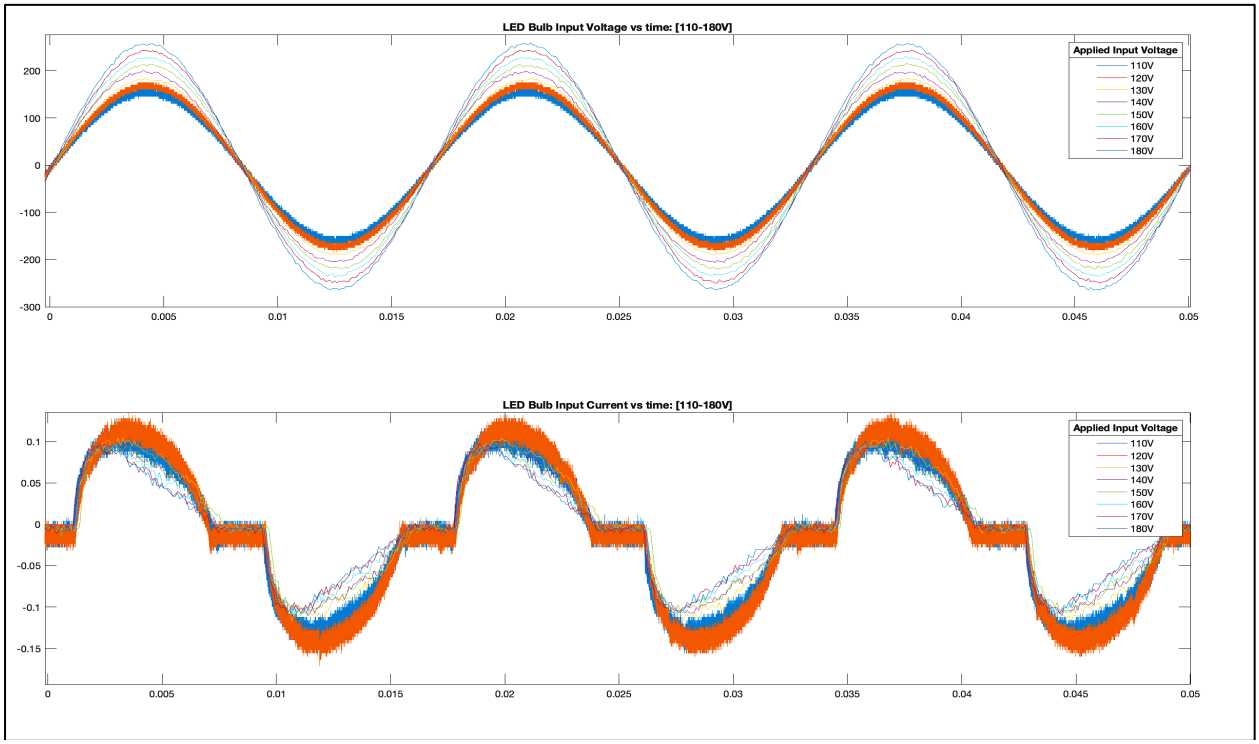

Figure 30. Continued Input, Constant Behavior Laboratory Testing

Graphic depicting the constant behavior of input current response condition under supply rated above 110 V.

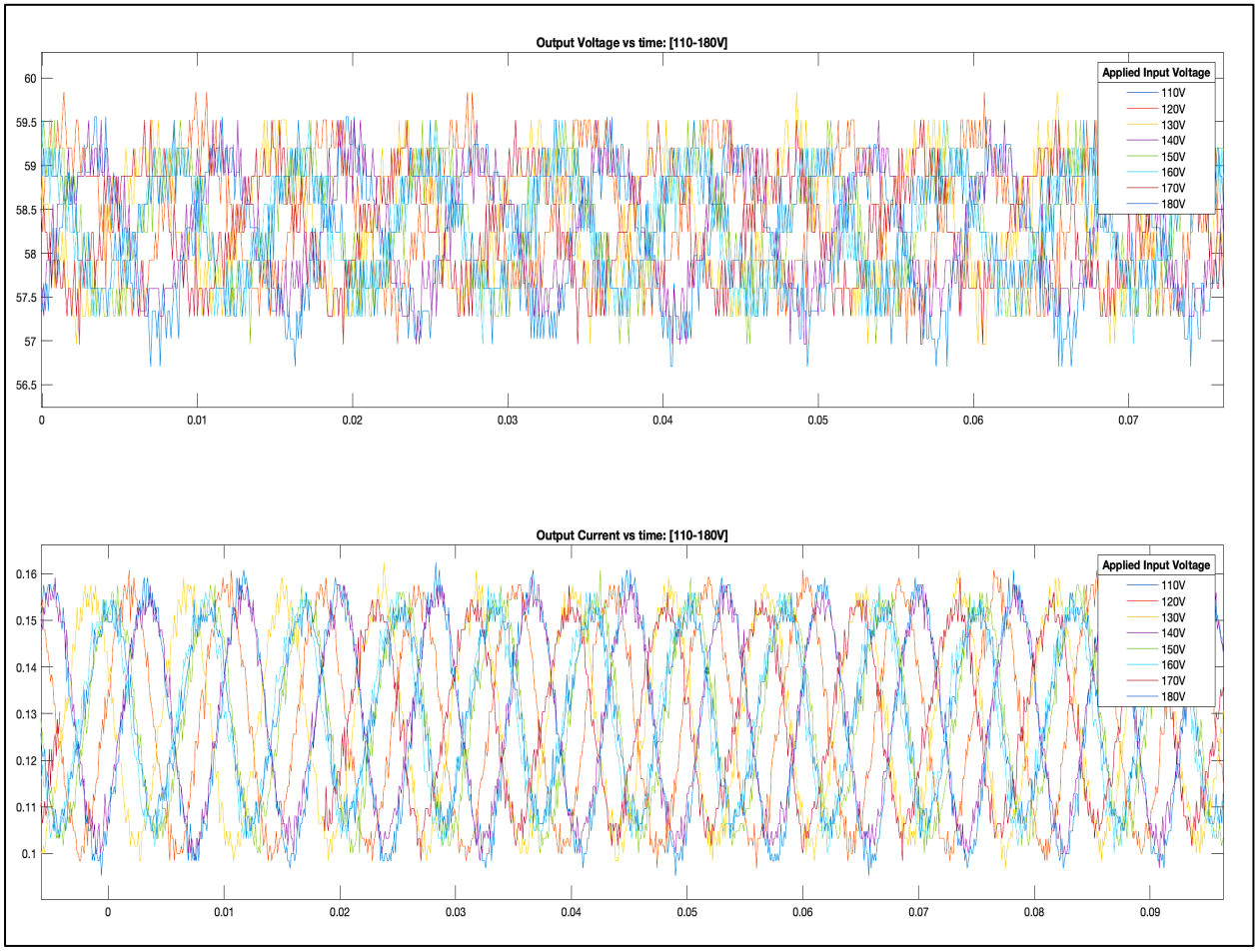

Figure 31. Continued Output, Constant Behavior Laboratory Testing

Graphic depicting the constant behavior of output waveforms under supply rated above 110 V.

provided for means of plotting the voltage and current waveforms at the input and output terminals of the load model. In doing so, comparison of the load model behavior could be drawn to the DUT's behavior, observed during laboratory testing.

The chosen topology was developed with respect to the manufacturer's design of the physical device. The developed model was segmented into AC (left) and DC (right) sides, separated by a diode bridge, for comprehension of the device's inner workings. On the AC side, capacitive and inductive elements were incorporated for additional smoothing and blockage of supply oscillations for rectification. The full wave bridge rectifier, at the front end of the module, was modeled with diodes. It enabled the transformation of AC supply voltage to DC voltage for more consistent conduction throughout the LED load.

On the DC side, a low voltage diode was used to permit DC voltage supply across the LED load. Capacitive and inductive components stored energy during off-cycles for operation of the LED load and provided additional smoothing of oscillations. Finally, the WBG SiC MOSFET acted as an active switch to achieve flow of current throughout the load, with more constant behavior.

The established load model was run at laboratory test supply conditions, in the range of 0-120 V. In simplification of the various simulated test conditions, the Simulink load model was inserted into a subsystem. The AC voltage power supply was removed, and terminals were placed inside of the substation at the nodes where the power supply had been connected. This allowed for application of supply conditions in the external model environment. Additionally, signal ports were used to replace the measurement probe's scoped signals. In doing so, the behavior of the subsystem was able to be monitored in the external model environment, as well. Depiction of the adjusted subsystem model, for supply condition simulation, is provided in Figure 33.

Within the external model, power supply conditions from 10 V to 120 V were applied to the load model, as shown in Figure 34. Monitored behavior of the load model was recorded for current and voltage waveforms at the input and output terminals. Similar to the extraction of laboratory data, input current waveforms at each supply state were plotted in the same figure, as was input voltage waveforms. These figures were combined in the same window, just as the laboratory data extraction was visualized.

In the same manner, the load model's output current and voltage waveforms were formulated for visual representation and analysis. Through this simulated behavior at load model input and output terminals, a comparison can be drawn between laboratory and simulation data for verification of the established load model. The simulated component-based load model data showing input and output behavior of the device is provided in Figures 35 and 36, respectively.

4.2.2 Simulated LED Bulb Load Model Data Analysis

Data acquired during simulation of the load model was compared to the measured data from laboratory testing. The behavioral response of the derived component-based load model was observed to mimic characteristics exhibited in laboratory analysis. As supply conditions increased in magnitude, in the range of 0 V to 100 V, simulated data also increased in proportion. Exhibiting this relationship indicated that the simulated model was able to depict constant impedance characteristics, similar to laboratory measurements.

When the applied supply conditions were above 100 V, the simulated load model was successful in exhibiting an approximate constant power type characteristic, similar to the DUT. While simulation results had exhibited a marginal increase within this range, it is evident that the load model converged within this range.

When behavioral ratings are addressed, in comparison to the DUT's measurements, the

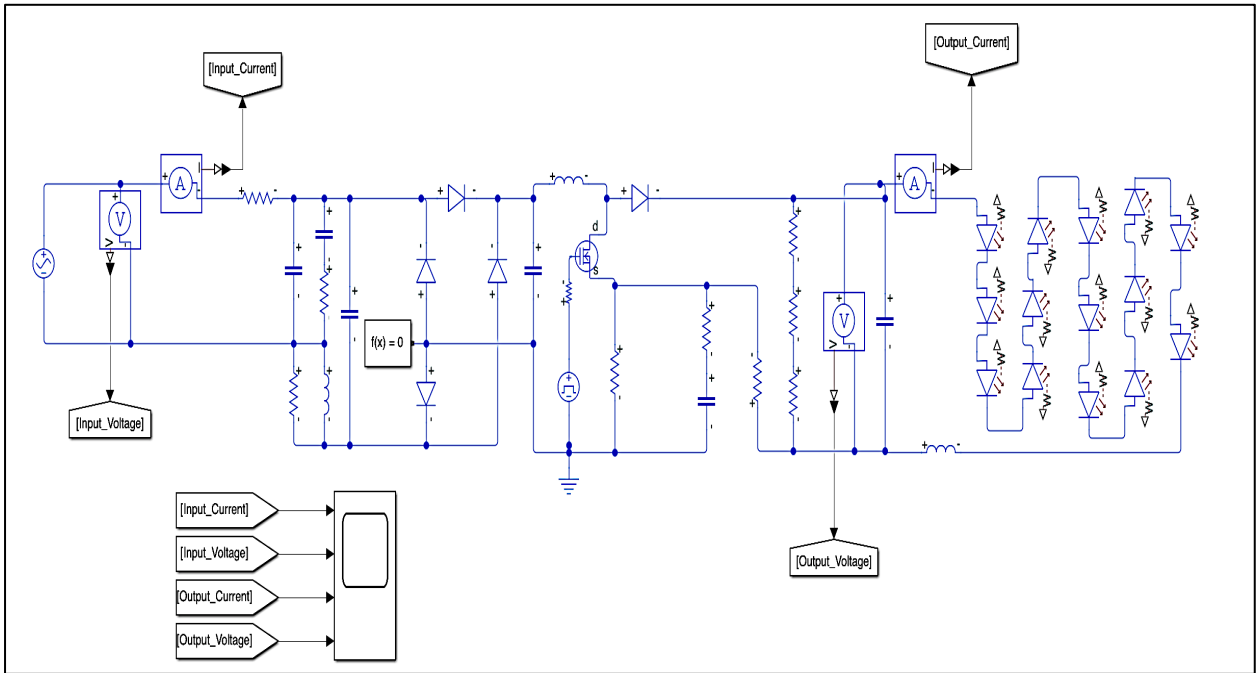

Figure 32. Simulated Load Model Measurement Configuration

Graphic depicting the load model, formulated in MATLAB Simulink Software, with inclusion of measurement probes and scope for plotting behavioral waveforms.

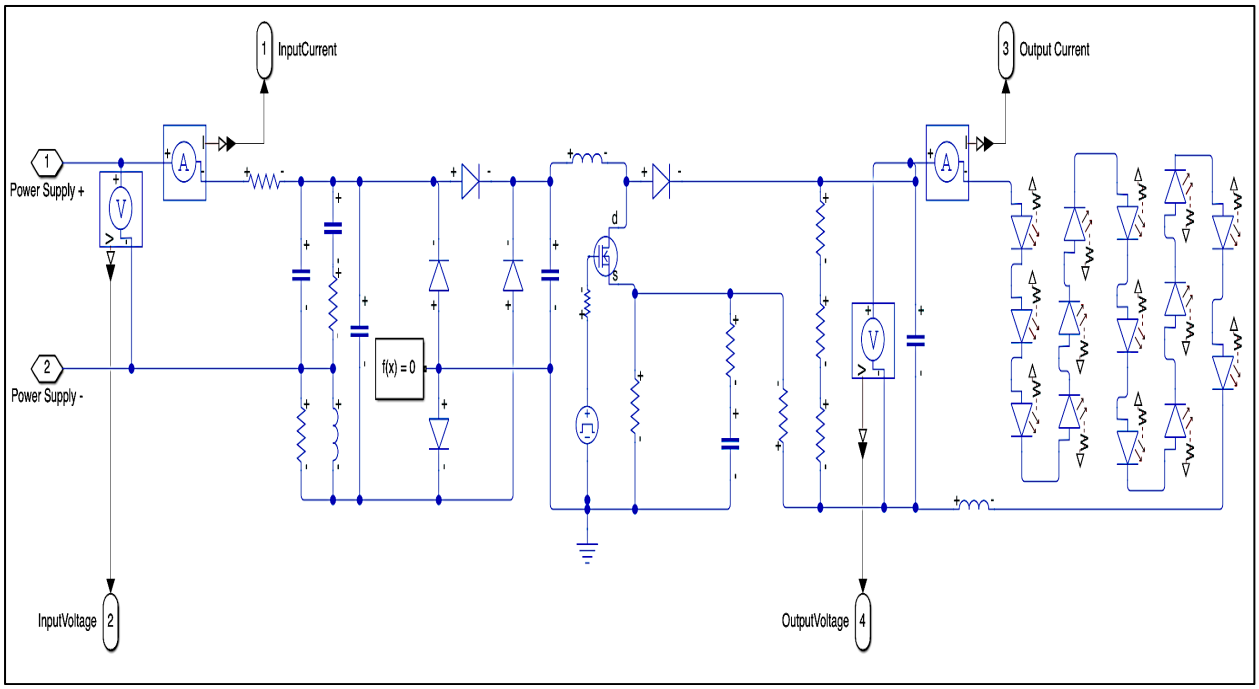

Figure 33. Simulated Load Model Subsystem

Graphic depicting the modified load model, in formulation of a subsystem, for convenience in testing supply states in the range of 0 V to 120 V.

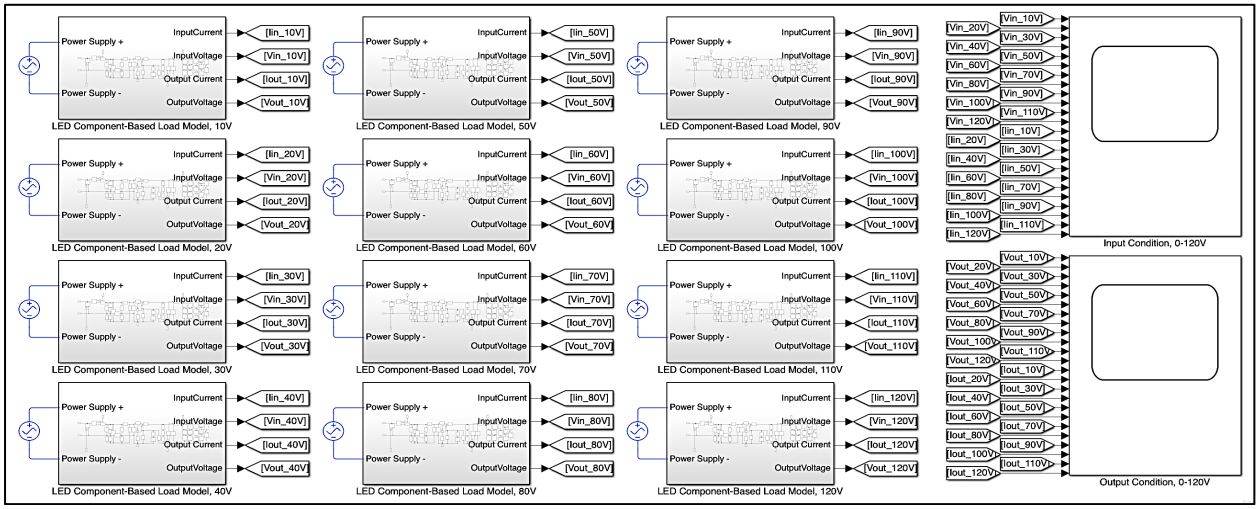

Figure 34. Simulated Load Model Subsystem

Graphic depicting the modified load model, in formulation of a subsystem, for convenience in testing supply states in the range of 0 V to 120 V.

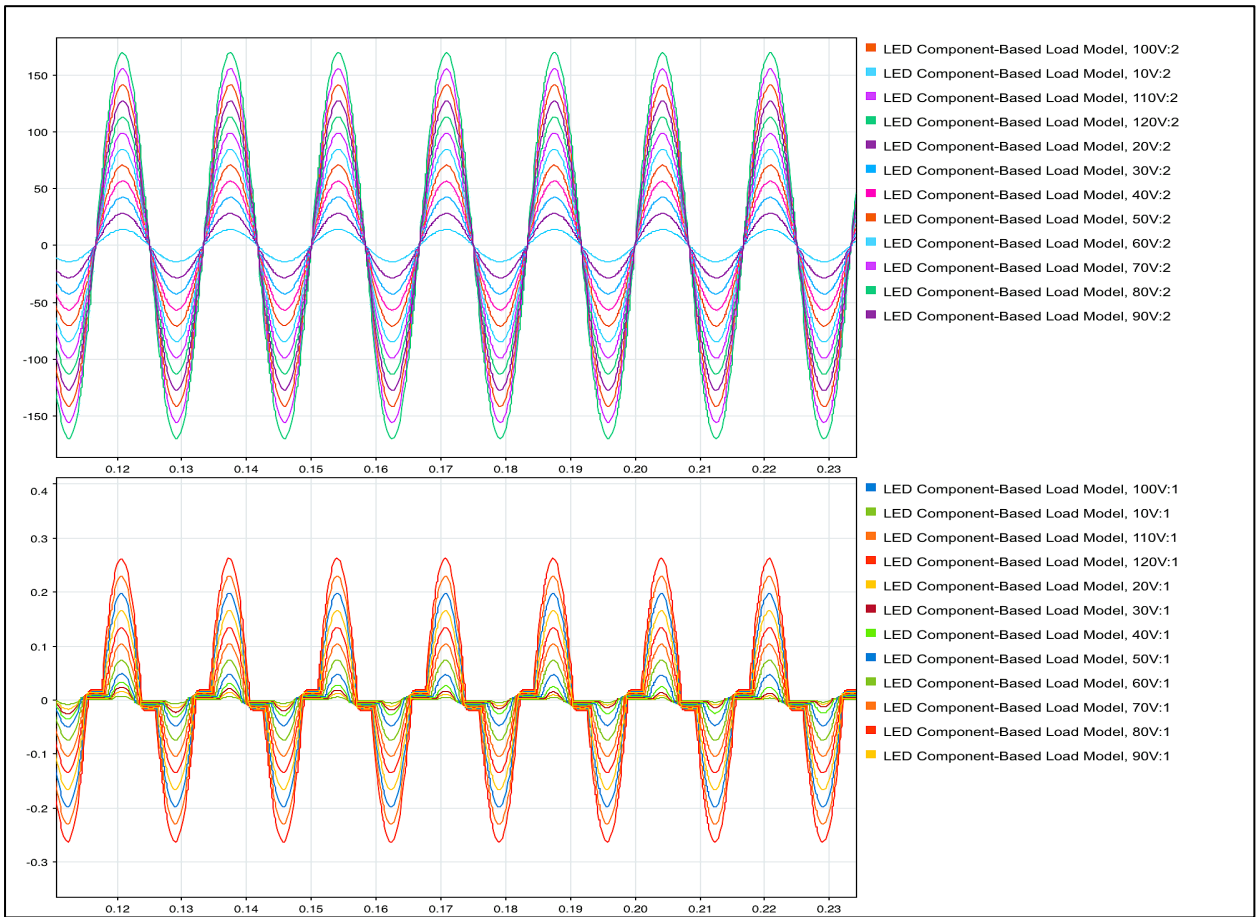

Figure 35. Simulated Load Model Input Condition Data

Plot depicting the voltage (top) and current (bottom) waveforms at the input terminals of the simulated load model with applied operating conditions in the range of 10 V to 120 V.

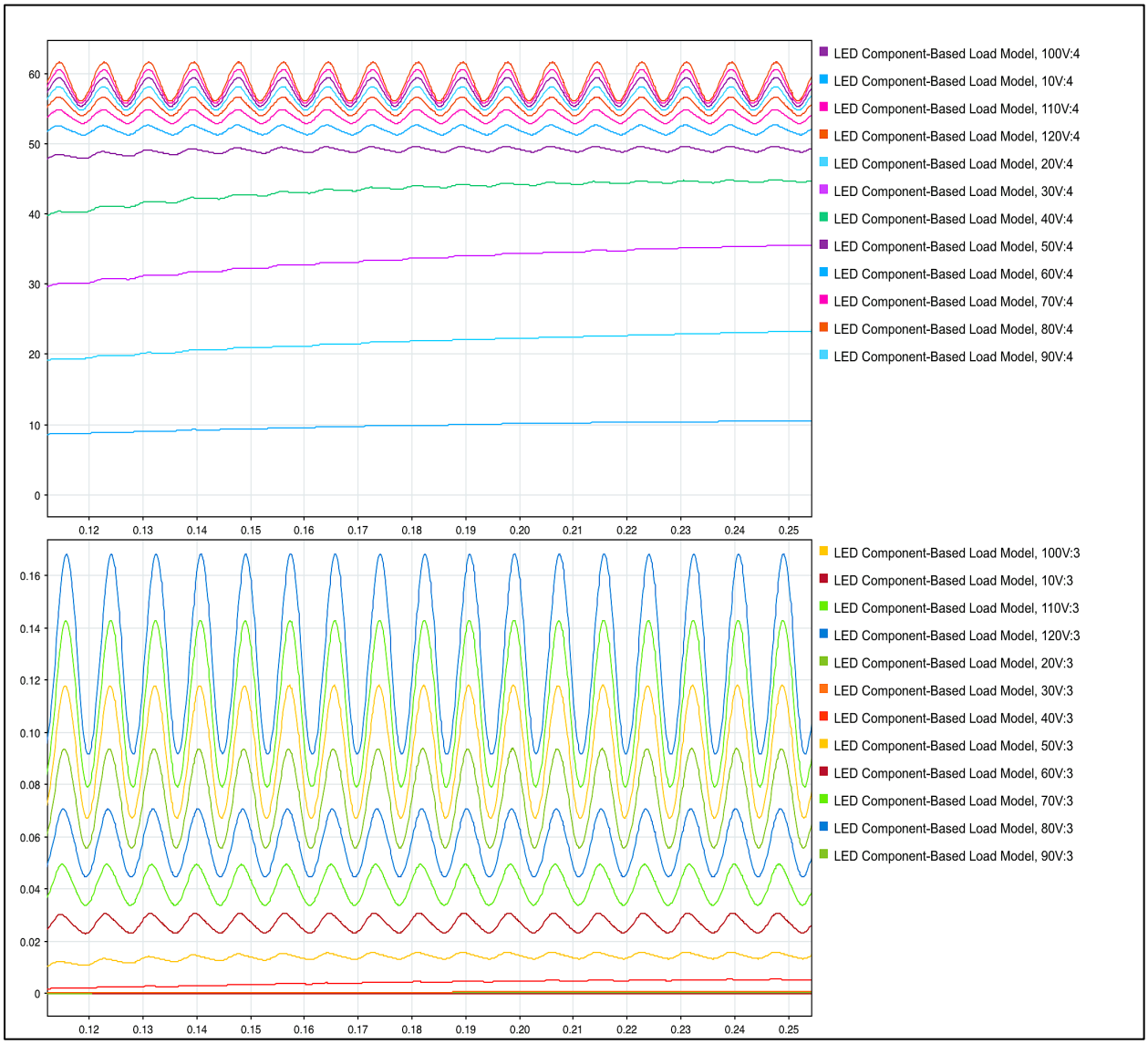

Figure 36. Simulated Load Model Output Condition Data

Plot depicting the voltage (top) and current (bottom) waveforms at the output terminals of the simulated load model with applied operating conditions in the range of 10 V to 120 V.

Simulink load model emulated the DUT within reasonable margin. The result obtained from the Simulink model had slightly higher response ratings than those measured in laboratory analysis. The difference in magnitude, at equivalent operating conditions, can be attributed to the omission of protection components utilized in the DUT. The physical Feit bulb incorporated a front end varistor and fuse in implementation. In an effort to characterize a conventional LED bulb, protection components such as these, were omitted, as they were not prevalent in other manufactured devices.

Additionally, Simulink software operates under idealized operating conditions of all components within the model. While tolerance of component ratings and parasitic effects of active components were incorporated in topology design, the real-time device was subject to more drastic effects from these factors. Further, losses in laboratory testing are more common due to switching of active components, orientation of connections, and affiliated probe characteristics. Thus, marginal differences, such as those observed, were considered negligible.

Further confirmation of the simulated model's successful emulation of the device is depicted by the change in response between 30 V and 40 V supply states. As laboratory testing indicated the observation of illumination at ~34 V, laboratory testing had shown a change in the DUT's output condition between testing conditions of 30 V and 40 V. The simulated model also portrayed a distinct change in waveforms between these states, showing more oscillation and a distinct increase in conduction throughout the load.

As behavioral response of the designed, component-based load model performed congruently to the tested bulb, the established model was deemed successful in representation of the LED device as a load. Since the established model is to be utilized for testing in integration

with the power grid, further simulations must be run for portrayal of the device's behavior under dynamic conditions.

4.3 Chapter Four Summary

In this chapter, a testing procedure and analysis of the physical device was addressed. The device chosen for laboratory testing was outlined, and reasoning behind choice of bulb was explained. The procedure formed and utilized in testing of this LED bulb was described in detail. An overview of laboratory measured test conditions was provided, which provide a qualitative observation of the bulb's illumination state. Utilization of the affiliated equipment throughout testing was explained and the process of extracting measurements realized. Analysis of the observed measurements of the device under supply states in the range of 0-120V was portrayed.

Associated laboratory data plots were formulated depicting synonymous waveforms at each supply condition with the same figure. Current and voltage waveform measurements taken at terminals alike were established in the same figure for analysis of the DUT's behavior at input and output nodes. Operational ranges were separated into two behavioral trend categories. Trends are depicted at above and below 100 V, where the device was likened to load type characteristics of constant power and constant impedance behavior, respectively. Irregularities and discrepancies observed in testing were negated through additional testing of the device at increased supply conditions in the range of 110 V to 120 V, in support of the determined behavior trends.

The process of orienting the component-based load model in simulation software was outlined and adjustments made to the model for measurement and testing of the model's behavioral relation to operating conditions. Simulation of the load model and acquired data at input and output terminals was provided and comparison was drawn to the DUT's laboratory response.

General response trends of the load model were likened to the DUT, and minor discrepancies were addressed. Observations made in output load conduction were utilized to further illustrate the load model's emulation of the DUT. The formulated component-based load model was ultimately deemed successful in emulation of LED bulb behavior.

CHAPTER 5
DYNAMIC RESPONSE OF THE LED BULB'S LOAD MODEL

5.1 Overview of Dynamic Response Emulation

5.1.1 Purpose of Dynamic Testing

Formulation of a component-based load model was designed with the intention of providing representation of the device's behavior in grid level applications. Previous testing of the load model portrayed behavioral response under a range of steady-state operating conditions. In doing so, the load model's steady-state response was portrayed for verification of the topology, in comparison to the physical device's response. Once the load model was established and verified in approximate representation of the physical device, testing of the model's behavior in utility applications can be addressed.

Since the power grid does not consistently operate in steady-state, dynamic testing illustrates the effects of integrating the device within the grid. Analysis of the load model's response, under the presence of dynamic conditions such as voltage sag or swell due to system faults, provides information on potential disturbances, associated with the grid level and intrinsic device function, resulting from market utilization of the device. Characterization of these effects through load model analysis in real-time operation can preemptively implement compensation tactics in mitigation of detriment to device and grid. In doing so, increased reliability in functionality of the device and power grid may be achieved.

5.1.2 Application of Dynamic Response Emulation

In lieu of the established systems at UTK, dynamic emulation of the LED bulb load model is addressed in correspondence to the HTB emulator. Design of the model was formulated in representation of a standard LED device utilized throughout the power grid. Through dynamic

analysis of the load model's behavior, comprehension of the device's effects on affiliated utility technologies may be achieved.

5.2 Dynamic Response of the Load Model

5.2.1 Dynamic Response Simulation Procedure

In characterization of the load model's behavior under dynamic conditions, manipulation of supply state conditions was implemented within the simulation load model. Characterization of the device's response to dynamic conditions was designed to obtain data at supply conditions commonly associated with grid level disturbances. Since the DUT was rated for operation at 120 V, the load model reflected this as the baseline source condition.

The model was designed to initially portray steady-state operation, undergo a dynamic event in supply condition, for a duration of time, then return to steady state. Adoption of this technique provided for characterization of the device's behavior prior to, during, and following a grid disturbance. Further, analysis of the effects on device behavior was exhibited throughout the transition from standard ratings to induced fault condition.

In this regard, testing scenarios were designed to initiate dynamic faults of various magnitude and duration. The magnitude of fault was described as the voltage drop applied to the supply condition. Magnitudes of faults (voltage decrement) were tested within the range of 10 V to 120 V, in 10 V increments. Duration of fault was described as the time duration, in milliseconds, which the fault magnitude was applied to the supply source. Fault durations were tested in the range of 10 ms to 50 ms, in 5 ms increments.

As described, the load model was simulated with initial device operating at rated conditions (120 V). Fault magnitude of each test was held constant, and the duration that the fault was induced

was incrementally increased on each measured signal. The following fault, within one test cycle, maintained the equivalent fault magnitude and was incremented in duration by 5 ms.

Once the test was run, measured signals exhibited the designated fault magnitude at each duration of time. Measured response of voltage and current at the load model's input and output terminals were exported to the model workspace and saved as a variable. Once the test was complete, the next test was configured with incremented fault magnitude induced in the same manner. Upon obtaining measurements at all fault magnitudes, the exported files were plotted for comparison and analysis.

5.2.2 Dynamic Response of the LED Load Model

Implementation of the dynamic response procedure began with modification of the established load model power supply component. The standard AC voltage source was replaced with a programmable voltage source component with input sinusoidal signal, shown in Figure 31. A sinusoidal signal was applied to the programmable source with a frequency of 60 Hz. The magnitude of the signal was set to an equation with incorporation of a global variable (Induce_Fault), shown in (29).

$$\boldsymbol{Signal\ Magnitude = 120\sqrt{2} - (Fault\ Magnitude\sqrt{2} * Induce\_Fault)} \quad \textbf{(29)}$$

When a load model was operating in steady-state, the global variable was set to 0, making the signal equivalent to 120 V. However, when the load model was under the presence of a fault, Induce_Fault was set to 1, meaning the fault magnitude was subtracted from the steady-state 120 V condition. The value of Induce_Fault was controlled through a subsequent system within the load model environment.

Within the subsequent system, start and stop times for each duration of fault were calculated, as shown in Figure 37. A comparison was drawn between the simulation model time

and the range of time between start and stop of the fault.

When simulation time fell within the range of a fault, Boolean logic gates returned a true signal, equivalent to 1. When simulation time was not within a fault duration range, the Boolean logic gates returned a false signal, equivalent to 0. This signal was used to set the value of the global variable, Induce_Fault, depicted in Figure 38.

Tests were run with fault magnitudes ranging from 10 V to 120 V (amount of voltage decrement from a nominal 120 V). Current and voltage waveforms depicting the behavior of the device under fault conditions were observed at the input and output terminals of the load model. In doing so, the load model's behavior under dynamic conditions was visualized for analysis. The established plots depicting input and output behavior of the load model during dynamic events are provided in Figures 39 and 40, respectively.

Observation of the established waveforms provided information on the device's operation under dynamic supply conditions. Analysis of the waveforms proves that the output conditions operated as expected. Current and voltage at the output terminals decreased under the presence of a fault. However, under the presence of a fault, for 50 ms or less, voltage and current waveforms internal to the LED did not drop beneath the threshold of LED load operation. In lieu of this, it was determined that at fault durations under 50 ms, the bulb will maintain function as an illumination device, as measurements remained above the 34 V supply state response. Further, longer duration of faults posed more concern, for effects on device operation in exhibiting illumination.

When the obtained input current conditions are addressed, the load model response exhibited more ambiguous behavior under the presence of dynamic conditions. A spike in current condition was exhibited when the fault was induced on the load model. The current impulse

increased in magnitude in proportion to fault magnitude, with little correlation observed with respect to fault duration. When the fault began or stopped at the zero-crossing of supply waveforms, a spike in current was not induced. However, when a fault began or ended in proximity to the peak of supply waves, the impulse was more prevalent, as depicted in Figure 40. This pulse was deemed a concern in operation with grid affiliated technologies, with the potential requirement of compensation to be addressed.

As previously described, protection elements were not incorporated in the established load model. There is potential that the device, with incorporation of these elements, would mitigate concerns pertaining to input current dynamic response. However, comprehension of this worst-case scenario, allows researchers to address it for mitigation and prevention.

5.2.3 Dynamic Input Current Response of the LED Load Model

Further analysis of the current impulse associated with the LED load model was complete in portrayal of the relationship which fault location has on input current behavior. Fault scenarios, ranging in magnitude, were induced on the model at various locations. In doing so, a relationship was observable between the location of the fault scenario initiation and current impulse resulting from the grid level event at each fault magnitude.

Each fault scenario was induced upon the input source voltage. As the input voltage is sinusoidal, the fault scenarios were introduced to the system at varied point on the sinusoidal input waveform. The initiation of each fault occurred through the periodic wave at unit circle degrees ranging from 30-degrees to 360-degrees, in 30-degree increments. Locations of faults tested are portrayed in Figure 41 with respect to standardized voltage waveform for reference.

Faults were induced in 30-degree increments over the period of the input voltage condition. Additionally, the fault magnitude of each grid simulated scenario was tested in the root-mean-

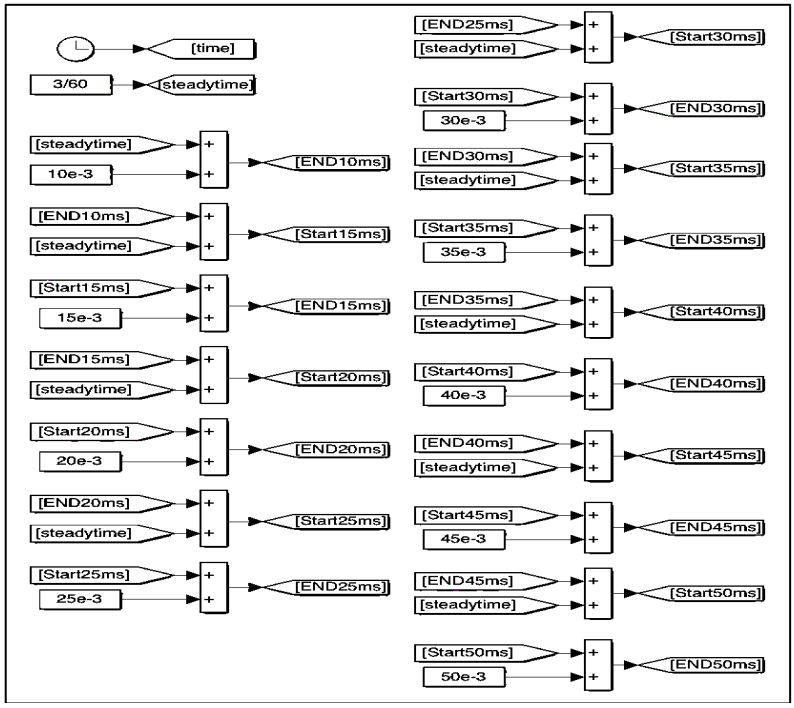

Figure 37. Fault Duration Start and End times

Start and stop times for each duration of fault, ranging from 10 ms to 50 ms, are calculated in a subsystem of the load model.

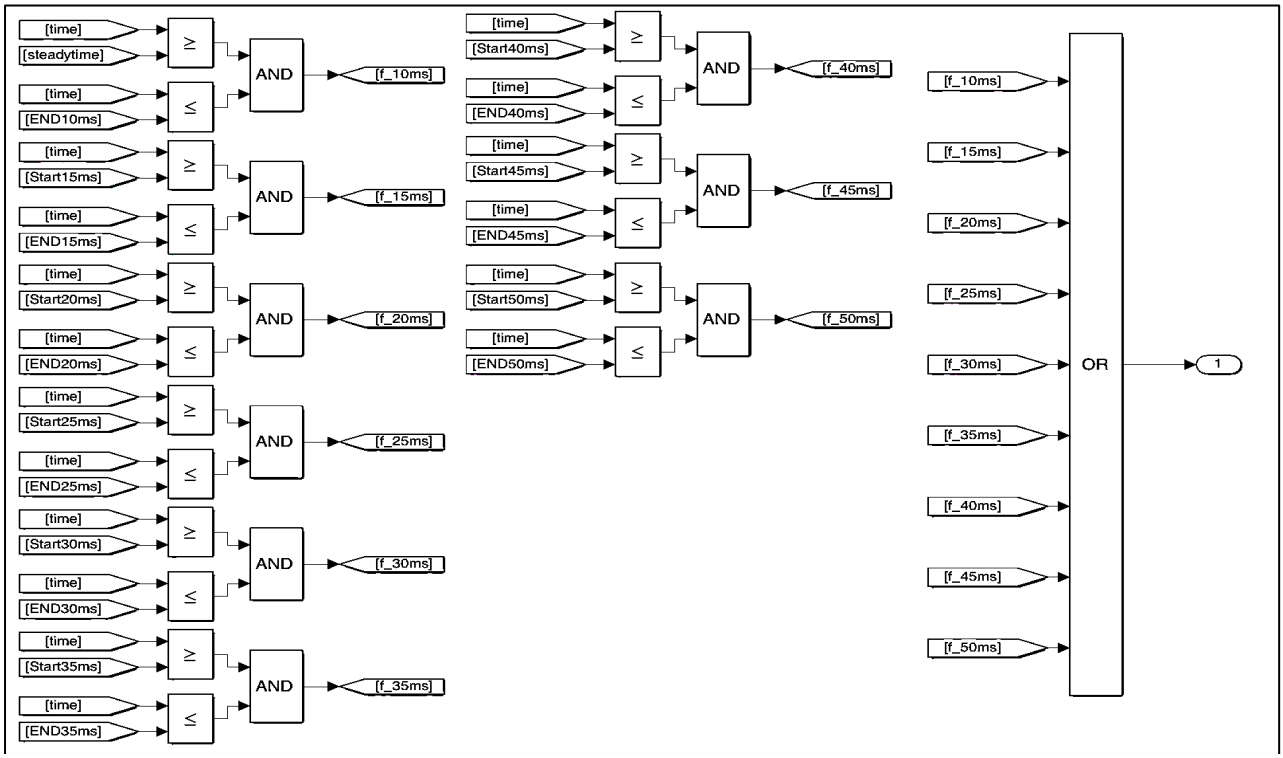

Figure 38. Fault Duration Logical Implementation

Logic design utilized in implementing a Boolean signal, initiating each fault at the established time range.

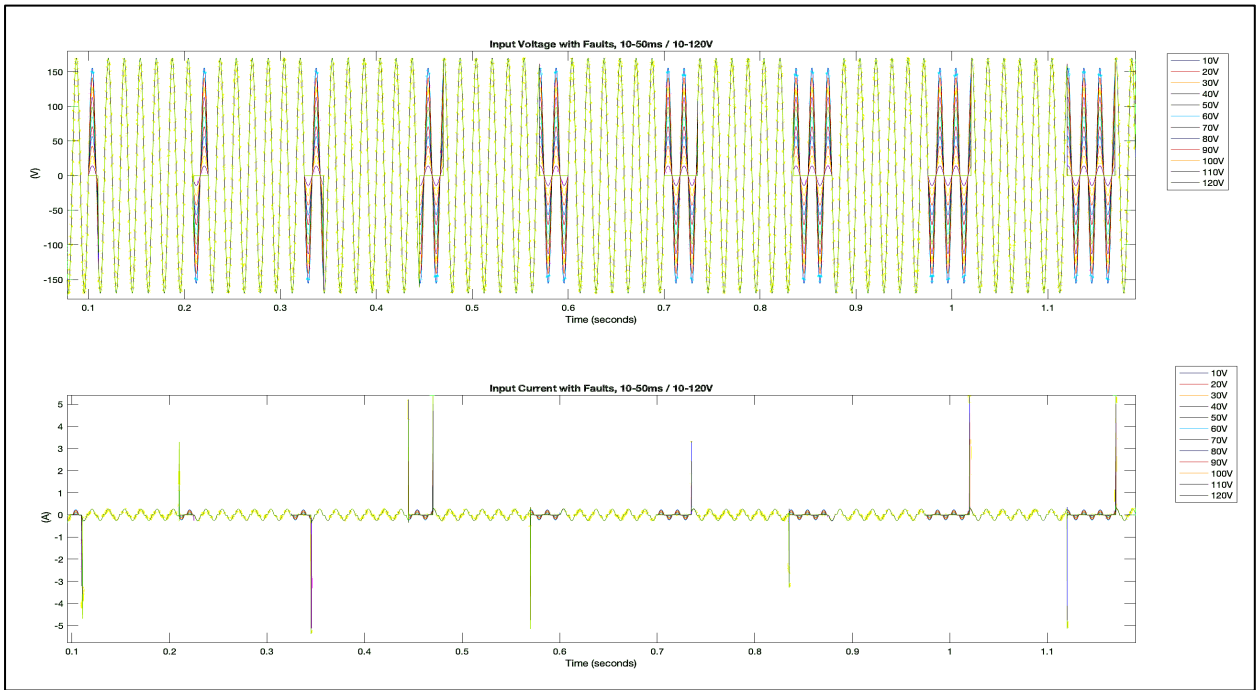

Figure 39. Load Model Input Behavior During Fault Scenarios

Current and Voltage Waveforms characterizing input behavior of the load model under faults of 0 V to 120 V, for 10 ms to 50 ms.

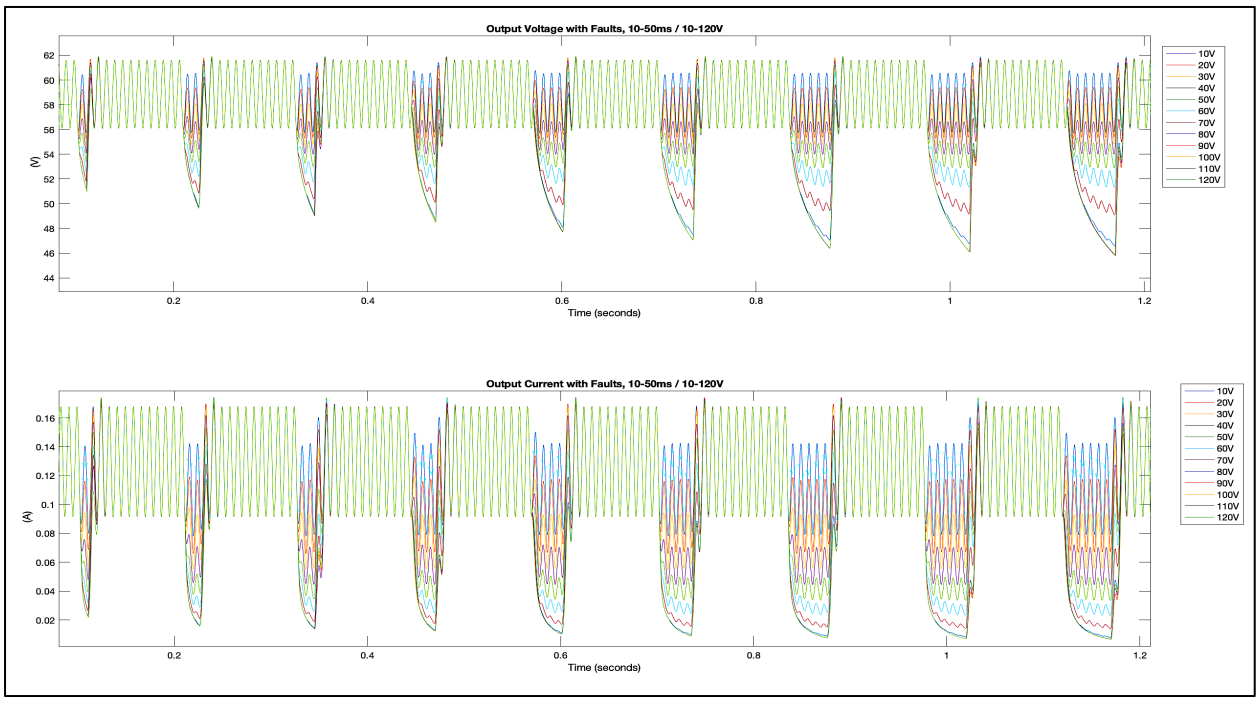

Figure 40. Load Model Output Behavior During Fault Scenarios

Current and Voltage Waveforms characterizing output behavior of the load model under faults of 0 V to 120 V, for duration of 10 ms to 50 ms.

square range of 10 V to 120 V difference from rated operation, of 120 V_{RMS}. Data extrapolated from testing was plotted for visualization of the relationship which fault location has on current impulse during fault initiation. The observed relationship is portrayed in Figure 42.

As Figure 41 illustrates, the magnitude of current impulse was observed to increase in proportion to the increase in fault magnitude within the system. Further, the impulse is observed to have a sinusoidal relationship with fault location. When a fault is induced at the zero crossing of voltage input, the input current does not exhibit a spike in current. However, the input current impulse increases in magnitude with a fault introduction in closer proximity to the peak condition of input voltage condition.

5.3LED Bulb Load Model Fault Scenario Interactive Test Interface

5.3.1 Interactive Interface for Dynamic Load Model Testing

The LED bulb load model was designed with the intent to emulate device behavior during grid scenarios, similar to that established at UTK's HTB. Further manipulation of the dynamic test model was implemented, in creation of an interactive user interface. The established component-based load model simulation was used as a baseline in accomplishment of this interfaced design.

Trivial adjustments were made to the model such that a user could apply a chosen disturbance to be visualized during simulation. The constant value for magnitude of fault, at the voltage power supply, was replaced with a global variable. This variable was linked to a dial on the dashboard window, that allowed the user to adjust the value of fault magnitude during testing.

Additionally, the Induce_Fault variable, that had been previously used in implementation of fault duration, was adjusted to portray the state of a button, placed within the dashboard. When the button was held, a Boolean truth, equivalent to 1, was sent to Induce_Fault. In doing so, the

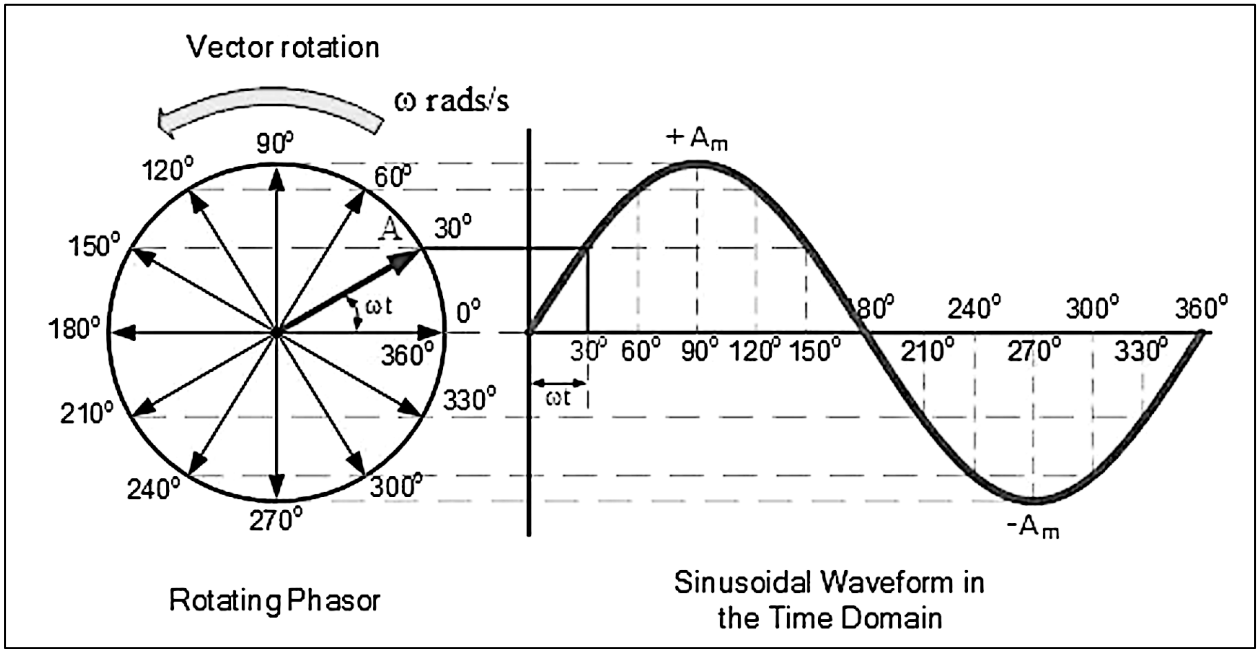

Figure 41. Fault Locations Unit Circle Representation

Visualization of the locations utilized for testing various fault locations on input voltage condition for analysis of the effects on input current behavior [85].

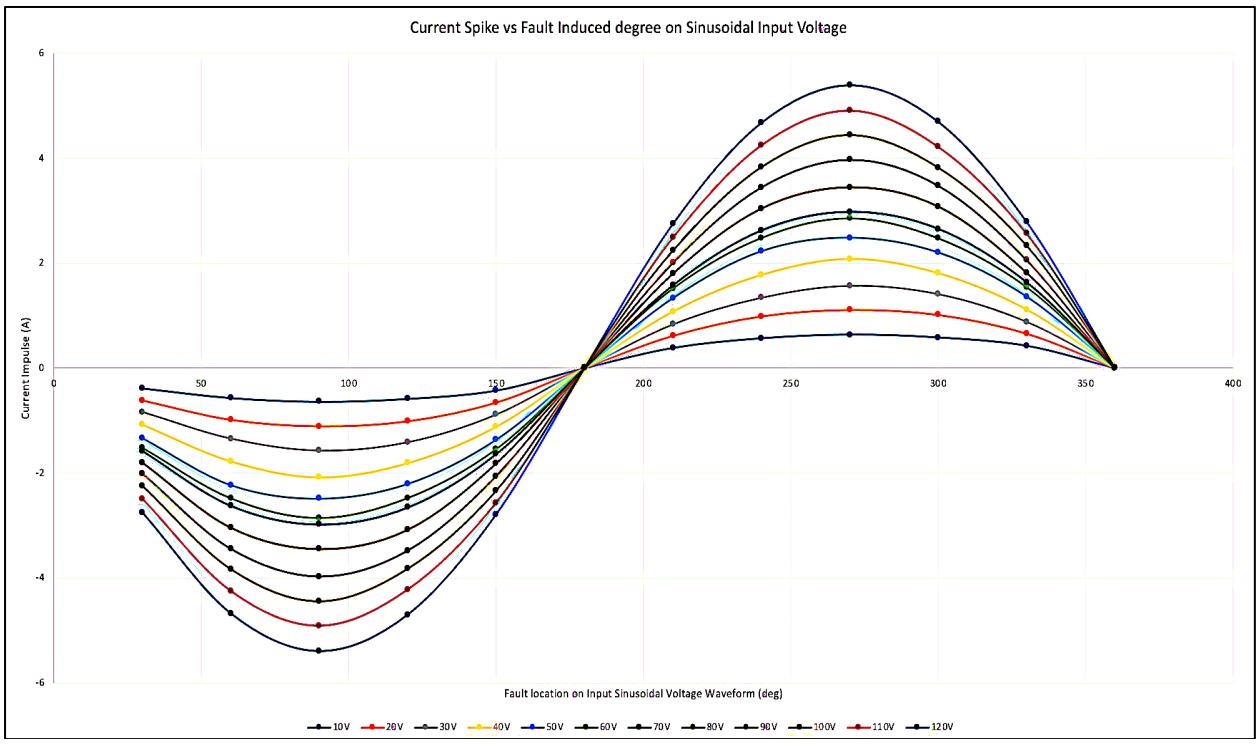

Figure 42. Fault Locations Unit Circle Representation

Visualization of the locations utilized for testing various fault locations on input voltage condition for analysis of the effects on input current behavior.

fault condition was implemented across the load model's supply terminals. The subsequent system pertaining to fault duration was removed from the model, as the duration of time the button was held by the user directly correlated to the duration of time the fault would remain.

Dashboard scopes that exhibited input and output conditions are also included for observation of the load model behavior throughout testing. These scopes were oriented to include a small snapshot of the model's working behavior at input and output terminals throughout the duration of the test. Once testing was complete, the modified load model simulation was accessible to users from the dashboard. Primary scopes with improved visualization of the load model's behavior were accessible within this system.

Further, depiction of the illumination state of the bulb was depicted on the user interface dashboard of the load model. Logic design principles were utilized in analysis of the output conditions of the load model. When the measured output conditions did not reflect those necessary for illumination of the device, the dashboard light would turn off, signifying the cease in function of the device for intended purpose. Depiction of the dashboard with on and off state light and randomized fault scenarios are provided in Figures 43 and 44. In establishment of a dashboard interface which allows users to interact with the model, the component-based load model provided improved comprehension of device operation in real time conditions.

5.3.2 Duration of Fault Scenarios for Bulb Failure in Illumination Test Procedure

The formulated interactive interface, for observation of the LED Bulb's dynamic behavior, was utilized in observation of device illumination throughout fault events. Within the interactive module, the acquired simulation data is recorded throughout induced fault scenarios. Access to the numerical data is automatically exported to the MATLAB workspace environment for compilation and analytical analysis.

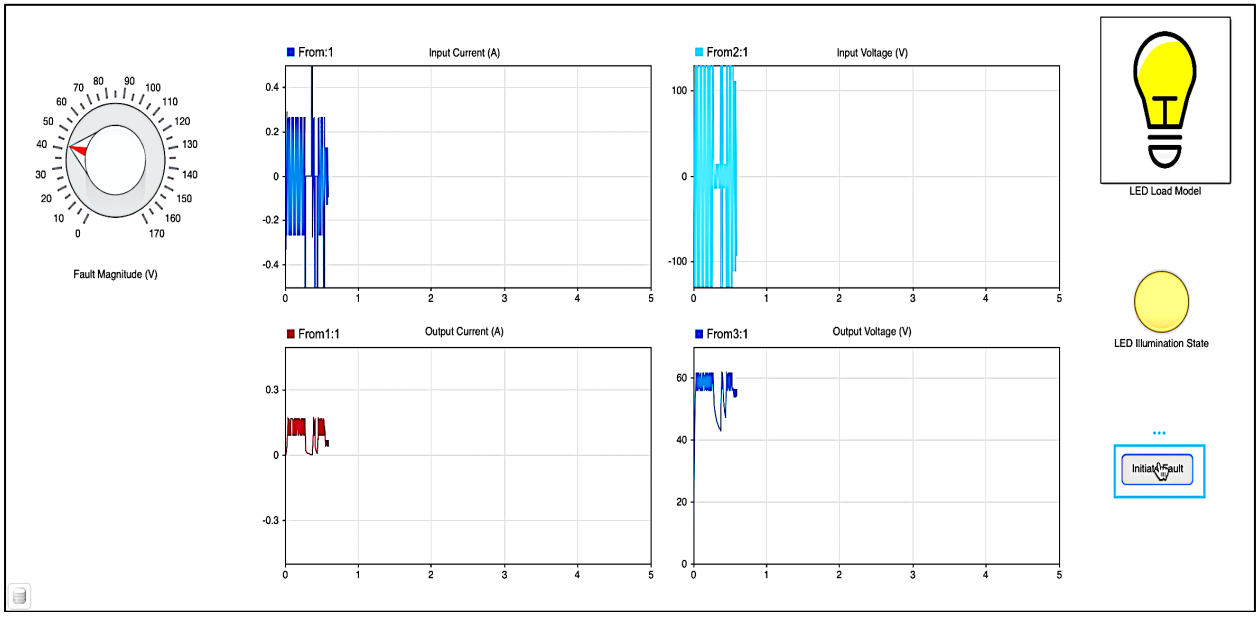

Figure 43. Interactive Dynamic Load Model with Illumination

Visualization of the interactive, user dashboard formulated for comprehensive dynamic testing of the load model during real time. Randomized faults are implemented using the by setting fault magnitude with the dial and holding the button for desired fault time. Illumination state remains on under the presence of a 40 V fault.

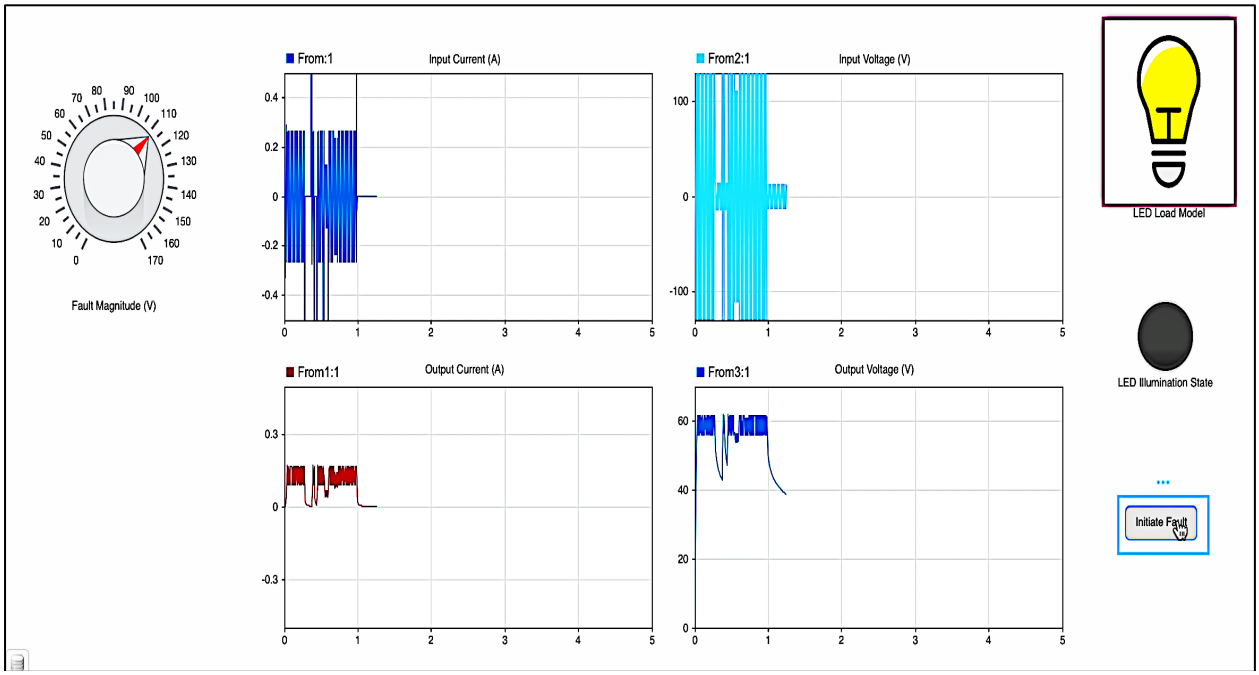

Figure 44. Interactive Dynamic Load Model with Affected Illumination

Visualization of the interactive, user dashboard formulated for comprehensive dynamic testing of the load model during real time. Randomized faults are implemented using the by setting fault magnitude with the dial and holding the button for desired fault time. Illumination state becomes affected under the presence of a 110 V fault for long duration of time.

Observation in simulated and laboratory testing showed that illumination of the LED bulb is not perceptible to the naked eye when output voltage conditions are below 40 V. Preliminary testing was completed, within the interactive dynamic test interface, in exploration of the minimum fault voltage magnitude which would affect device illumination. Fault voltage magnitude was defined as the difference in applied input voltage from standard operation, being 120 V_{RMS} condition, expressed in **(30)**.

$$\boldsymbol{V_{During\ Fault} = 120\sqrt{2} - (Fault\ Magnitude) * \sqrt{2}} \quad \textbf{(30)}$$

Initial exploration of the minimum fault magnitude, that would affect device illumination, was completed in 10 V decrements beginning at 120 V. Faults were induced for an extended duration of time until steady-state conditions were achieved, in the presence of the fault. It was observed, through the simulation interface, that device functionality in lighting no longer became affected at a fault magnitude of 80 V. Meaning, any fault possessing a magnitude less than 80 V would not affect the illumination of the device, regardless of the duration which the fault was present. Thus, the LED bulb was able to ride through faults of less that 80 V magnitude and maintain functionality.

Once the approximate minimum was retained for fault magnitude, testing commenced in investigation of the fault duration at various magnitudes. Fault duration referred to the amount of time, in seconds, that the fault would be present within the system. Through comprehensive simulation scenarios, the time necessary for the bulb's illumination to be affected was quantified at respective fault magnitudes.

Beginning at a 120 V magnitude, the interface was utilized to implement a fault throughout the device until illumination state became affected, allowing output voltage to sag below the 40 V threshold for functionality. Once illumination state was affected, the fault was removed from the

system and operation was allowed to return to the rated operating conditions. Following this, the magnitude of the fault induced was decremented by 1 V and introduced to the system once more until illumination became affected.

5.3.3 Fault Duration at Various Fault Magnitudes for Illumination Failure Results

This testing process was repeated until device illumination no longer became affected by the fault magnitude, with final test condition occurring at exactly 87 V. At a fault magnitude of 87 V (120 V nominal – 87 V sag such that system dropped to 33 V), the output voltage waveform oscillated above and below the functional threshold. As a result, the simulation appeared to initially flicker between on and off state prior to setting in the off state, with no illumination. At fault magnitude conditions below 87 V, the bulb remained with illumination and did not exhibit flickering, making this the minimum rated magnitude for fault duration testing in observation of bulb functionality throughout dynamic events.

Data which had been exported to the MATLAB model workspace from testing was observed through code-based analysis. The associated waveforms were compiled and plotted for comparison. Input behavior waveforms are plotted in Figure 44 and output conditions are visualized in Figure 45. Additional incorporation of a test condition with fault magnitude of 86 V was incorporated for illustration, showing that while dimming at lower conditions occurs, the bulb's illumination state remained on, as conditions do not cross the 40 V functional output condition threshold.

Data was extrapolated from the behavioral waveforms pertaining to input and output voltage conditions. The time of fault introduction was recorded with respect to each fault magnitude scenario from the observed input voltage behavior. Further, the output voltage behavior was utilized in determination of the time which voltage sagged below the 40 V illumination

threshold. The difference in time between fault introduction and sag to 40 V condition was calculated. This difference represented the duration of time, at specified fault magnitude, for the bulb's illumination to be affected, as shown in **(31)**.

$$t_{illumination\ failure} = (t_{fault\ introduced}) - (t_{V_{output}\,=\,40\,V}) \quad (31)$$

The duration of time for the bulb's illumination to be affected was compiled with respect to the tested fault scenario's magnitude of fault. The acquired data was plotted for representation of the relationship between fault duration and fault magnitude, which exhibited exponential decay. It was determined that at fault magnitudes of 87 V to 90 V the duration of time for illumination failure exhibited an exponential decay relation, displayed in Figure 46.

Upon reaching 90 V, all fault magnitudes above this condition remained relatively constant in duration of time for failure in illumination. At fault magnitudes of 90 V and above, a dynamic event for approximately 194.5 ms would result in effects on bulb illumination. Thus, faults of 87 V magnitude, and above, require mitigation in 194.5 ms to maintain operation of the device for lighting.

5.4 Chapter Summary

In chapter five, the methodology and reasoning behind dynamic characterization of the established load model was discussed in detail. Simulation and affiliated measurements, in observation of load model behavior, under the presence of faults, ranging in magnitude and duration were exhibited. Analysis on the effect of fault duration and magnitude on the load model's behavior and functionality as a lighting device was illustrated.

Findings were correlated in relationship to power grid operation. Utilization of these methods, for improvement in both device and integrated system reliability, were discussed. The

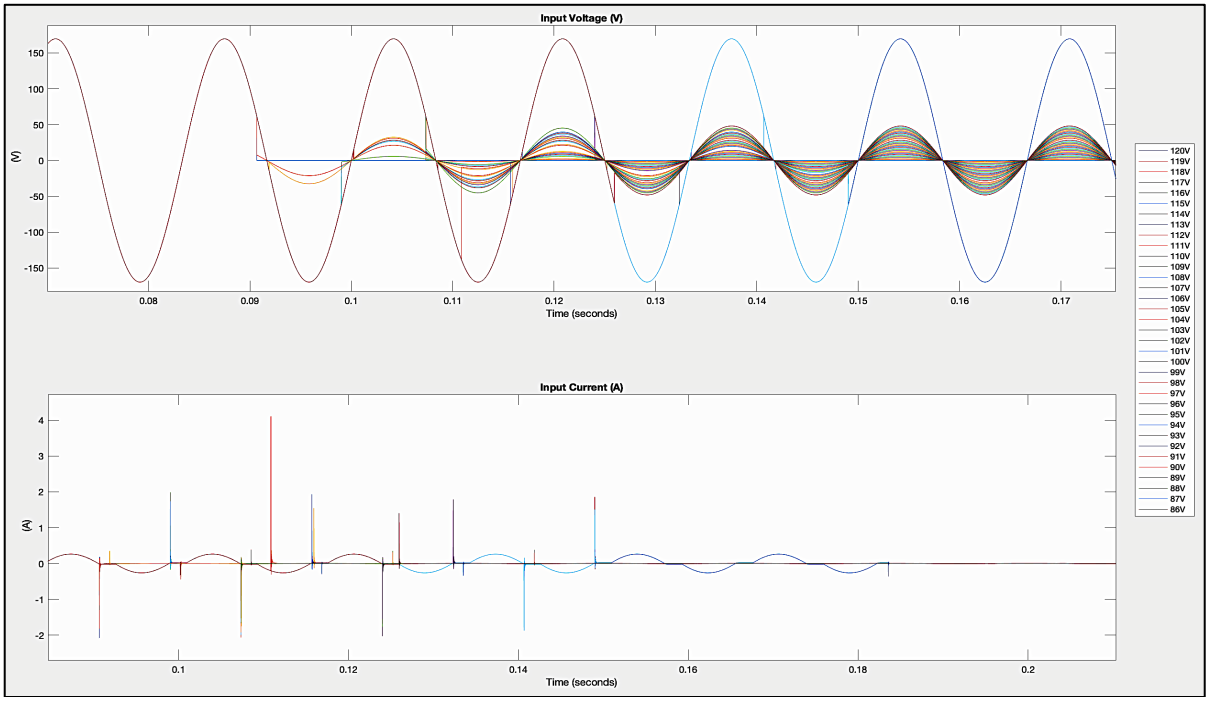

Figure 45. Input Waveforms for Fault Induced Illumination Failure

Visualization of the input voltage and current waveforms for determination of the effects on fault magnitude and fault duration on bulb illumination.

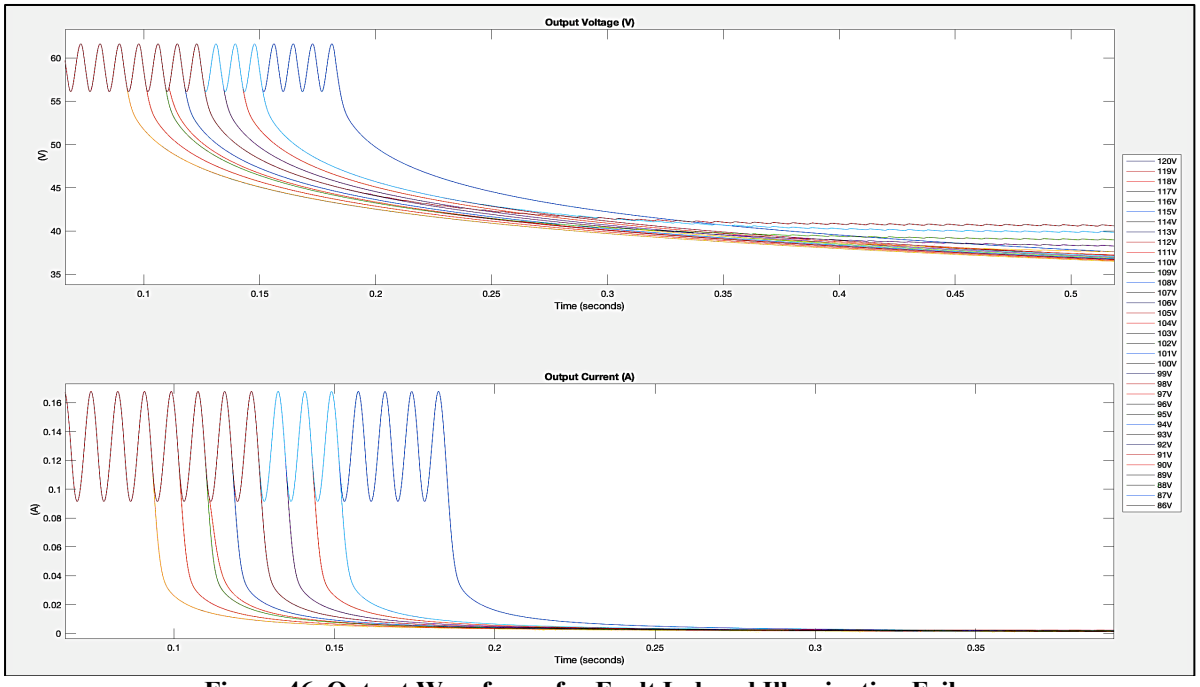

Figure 46. Output Waveforms for Fault Induced Illumination Failure

Visualization of the output voltage and current waveforms for determination of the effects on fault magnitude and fault duration on bulb illumination.

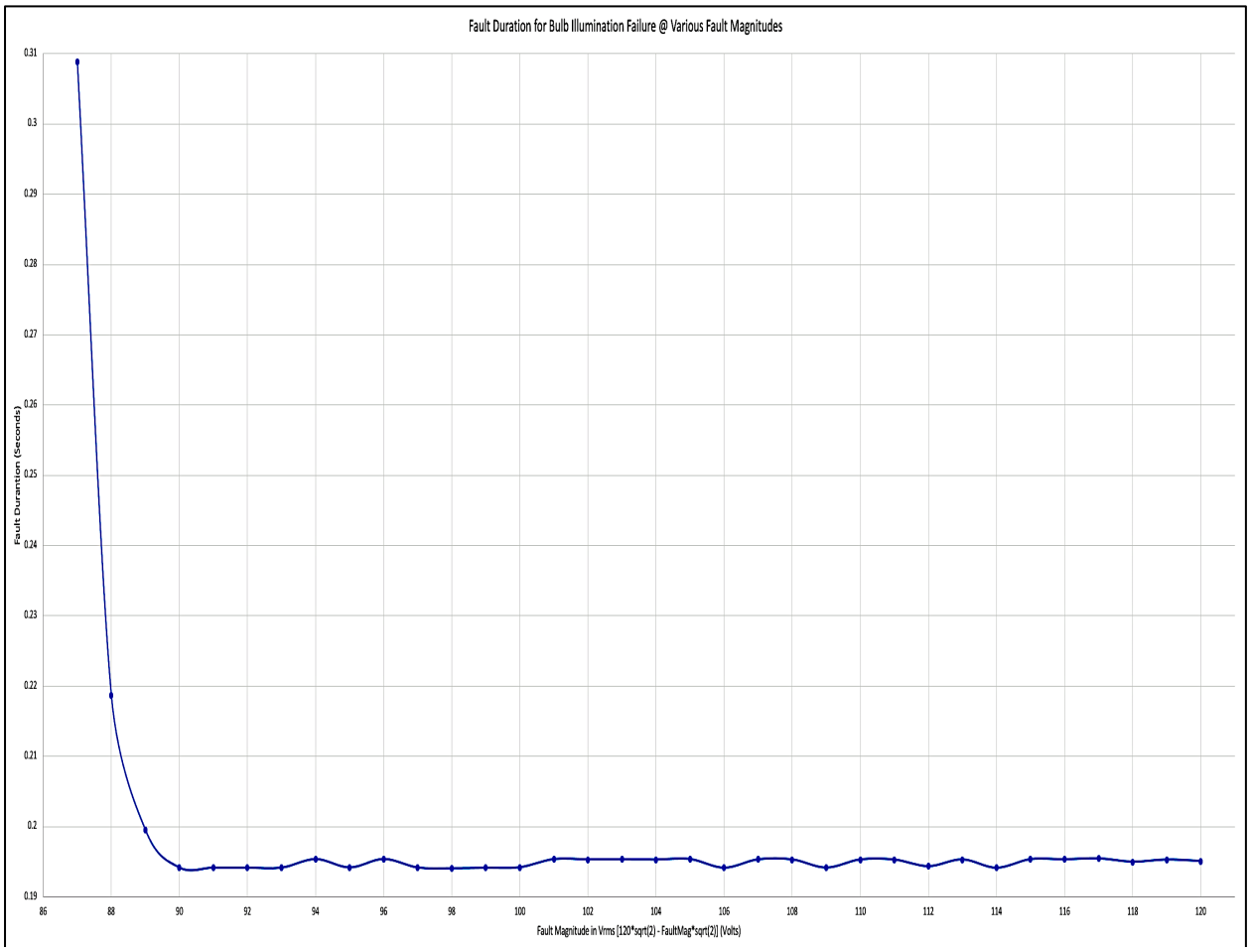

Figure 47. Interactive Dynamic Load Model with Affected Illumination

Visualization of the interactive, user dashboard formulated for comprehensive dynamic testing of the load model during real time. Randomized faults are implemented by setting fault magnitude with the dial and holding the button for desired fault time. Illumination state becomes affected under the presence of a 110 V fault for long duration of time.

benefit of dynamic characterization of load models was emphasized to provide future researchers opportunity for mitigation of threats to the system's reliability. In doing so, they might establish working systems in integration that compensate for the impending effects associated with LED bulb usage under worst case scenario fault.

Work exhibited in the characterization of dynamic faults was applied in the formulation of an interactive, real-time load model test interface. With reference made to UTK HTB grid emulators, the interactive dashboard and affiliated load model were adjusted for user input, via dashboard, in dynamic analysis of the device model. The benefit of interactive elements allowing user defined disturbance was highlighted with additional features addressed, such as the depiction of the modeled device's illumination.

The established emulation module allows users to not only interact with the load model in observation of the impending effects of fault scenarios on the system of integration, but also observe the effect of an induced fault scenario of the function of the device for intended purpose. Inclusion of this component aimed to additionally provide researchers opportunity for providing supply conditions that enabled consistently accessible lighting to users.

CHAPTER 6
CONCLUSIONS AND RECOMMENDATIONS

In recent years, the lighting industry has been revolutionized through the invention and adoption of the LED bulb. As historical lighting trends indicate, the commercial and residential market has enthusiastically welcomed the adoption of LED bulbs as a primary source of lighting. Capable of improved efficiency, operational lifespan, minimal power consumption, and quality of illumination, LED bulb utilization has steadily been adopted throughout all utility sectors. The device currently occupies the majority of the market for area lighting and is predicted to continue to show increased integration in coming years.

Due to the rapid adoption of LED bulbs for lighting, the effects of the device's integration within the power grid must be addressed. Analysis of end-use power consumption, throughout utility sectors, indicates the influential nature of lighting devices within the power grid. For improved operation, reliability, and security of the power grid, behavior of the LED as a load requires comprehension. Load modeling methodologies in device characterization assist in describing the bulb's behavior within ambient conditions, providing vital information on the effects of device utilization on affiliated grid technologies and function of the device for illumination.

Through various techniques of load modeling, a simplified model that represents the device's behavior as a load may be achieved, approximating the relationship between voltage and current within the device to a constant impedance, voltage, or current relationship. For complex power electronic devices, load modeling becomes more convoluted. Attributes and pitfalls of each load modeling technique influences choice of implementation for analysis of the device's behavior in characterization.

Previously, researchers employed measurement-based ZIP modeling principles, in characterization of the LED bulb as a load. Measurement-based techniques are restricted in accurate representation to conditions tested in establishment of the model. In this regard, transient behavior of the modeled device throughout dynamic events is not efficiently addressed in measurement-based load models. Adoption of ZIP modeling, for analysis of a power system with LED bulb integration, can provide ambiguities in operation, hindering accuracy in emulation.

Emulation of grid-level scenarios provides comprehensive understanding on the effects of disturbances and opportunity for mitigation of failures within the system. For accurate reflection of grid behavior, emulators require consistent adaptation in reflection of emerging technologies in utilization, achievable through development and aggregation of load model profiles. As LED bulbs are considered an emerging and influential device within utility applications, design of a load model that depicts accurate behavior of a standard bulb is crucial for maintaining precision in grid emulation. As effort in this thesis was focused on establishing a working load model of the LED bulb for analysis, future work toward the integration of the established model within grid emulator systems, such as the UTK HTB, will provide comprehensive illustration of the LED bulb's effect on affiliated technologies throughout the grid.

A component-based load model, in representation of the LED bulb, provides improved accuracy in characterization of the device, with inclusion of transients under a plethora of grid-level scenarios. In depiction of a conventional bulb's behavior, the model must pay respect to LED bulbs within the lighting market. Through analysis of LED device market trends, power electronic principles, and comparison of manufactured topologies, a generalized load profile can be formulated in depiction of a LED bulb as a load.

In formulation of a standard LED bulb's component-based load model, parameters of electrical elements within the topology were tuned to represent typical bulbs and specified to a particular device utilized during laboratory testing. Comparison was drawn between exhibited behavior of the device during the described laboratory testing and simulation of the load model. Verification of the established load model's emulated device behavior is achieved through this steady-state analysis and comparison. As the established model acts a baseline for representation of a typical LED bulb, future work toward application of the load model for various manufactured LED bulbs can further provide precision in grid emulation.

Behavior of the device and load model was observed to portray both constant impedance and constant power type load characteristics, dependent on the applied steady-state operating condition. Simulation of the verified load model was adjusted for representation of device behavior under the presence of dynamic grid conditions, with a range of fault magnitudes and durations. Transient effects and mitigation of potential failures, caused by load model dynamic response, is addressed through simulation of conventional fault scenarios. Research may be furthered through testing of dynamic disturbances in a wider range of fault magnitudes and fault duration. In doing so, compensation techniques, for the load model's dynamic response, have the potential to be designed for incorporation within the grid providing improved system reliability.

A dashboard interface was established for user interaction in real-time manipulation and observation of load model behavior during an induced fault. From this, emulation of the LED bulb as a grid load is visualized for analysis of effects on affiliated grid technologies. Inclusion of device function, for the manufactured intention of light production, is incorporated for illustration of the additional effect dynamic conditions have on the device itself. In doing so, researchers are provided the opportunity to not only work toward incorporating compensation technologies in the mitigation

of failures and improved reliability of the grid, but also work toward maintaining supply conditions to the bulb that allow for continuous access to lighting. With this regard, a brighter future may be achieved.

LIST OF REFERENCES

[1] N Grandjean 2010 J. Phys. D: Appl. Phys. **43** 350301

[2] Susan Walsh Sanderson, Kenneth L. Simons, Light emitting diodes and the lighting revolution: The emergence of a solid-state lighting industry, Research Policy, Volume 43, Issue 10, 2014, Pages 1730-1746, ISSN 0048-7333, https://doi.org/10.1016/j.respol.2014.07.011.

[3] Edirisinghe, Kamal & Abeyweera, Ruchira & Senanayake, N.. (2016). Evaluation of Effectiveness of LED Lighting in Buildings. SLEMA Jornal. 19. 10.4038/slemaj.v19i2.10.

[4] Krch, Anas Al. "LED ZIP Model Development." University of Nebraska-Lincoln, The Graduate College of The University of Nebraska, 2020, pp. 2–122.

[5] A. Arif, Z. Wang, J. Wang, B. Mather, H. Bashualdo and D. Zhao, "Load Modeling—A Review," in IEEE Transactions on Smart Grid, vol. 9, no. 6, pp. 5986-5999, Nov. 2018, doi: 10.1109/TSG.2017.2700436.

[6] Collin, A.J. & Acosta, J.L. & Hayes, Barry & Djokic, Sasa. (2010). Component-based aggregate load models for combined power flow and harmonic analysis. 1 - 10. 10.1049/cp.2010.0901.

[7] Ayothi, Manimuthu. "What Is Power System, How Power System Works." Electrical4u, 23 June 2018, https://www.electrical4u.net/electrical/power-system/#:~:text=Power%20system%20is%20a%20network,transferred%20to%20the%20transmission%20line.

[8] Sairam, Seshapalli & Daram, Suresh & Venkataramu, P..s & Nagaraj, M.. (2018). Analysis of exponential and polynomial load models using newton-raphson method with hybrid power flow controller. International Journal of Control and Automation. 11. 43-56. 10.14257/ijca.2018.11.11.04.

[9] Kuphaldt, Tony R., and John Haughery. "Power Factor Correction." *Applied Industrial Electricity*, Iowa State University Digital Press, 1 June 2020, https://iastate.pressbooks.pub/electriccircuits/chapter/power-factor-correction/#:~:text=For%20the%20purely%20resistive%20circuit,the%20reactive%20power%20equals%20zero.

[10] Eugen. "Are LED Lights Inductive or Resistive Load? - Led & Lighting Info." *LED & Lighting Info - Useful Tips To Improve Design*, 21 Nov. 2021, https://ledlightinginfo.com/are-led-lights-inductive-or-resistive-load.

[11] Bhuiyan, Md Abul Ehsan & Yang, Feifei & Biswas, Nishan Kumar & Rahat, Saiful & Neelam, Tahneen. (2020). Machine Learning-Based Error Modeling to Improve GPM IMERG Precipitation Product over the Brahmaputra River Basin. Forecasting. 2. 248-266. 10.3390/forecast2030014.

[12] J, Gaurav. "Types of Electrical Load: Resistive, Inductive & Capacitive Load." *TheElectricalGuy*, Gaurav J Https://Secure.gravatar.com/Avatar/87a2d2e0182faacb2e003da0504ad293?s=96&d=Mm&r=g, 30 Aug. 2020, https://www.theelectricalguy.in/tutorials/types-of-electrical-load-resistive-inductive-capacitive-load/.

[13] *What Is a Power Triangle? - Quora*. https://www.quora.com/What-is-a-power-triangle.

[14] Gopstein, Avi, et al. “Summary Report on NIST Smart Grid ... - TSAPPS at NIST.” *National Institute of Standards and Technology*, U.S. Department of Commerce, Mar. 2021, https://tsapps.nist.gov/publication/get_pdf.cfm?pub_id=931609.
[15] *Curent*, https://curent.utk.edu/contact-us/facilities/university-of-tennessee/.
[16] Dingrui Li1, Yiwei Ma1, Chengwen Zhang1, He Yin1, Yu Su1, Ishita Ray1, Lin Zhu1, Montie Smith1, Evan McKee1 Fred Wang1,2, Leon Tolbert1,2, Yilu Liu1,2 1 The University of Tennessee, Knoxville 2 Oak Ridge National Laboratory. “Microgrid Test with Hardware Testbed Platform - Curent.utk.edu.” *Microgrid Test with Hardware Testbed Platform*, CURENT, https://curent.utk.edu/2018SiteVisit/Li_Dingrui_UTK_Wang_1.pdf.
[17] Center for Ultra-Wide-Area Resilient Electric Energy Transmission Networks, et al. “2021 Annual Industry Conference.”
[18] Tolbert, Leon M. “Reactive Compensation.” 8. ECE 625 fall 2021 lecture 8, Knoxville, University of Tennessee.
[19] Tolbert, Leon M. “Diode Rectifiers.” 13. ECE 625 fall 2021 lecture 13, Knoxville, University of Tennessee.
[20] Tolbert, Leon M. “Generalized Power Theory.” 7. ECE 625 fall 2021 lecture 7, Knoxville, University of Tennessee.
[21] Tolbert, Leon M. “Transmission Interconnections.” 1. ECE 625 fall 2021 lecture 1, Knoxville, University of Tennessee.
[22] Wang, Shuyao. *Grid Frequency in Normal Summer with Responsive Load Support V.s. without Responsive Load Support*. University of Tennessee, Knoxville, 2020.
[23] Tolbert, Leon M. “CURENT System Demonstration in HTB.” 10. Year 10 HTB Mini-Report Quad-Chart Spring 2021, Knoxville, University of Tennessee.
[24] Kurtus, Ron. “List of Worldwide AC Voltages & Frequencies.” *Ron Kurtus' School for Champions*, Ron Kurtus, 13 Feb. 2016, List of Worldwide AC Voltages & Frequencies.
[25] “Frequently Asked Questions.” *SST Inc*, https://www.sunlitest.com/faq/do-led-lights-run-on-ac-or-dc-current/.
[26] “What Is the Most Common Light Bulb Size?” *True DIY : Your Number One Source for Everything DIY, Crafts and Handmade*, 12 Nov. 2021, https://truediy.net/diy-crafts/what-is-the-most-common-light-bulb-size/.
[27] Staff, Waveform. “Everything You Need to Know about A19 Bulbs.” *Waveform Lighting*, Waveform Lighting, 10 July 2018, https://www.waveformlighting.com/home-residential/everything-you-need-to-know-about-a19-bulbs/.
[28] Silvan, Nyla, and About The Author Nyla Silvan. “Decoratingspecial.com.” *Counter Create Hit*, 28 Dec. 2015, https://www.decoratingspecial.com/standard-light-bulb-dimensions/.
[29] Nick. “Top 10 Largest LED Lighting Manufacturers in 2019: Global Led Market.” *Technavio*, Technavio, 25 Mar. 2020, https://blog.technavio.org/blog/top-10-largest-led-lighting-manufacturers.
[30] Anwell Semiconductor Corp. “AP1910 Universal High Brightness LED Driver Controller.” AnSC, 2012.
[31] SILERGY. “Applications Note: SY22653 Single Stage Non-Isolated Flyback and PFC Regulator for Warm/Cold White LED Color Mixing and Dimming Application.” Silergy Corp. Confidential, 2018.
[32] Rowe, Martin. “Teardown: A19 Led Bulb.” *EDN*, 22 Jan. 2018, https://www.edn.com/teardown-a19-led-bulb/.

[33] Texas Instruments Incorporated. “Using the TPS92075 BUCK Converter.” TI, 2013.
[34] OF-SMD3528WW. “Specification For 3528 Single Chip Warm White Color Top LED.”
[35] California Instruments. “Portable AC Power P Series.” California Instruments Corp. , 1999.
[36] Stackpole Electronics, Inc. “CF / CFM Series Carbon Film Resistor.” Resistive Product Solutions, 3 Mar. 2022.
[37] Cornell Dubilier. “MKP Boxed Metallized Polypropylene Film Capacitor.” Illinois Capacitors Inc., Sept. 2021.
[38] Yageo. “DATA SHEET GENERAL PURPOSE CHIP RESISTORS RC_L Series.” PhiCorp, 15 May 2020.
[39] TDK Capacitors. “Capacitor with Multi-Layer Lead FK Series.” TDK, 2015.
[40] Bourns. “RLB Series Radial Lead Inductors.” Bourns Inc., 31 Mar. 2015.
[41] Taiwan Semiconductor. “ABS02-ABS10 1A, 200 - 1000V Standard Bridge Rectifier.” TSC, 18 Aug. 2004.
[42] Knowles. “High Q Capacitors - Q(MS) & U Ranges.” DLI-JohansonMFG-Novacap-Syfer-Voltronics, 2015.
[43] Unisonic Technologies Co., LTD. “4N60- 4A, 600V N-CHANNEL POWER MOSFET .” UTC LTD, 4 Sept. 2013.
[44] Panasonic. “Anti-Surge Thick Film Chip Resistors (Double-Sided Resistive Elements Structure) 0805.” Panasonic Industry, 1 Oct. 2019.
[45] Nexperia. “RB751 Series Schottky Barrier Single Diodes.” Nexperia BV, 21 May 2007.
[46] Panasonic. “Thick Film Chip Resistors- ERJ Type.” Panasonic Industry, 1 Oct. 2019.
[47] Samsung. “CL05A104KA5NNNC Specification Sheet.” Samsung Electro-Mechanics.
[48] OF. “Specification For 3528 Single Chip Warm White Color Top LED.” RoHS, 2019.
[49] Hummel, Anita. “What Are the Standard Light Bulb Base Socket Types and Sizes?” *Mondoro*, Mondoro, 12 Jan. 2022, https://mondoro.com/what-is-the-standard-light-bulb-base-different-e-socket-types/.
[50] Feit Electric Store. “FEIT Electric Led Light Bulbs, 60 Watt Equivalent (8.8 ...” *Feit Electric LED Light Bulbs, 60 Watt Equivalent (8.8 Watt) A19 Dimmable LED Bulb, Color Daylight (5000K) 800 Lumen, CEC Title 20 Compliant Energy Star 90+ CRI Light Bulb, 4-Pack*, Amazon, https://www.amazon.com/Feit-Electric-Equivalent-Dimmable-Compliant/dp/B07P5HBD91.
[51] “Leviton 600-Watt 250-Volt White Outlet Box Lampholder R50-49875-000.” *The Home Depot*, https://www.homedepot.com/p/Leviton-600-Watt-250-Volt-White-Outlet-Box-Lampholder-R50-49875-000/207106566.
[52] CURENT. “Curent Student Wiki.” *Start [CURENT Student Wiki]*, The University of Tennessee Knoxville EECS, https://wiki.curent.utk.edu/.
[53] “X-Tronic - Model 3020-XTS Led Soldering Station.” *XTronicUSA*, XTronic, https://xtronicusa.com/X-Tronic-Model-3020-XTS-LED-Display-Soldering-Station-p74220205.
[54] “Single Strand Hookup Wire - 22AWG (Gauge) - Red - 5 Metre.” *ElectronicsComp.com*, Electronics Co., https://www.electronicscomp.com/single-strand-hookup-wire-22awg-red-5metre.
[55] “Single Strand Hookup Wire - 22AWG (Gauge) - Black - 5 Metre.” *ElectronicsComp.com*, Electronics Co., https://www.electronicscomp.com/single-strand-hookup-wire-22awg-black-5metre?search=Single+Strand+Hookup+Wire+-+22AWG.

[56] "Wire Stripper 22-10 AWG." *ElecDirect*, https://www.elecdirect.com/tools/wire-cable-strippers/wire-stripper-22-10-awg.
[57] "Chicago Electric 9.6 Volt Cordless Variable Speed Rotary Tool Kit – Item 63389 / 63234 / 69336 / 69946 / 92880." *Harbor Freight Coupons*, Harbor Freight , https://go.harborfreight.com/sku/63389/.
[58] "Klein Tools 7-Piece Cushion-Grip Screwdriver Set." *KleinTools.com*, 16 Apr. 2022, https://www.kleintools.com/catalog/screwdriver-sets/screwdriver-set-slotted-and-phillips-7-piece.
[59] "About the U.S. Electricity System and Its Impact on the Environment." EPA, Environmental Protection Agency, https://www.epa.gov/energy/about-us-electricity-system-and-its-impact-environment#about.
[60] Zohuri, Bahman. (2016). Electricity, an Essential Necessity in Our Life. 10.1007/978-3-319-23537-0_2.
[61] "Electrification in Industrials." *Deloitte Insights*, https://www2.deloitte.com/us/en/insights/industry/power-and-utilities/electrification-in-industrials.html.
[62] "U.S. Energy Information Administration – EIA – Independent Statistics and Analysis." *Electricity Generation, Capacity, and Sales in the United States – U.S. Energy Information Administration (EIA)*, https://www.eia.gov/energyexplained/electricity/electricity-in-the-us-generation-capacity-and-sales.php.
[63] Lars Schmitz, Ryosuke Motani, Morphological differences between the eyeballs of nocturnal and diurnal amniotes revisited from optical perspectives of visual environments, Vision Research, Volume 50, Issue 10, 2010, Pages 936-946, ISSN 0042-6989, https://doi.org/10.1016/j.visres.2010.03.009.
[64] "Photoreception: Media." *Encyclopædia Britannica*, Encyclopædia Britannica, Inc., https://www.britannica.com/science/photoreception/images-videos.
[65] Madani, Vahid & Das, Ratan & Aminifar, Farrokh & McDonald, John & Venkata, S.s & Novosel, Damir & Bose, Anjan & Shahidehpour, M.. (2015). Distribution Automation Strategies Challenges and Opportunities in a Changing Landscape. IEEE Transactions on Smart Grid. PP. 10.1109/TSG.2014.2368382.
[66] *Griffith Institute: Carter Archives – 041A*, http://www.griffith.ox.ac.uk/perl/gi-ca-qmakesumm.pl?sid=141.211.81.29-1643996061&qno=1&curr=041a.
[67] Staff, Stouch Lighting. "The Historical Evolution of Lighting." *LED Lighting Distributor and Implementation Company*, 10 Feb. 2016, https://www.stouchlighting.com/blog/the-historical-evolution-of-lighting.
[68] "London's History of Gas Lamps." *Gas Lanterns and Lights*, 19 Jan. 2018, https://gaslanternsandlights.com/londons-history-gas-lamps/.
[69] "Revolución Industrial 1825882 Timeline." *Timetoast Timelines*, 1 Jan. 1764, https://www.timetoast.com/timelines/revolucion-industrial-1825882.
[70] "Edison's Lightbulb." *The Franklin Institute*, 19 May 2017, https://www.fi.edu/history-resources/edisons-lightbulb.
[71] BAKER, RAY STANNARD. *Boy's Second Book of Inventions*. OUTLOOK VERLAG, 2020.
[72] "40 Watt Standard Spiral CFL Bulb 2700K." *Shades of Light*, https://www.shadesoflight.com/products/40-watt-standard-spiral-cfl-bulb-2700k.

[73] Staff, Stouch Lighting. “Lighting Comparison: Led VS Fluorescent and CFL.” *LED Lighting Distributor and Implementation Company*, 13 Jan. 2016, https://www.stouchlighting.com/blog/fluorescent-vs-led-vs-cfl.
[74] “Led vs CFL: Which Lightbulb Is Most Energy Efficient.” *LED vs CFL Bulbs: Which Is Most Energy Efficient? | Perch Energy*, https://www.perchenergy.com/blog/energy-101/led-vs-cfl.
[75] “History of Leds - Light Emitting Diodes.” *History of LED - Development of Light-Emitting Diodes*, http://www.historyoflighting.net/light-bulb-history/history-of-led/.
[76] Edwards, Kimberly D. "Light Emitting Diodes" (PDF). *University of California at Irvine*. p. 2. Archived from the original (PDF) on February 14, 2019. Retrieved January 12, 2019.
[77] Admin, et al. “Nick Holonyak, ‘the Father of the LED."." *My LED Passion*, 15 Dec. 2020, https://myledpassion.com/history/nick-holonyak/.
[78] “Light Emitting Diode Working, Construction, Types and Application.” *Microcontrollers Lab*, 24 Apr. 2019, https://microcontrollerslab.com/light-emitting-diode-working/.
[79] “Candlelight-Style Organic Leds: A Safe Lighting Source after Dusk.” *SPIE Homepage*, https://spie.org/news/5070-candlelight-style-organic-leds-a-safe-lighting-source-after-dusk?SSO=1.
[80] *Light Bulb Comparison Chart Leds vs. Cfls vs ... - Energitix*. http://www.energitix.com/wp-content/uploads/2015/07/LED-vs-CFL-vs-Incandescent-Light-Bulb.pdf.
[81] “Led Light Bulb Conversion Chart.” *Lampsone*, https://www.lampsone.com/blog/led-light-bulb-conversion-chart/.
[82] Iea. “Global Lighting Sales, Historical and in the Net-Zero Scenario, 2010-2030 – Charts – Data & Statistics.” *IEA*, https://www.iea.org/data-and-statistics/charts/global-lighting-sales-historical-and-in-the-net-zero-scenario-2010-2030.
[83] M. Yamada, J. Penning, S. Schober, K. Lee, C. Elliott, and Navigant Consulting, Inc., “Energy Savings Forecast of Solid-state Lighting in General Illumination Applications,” Navigant Consulting, Inc., Washington, DC, Dec. 2019. Accessed: Mar. 01, 2022. [Online]. Available: https://www.energy.gov/sites/default/files/2020/02/f72/2019_ssl-energy-savings-forecast.pdf.
[84] “U.S. Energy Information Administration - EIA - Independent Statistics and Analysis.” *Use of Electricity - U.S. Energy Information Administration (EIA)*, https://www.eia.gov/energyexplained/electricity/use-of-electricity.php.
[85] *Why Is Sine Not a Wave Function? - Quora*. https://www.quora.com/Why-is-sine-not-a-wave-function.

VITA

Jillian Ruff was born in Lake Forest, IL, and raised in Libertyville, IL. She began her undergraduate studies in electrical engineering at The University of Tennessee, Knoxville in 2016. During her undergraduate years at UTK, Ruff spent the Fall semester of her sophomore year contributing to undergraduate research work within the College of Electrical Engineering and Computer Science. In the remaining semesters of her Bachelor's Degree, Ruff joined the Neutron Technologies Team at Oak Ridge National Laboratory's Spallation Neutron Source, in neutron polarization research and experimentation. Upon graduating with her B.S.E.E. from The University of Tennessee, Knoxville in 2020, Ruff was admitted to the UTK Graduate School through the WBG Power Electronics Graduate Student Traineeship program in pursuit of her Master's Degree. Ruff graduated from the program with her M.S.E.E. in May of 2022.